

---

Dynamics of sensorimotor  
behavior in electrolocation and  
electrocommunication

---

Dissertation ° Federico Pedraja ° Bielefeld University









**Dynamics of sensorimotor behavior in  
electrolocation and  
electrocommunication**

**Dissertation presented in partial fulfillment  
of the requirements for a Doctorate degree (Dr. rer. nat.)  
at the Faculty of Biology, Bielefeld University**

**by MSc. Federico Pedraja  
supervised by Prof. Dr. Jacob Engelmann**

**Bielefeld, May 2019**



---

## Preface

How are external sensory stimuli perceived, integrated and represented within the central nervous system? How does the nervous system generate appropriate behavioral responses based on this input and how does this behavior affect perception?

The above questions have in common that they view sensory input and motor control as two sides of the sensorimotor loop. In this closed-loop system, actions inevitably generate sensory flow<sup>1</sup> that can serve to organize behavior. To look, to smell, to touch, etc. are perceptual acts that depend on the interaction, coordination and interpretation of motor and sensory information through neural mechanisms. Active sensory systems<sup>2</sup> are particularly amenable to the study of the reciprocal relations of motor and sensory components, as parts of closed loop control structures. A notable advantage of these sensory systems is the experimental accessibility of their sensory input, both in terms of its measurement and in terms of detailed modeling reconstructions of the input. In the case of weakly electric fish studied in this thesis, the animals sense and process environmental perturbations of a self-generated electric field. The fact that this field serves as the carrier of sensory information and at the same time is controlled by the animal, enables to precisely determine aspects of sensing that are often hard to obtain or quantify in sensory systems that do not actively generate the carrier: where, when and what an animal samples.

Drawing on these benefits, my thesis focuses on the role of motor and electromotor behavior in sensorimotor integration. For this, a biophysical model for the active and passive electroreception was combined with physiological recordings and behavioral approaches. The central topics addressed are:

---

<sup>1</sup> Modulation of the sensory input produced by movement, self- or externally generated.

<sup>2</sup> Sensory systems where the energy (carrier) that stimulates the receptors is self-generated, as in somatosensory and echolocation systems.

---

(i) **Object detection and sensorimotor learning.** The sensory information obtained by the African species *Gnathonemus petersii* while learning a detection task was computationally reconstructed using boundary element methods (BEM). This revealed that the improved task performance was paralleled by an enhancement of the quality of the sensory information, which was mediated by changes of the electromotor patterns. The versatile manner in which the fish changed the spatial and temporal allocation of otherwise stable motor components not only improved the quality of the sensory input, but also resulted in shifts of the animals' attention towards the object.

(ii) **Dynamic choice of optimal behavior.** Extending on the above results, I next explored how changing the distance of an object to be detected by the fish influenced the electromotor behavior. With increasing complexity (distance), the fish resorted to a new motor strategy. This consisted in first approaching a salient element in the arena, from where the fish then made a perceptually-guided decision. This interpretation is backed up by analyzing the trajectories in the context of attractors, revealing that the focus of attention was altered in a task-dependent manner.

(iii) **Distance estimation using a non-visual form of motion parallax.** In the above experiments it is implicitly assumed that electric fish acquire spatial information like the position and distance of a target. How this is achieved dynamically has been addressed recently. Based on the properties of the electric field geometry, theoretical considerations indicated that relative movements might provide depth information. In a behavioral assay, I show that this novel form of electric parallax exists and is used across phylogenetically distant taxa of weakly electric fish (*Apteronotus albifrons*, *Eigenmania virescens* and *Gnathonemus petersii*). Notably, these species electrically sample the environment in temporally distinct ways (using discrete pulses or quasi-sinusoidal waves), suggesting an ubiquitous role for parallax in electric sensing.

(iv) **The role of multi-modal integration in socially relevant agonistic behaviour.** Extending on the above results, I next addressed if passive as well as active electric sensory information can be used to evaluate more complex features of the environment. For this I turned to social interactions

---

of the South American species *Gymnotus omarorum* to study if an electrical assessment of a competitor is possible. Based on modeling the sensory consequences of dyadic encounters, I showed that passive as well as active sensory information can drive agonistic interactions. This suggests that aggressive interactions may be triggered by information about contenders obtained through the active and passive electrosensory system.

(v) **Hierarchy as a social consequence of electric interactions.** The above analysis indicated that active as well as passive electrolocation may contribute in a non-reciprocal manner to social interactions. *Gymnotus omarorum* then was tested in intra- and intersexual dyads in small plain arenas. A sex-independent dominant-subordinate status emerged after highly aggressive contests. Subordinates signaled their submission by retreating and emitting specific (submissive) electric signals. The emergence of a dominant-subordinate status was also observed in a larger arena after longer but milder contests with rare electric signaling of submission with a unique consequence: the persistence of dominance over time with no outcome reversion.

---

# Contents

---

<b>1. Introduction</b>	<b>1</b>
1.1 Image formation .....	5
1.2 Electrosense .....	6
1.3 Electrolocation tasks and their sensory-motor consequences.....	13
1.3.1 Detection in electric sensing: motor learning to enhance sensory information .....	15
1.3.2 Distance estimation in the electric sense: motion parallax as a mechanism for distance estimation .....	19
1.3.3 Discrimination in the electric sense: Electric image formation from conspecifics .....	22
1.4 Bibliography .....	26
<b>2. Task related sensorimotor adjustments increase the sensory range</b>	<b>35</b>
2.1 Introduction .....	36
2.2 Methods.....	39
2.2.1 Animals.....	39
2.2.2 Behavior .....	39
2.2.3 Physiology .....	45
2.3 Results.....	48
2.3.1 Detection limits based on neuronal recordings in ELL.....	48
2.3.2 Task learning is paralleled by sensorimotor alterations .....	51
2.3.3 Motor behavior changes through differential recruitment of basic kinematic components.....	54
2.3.4 Altered behavior is reflected by the formation of an attractor .....	56
2.3.5 Electromotor behavior adapts alongside kinematics.....	58
2.3.6 Sensory consequences of behavioral adaptations.....	59
2.4 Discussion.....	64
2.5 Bibliography .....	69
<b>3. Shaping sensorimotor behavior in response to changes in cue saliency</b>	<b>77</b>
3.1 Introduction .....	79
3.2 Methods.....	82
3.2.1 Animals.....	82
3.2.2 Training setup .....	82
3.2.3 Training procedure .....	83
3.2.4 Video tracking .....	84
3.2.5 Data analysis and statistical tests.....	84
3.2.6 Electric images models.....	86
3.2.7 Fisher information analysis.....	86
3.3 Results.....	87
3.3.1 Performance and motor behavior change with object distance .....	87
3.3.2 Sensory consequences of decrease in object saliency .....	91
3.3.3 Modification of the electromotor behavior with the task .....	94
3.3.4 Spatial correlation of sensorimotor behavior .....	96
3.4 Discussion.....	97
3.5 Bibliography .....	104
<b>4. Motion parallax in electric sensing</b>	<b>111</b>
4.1 Introduction .....	112
4.2 Methods.....	114



---

4.2.1	Animals .....	114
4.2.2	Measuring the electric field and electric image .....	115
4.2.3	Modeling the electric field and electric image .....	116
4.2.4	Behavioral experiments.....	117
4.2.5	Behavioral Analyses.....	118
<b>4.3</b>	<b>Results.....</b>	<b>119</b>
4.3.1	Sensory basis of electrosensory motion parallax.....	119
4.3.2	Predicting the magnitude of the parallax-induced shift .....	122
4.3.3	Behavioral test of the electrosensory parallax hypothesis .....	124
<b>4.4</b>	<b>Discussion .....</b>	<b>130</b>
<b>4.5</b>	<b>Conclusion .....</b>	<b>132</b>
<b>4.6</b>	<b>Bibliography .....</b>	<b>132</b>
<b>5.</b>	<b>Electroreception during agonistic encounters in <i>Gymnotus omarorum</i></b>	<b>137</b>
<b>5.1</b>	<b>Introduction .....</b>	<b>138</b>
<b>5.2</b>	<b>Methods.....</b>	<b>141</b>
5.2.1	Behavioral Protocol .....	141
5.2.2	Behavioural Recording.....	142
5.2.3	Modeling the electric organ.....	143
5.2.4	Modeling electric images.....	145
<b>5.3</b>	<b>Results.....</b>	<b>149</b>
5.3.1	Experimental analysis of real pre-contest behavior .....	149
5.3.2	Canonical approaches .....	155
5.3.3	Parallel and anti-parallel approaches.....	158
<b>5.4</b>	<b>Discussion .....</b>	<b>160</b>
<b>5.5</b>	<b>Conclusion .....</b>	<b>163</b>
<b>5.6</b>	<b>Bibliography .....</b>	<b>164</b>
<b>6.</b>	<b>Non-breeding territoriality and context-dependent aggression in <i>G. omarorum</i></b>	<b>169</b>
<b>6.1</b>	<b>Introduction .....</b>	<b>170</b>
<b>6.2</b>	<b>Methods.....</b>	<b>175</b>
6.2.1	Animals .....	175
6.2.2	Laboratory Settings .....	176
6.2.3	Behavioral Experimental Procedures .....	177
6.2.4	Experiment 1 .....	177
6.2.5	Experiment 2 .....	178
6.2.6	Behavioral data processing .....	179
6.2.7	Statistics .....	181
<b>6.3</b>	<b>Results.....</b>	<b>181</b>
6.3.1	Experiment 1 .....	182
6.3.2	Experiment 2 .....	185
<b>6.4</b>	<b>Discussion .....</b>	<b>189</b>
<b>6.5</b>	<b>Bibliography .....</b>	<b>195</b>
<b>7.</b>	<b>Supplementary Material</b>	<b>201</b>
7.1	Supplementary figures .....	202
7.2	List of Acronyms .....	217
<b>8.</b>	<b>Documentation</b>	<b>I</b>
	<b>Author contributions .....</b>	<b>II</b>
	<b>Acknowledgements .....</b>	<b>VI</b>
	<b>Curriculum Vitae .....</b>	<b>VII</b>
	<b>Affirmation .....</b>	<b>XIII</b>

---

# Introduction

# 1

Sensing depends on the ability to capture and transduce energy that serves as a carrier of information. To optimize this information uptake, sensory systems with receptors of different complexity and tuned to different carriers have evolved (Fulton, 1946). Therefore, the properties of the receptor determine or restrict the spectrum of stimuli that can be detected (Hudspeth and Logothetis, 2000). Depending on the quality of the specific stimulus, different sensory modalities (e.g., touch, smell etc.) are distinguished. In each modality a specific sensory pathway arises from receptors that are often spatially clustered. This afferent pathway then provides input to specific regions of the central nervous system where the information is processed and transformed into a percept. The perception depends on several aspects. In vision for example, the primary visual pathway ensuing from the cones and rods that transduce the electromagnetic energy of photons in a specific wavelength-range, provides the input to the lateral geniculate nucleus (LGN) of the thalamus, from where parsed information is relayed to the primary visual cortex. Along this pathway specific features are encoded. This shaping of the sensory input does not only depend on neuronal processing and can already occur prior to

transduction, as I will address in more detail in a later sections of this introduction.

Despite substantial pre-processing, the sensory input does not always provide sufficient or unambiguous information. One solution to overcome this problem relies on the combination of different sources of information. Such multisensory integration allows to process information from two or more sensory modalities (cross-modal stimuli) (Meredith and Stein, 1986; Schumacher et al., 2017a, 2016; Stein and Stanford, 2008). The propensity to rely on the multimodality of sensory information is so strong, that it can be exploited in illusions, like the *McGurk illusion* (McGurk and MacDonald, 1976). Here, an auditory feedback of the syllable *ba* coupled with a visual feedback showing lip movements corresponding to the syllable *ga* consistently result in the subject perceiving *da* as the actual auditory input.

Another solution to counter the ambiguities of sensation relies on movements. These induce (predictable) changes in the sensory input that can be used to encode, decode and disambiguate biologically significant events in the external world. The extraction of information from the environment in this scenario cannot be defined as a purely passive process, but requires the animal to evaluate and use both motor and sensory information (Caputi and Budelli, 2006; Caputi, 2004). Motor behavior therefore endows animals with the opportunity to enhance the sensory input and to then produce an effective behavior in light of the self-generated sensory flow. Examples where movement and motor activity are an essential aspect of sensing include:

(a) **Movements that condition the sensory signal.** In several sensory systems pre-receptor mechanisms can condition the carrier, including

amplification, filtering and channeling of the energy to the sensory surface. Often, as in the visual system of vertebrates where the accommodation of the pupil adaptively regulates the light intensity at the level of the photoreceptors, these pre-receptor mechanisms involve active motor components.

(b) **Movements that re-orient the sensors.** Such movement may consist of moving the whole body or only parts of it (e.g. head or eyes). The structural counterpart of such movements is the heterogeneous and localized organization of the receptor mosaic. Again using the eye as an example, this heterogeneity includes the density of photoreceptors, their sensory aperture (receptive field), the density of their innervations and the occurrence of differently tuned receptors (rods and cones). Based on this heterogeneity, the sensory mosaic typically can be split in a foveal and peripheral part. As this design sacrifices resolution in the periphery and only devotes a small fraction of the receptor mosaic to optimal resolution, active re-orienting mechanisms, i.e., movements, are required to align sensory signals of interest with the foveal part.

(c) **Movement or motor activity as a source of the carrier for sensory signals.** In many active sensory systems, the perception of the environment is the consequence of a self-generated carrier that is modulated by the environment. Examples of this include active touch, echolocation, as well as active electroreception (Figure 1.1A).

Active sensory systems have facilitated research on the tight couplings between sensing and movements and revealed general fundamental results (Gordon et al., 2011; Noë, 2004). One aspect concerns the question how external stimuli can be distinguished from those that are due to an animal's

own activity. This is of particular importance in active sensory systems, as here the relevant sensory information is often embedded in weak modulations of the self-generated signal while the carrier is in addition strongly modulated by self-movements of the animals. Following the terminology of von Holst and Mittelstaedt (von Holst and Mittelstaedt, 1950) this requires to distinguish re-afferent input that is caused by the actions of the animal from ex-afferent input. An ubiquitous strategy to extract and thereby disambiguate the ex-afferent from the self-initiated re-afferent input is to route copies of motor commands to sensory structures. These copies are referred to as corollary discharge signals or, when they consist of an actual copy of the motor command, as efference copies (von Holst and Mittelstaedt, 1950; Sperry, 1950). Corollary discharge mechanisms can take place at different functional and operational levels of the nervous system (Crapse and Sommer, 2008). While lower-order corollary discharge mechanisms are based on inhibitory filters that act in phase with motor signals, higher-order corollary discharge mechanisms participate in functions such as sensory analysis and stability, including sensorimotor planning and learning (Crapse and Sommer, 2008). In the latter case, corollary discharge can be regarded as particular form of predictive signaling (Straka et al., 2018).

Another aspect that directly influences what an animal may perceive is the way in which the representation of the external actually depends on the receptors and the ability to behaviorally reconfigure the receptor/environment relation. Regardless whether the sensory process involves movement of the animal or is purely passive, the energy providing the sensory input typically impinges on an array of sensors (*sensory images*), that represent the external world in form of a differential neuronal

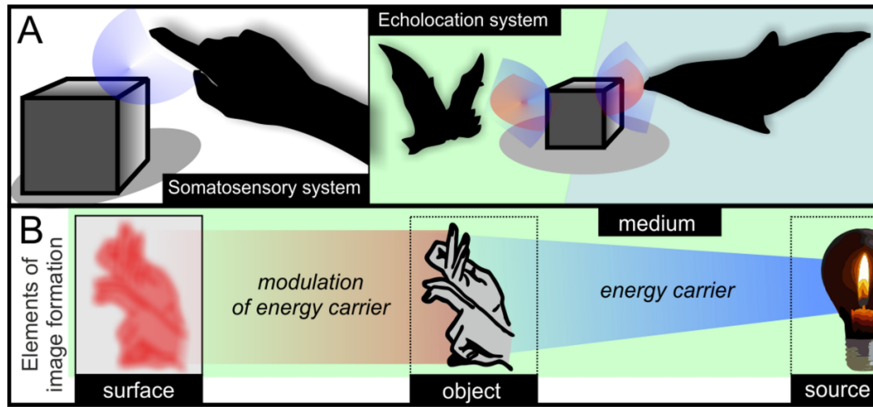
activation pattern (*neuronal images*). A central part of my thesis aims to elucidate how behavior can be used to influence this imaging process in active sensory systems. The next section thus addresses image formation in general, to then provide specific information on the electrosensory system studied in this thesis.

## 1.1 Image formation

Historically the concept of sensory images draws on optical images, where the optical apparatus of the eye forms a 2D representation (the image) of the three-dimensional world on the retina. This image formation process can be extended to any sensory system (Figure 1.1B) and allows distinguishing three aspects (Caputi and Budelli, 2006): (i) *the physical image* is the pattern of the energy parsed by, if present, pre-receptor structures. It can thus include aspects that the sensory system is not sensitive to (for example, in the human auditory system the physical images can include infra- and ultrasound, to which the sensory receptors are unresponsive). (ii) *The stimulus* or *receptor image* is the portion of the physical image that is transduced to be transformed into (iii) *the neural image* in the brain.

The physical image is either caused by changes of the source that generate the carrier, or by objects in the environment that modify the energy reaching the receptors. In this latter case the difference between the carrier with and without modulations by the environment is the actual carrier of sensory information. Since the carrier, traditionally termed the *perturbing carrier* (Lissmann and Machin, 1958), does not exist, it is also called the *virtual carrier* (Migliaro et al., 2005). Conceptually this virtual

carrier replaces the object(s) by an energy source that generate(s) a carrier equivalent to the feature(s) of the object(s). These feature(s) have been termed the *imprimance* of an object (Lissmann and Machin, 1958; Migliaro et al., 2005; Migliaro and Budelli, 2006). Note that this applies to both active and passive sensory systems, but due to the different sources passive and active images can be distinguished.



**Figure 1.1:** **A.** Active sensory systems form the source of the energy carrier used for sensing. Examples of the somatosensory and echolocation system are depicted. Note that in the haptic system the mechanical deformations of the carrier act directly on the sensory surface (contact sense, blue halo). In contrast the carrier needs to travel through a medium and return to the sensory surfaces in echolocating animals (teleceptive sense, blue and red halos show emitted and returned energy, respectively). **B.** Sketch of the process of sensory image formation using the theatre of shadows as an example. Image formation requires the spatial and temporal interaction of four elements: (i) an energy source that provides the information carrier, (ii) a medium that conducts the carrier, (iii) a modification of the carrier either by external objects as depicted here, or by changes in the source and (iv) a surface where the image is generated.

## 1.2 Electrosense

Many animals share the highly specialized ability of electroreception (Bullock and Chichibu, 1965; Lissmann, 1958). We can distinguish two sub-



modalities of electroreception (Coombs and Montgomery, 2005). **Passive electroreception** is the most primitive and oldest sub-modality of the electric sense (Bullock et al., 2006, 1993) and can be found in different chondrichthyes (Kalmijn, 1974), in catfish, in all electrogenic fish, tadpoles, salamanders, as well as in the mammalian platypus (Scheich et al., 1986) and in bees (Greggers et al., 2013). The widespread distribution highlights that this modality evolved several times (Baker et al., 2013). Passive electroreception allows the perception of electric fields produced by external electric sources. These sources can be of very different origin ranging from animate prey and predators to the metabolic activity of plants or the current induced when an animal moves through the Earth's magnetic field. In all these cases the sources are of low frequency content and thus this ability is referred to as *low frequency passive electroreception*. This is different when actively emitted electric signals of active electric fish are being sensed. This latter form has thus been termed *high frequency passive electroreception* (Figure 1.2A).

In contrast to the large number of species that are electroreceptive, the ability to actively emit electricity by aid of specialized electric organs (EO) to use it for predatory behavior, defense and active sensing has only been developed in a small group of teleost fish. These are commonly referred to as electric fish (Lissmann, 1958; Zupanc and Bullock, 2005). Strongly electric fishes (*Electrophorus electricus*, *Malapterurus electricus*, *Torpedo sp.*, *Astroscopus sp.*) use their electric organs to produce powerful electric organ discharges (EODs). These strong electric discharges purposely affect the target's motor neurons, easing the capture of the stunned prey or allowing the emitting fish to flight (Zupanc and Bullock, 2005). A second

extremely heterogeneous group of active electric fishes emits weak electrical pulses that support a specialized form of electrocommunication (Rajiformes, Uranoscopidae, Plotosidae, Siluriformes, Cladistia, Dipnoi and Amphibia). Here fish interact with conspecifics and use the EOD frequency, shape and/or the inter-pulse pattern of the EODs to signal information for the recognition of conspecifics, or to convey information required in specific interactions like spawning behavior or aggression. In *Sinodontis spp.* (Mochokidae) for example, the discharges are related to social interactions between individuals (Boyle et al., 2014); these fish also respond to external electrical stimulation (Orlov et al., 1993; Orlov and Baron, 2005). Another example is *Clarias macrocephalus*, where evidence suggests the use of episodic electric activity in the mating ritual. Female burst directly on the male's neuromuscular system results in tetanus-like axial muscle contractions, which in turn affect the sexual embrace, which is instrumental in egg release (Ol'shanskii et al., 2011).

In a third group of active electric fish, the EOD is used to communication as described above (Figure 1.2B)(Arnegard et al., 2010; Perrone et al., 2009; Silva et al., 2007; Zakon et al., 2002), but in addition is used for electrolocation. In this case the EOD functions as a carrier that provides re-afferent input to the emitting animal as well as ex-afferent input to other individuals. **Active electroreception** refers to the ability of these weakly electric fish to use the environmental modulations of the carrier to explore their environment (Figure 1.2C) (Bullock and Chichibu, 1965; Lissmann, 1958; Lissmann and Machin, 1958). Active weakly electric fish are divided in two evolutionary independent groups, the Mormyriiformes common to Africa and the Gymnotiformes of South America (Figure 1.2D).

In both groups the temporal profile of the EOD contains a sequence of elementary waves whose temporal relationship and relative amplitude are species-specific (Hopkins, 1980). In the following, I briefly summarize the major differences in the generation of this EOD.

In the majority of active electric fish species the EO is myogenic, that is, it is developmentally derived from muscle tissue. A neurogenic EO is known only in the South American Apterontids (Waxman et al., 1972). Independent of the developmental origin of the EO, in both lineages of fish a set of relay neurons of the pacemaker nucleus, the nucleus responsible for the generation of the signal for the EOD, project on spinal electromotorneurons (EMNs) that innervate the electrocytes. Electrocytes form the EO and generate the electric current that serves as a sensory carrier. One striking difference between the EO of South American and African species is that in the first, the EO is distributed along the longitudinal axis of the body with regional differences in electrocytes and their innervation that result in different regional EODs. The EO of the African Mormyriiformes however, is highly localized and composed by groups of homogeneous electrocytes. This allows the generation of comparatively stronger electric currents than in the Gymnotiformes species. The interval between consecutive discharges depends on the innervations pattern of the EO. High-frequency activation of the EO results in single discharges that merge into a continuous wave (100 to 1000 Hz fundamental frequency). When the interval between discharges is longer than the duration of the EOD, intermittent EODs are generated. Based on this differences weakly electric fish are often classified as *wave* or *pulse-like* fish. Nonetheless, this classification is strictly functional (Figure 1.2D); in both groups there are wave and pulse emitting species indicating a convergent

evolution of different electroreceptive strategies (Arnegard et al., 2010; Gallant et al., 2014). While the shape and frequency of the EOD is plastic, a given species cannot transition between these two different temporal modes of EOD emission.

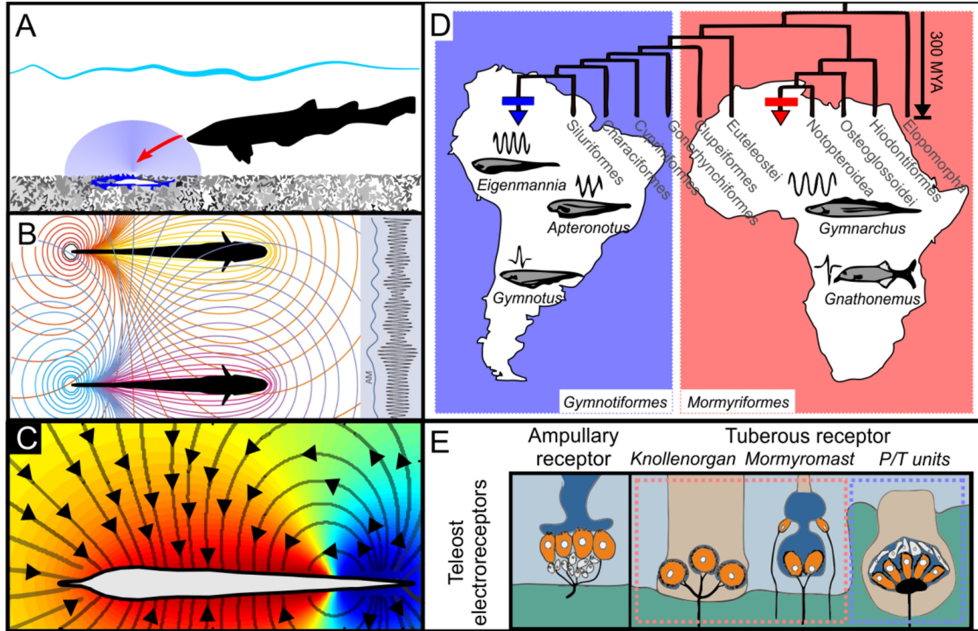
Independent of the difference in the way that the EODs are generated, the physics that govern active electric sensing are the same (Lewis, 2014; Moller, 1995). The resistive properties of the fish body shapes the electric field into an asymmetric dipole- or multipole-like electric field (Assad et al., 1999; Caputi and Budelli, 2006; Pedraja et al., 2014; Sanguinetti-Scheck et al., 2011) (Figure 1.2C).

Object in the environment that differ in their impedance from the water can perturb the electric field, be it self-generated or of external origin. This results in an object-dependent modulation of the spatial pattern of the current over the fish's skin that can be sensed by different receptors that are distributed over the body of the fish. The most common type of electroreceptor, found in active and passive electric fish, is the **ampullary electroreceptor** (Figure 1.2E). The name is derived from the morphology of the supporting structures that make these electroreceptors highly sensitive to low frequency electric fields. The ampullary system thus is responsible for low frequency passive electroreception which provides information of slow variations of the transcutaneous potential generated by sources external to the fish (Wilkins et al., 2002).

The properties of the self-generated EOD are perceived by **tuberous receptor organs** (Figure 1.2E) which are unique to weakly electric fish (Mormyriiformes and Gymnotiformes). These tuberous receptors can be grouped in phase and amplitude coders. Phase coders are sensitive to

changes in the EOD frequency. In Mormyrids fish, these are known as the Knollenorgan receptors and are sensitive to both the own EOD and that of conspecifics. As Knollenorgan receptors are generally not strongly affected by the intensity of the EOD, they are considered to be used to detect the EODs of other fish exclusively, i.e., they serve for communication (Bell and Szabo, 1986). In Gymnotiformes the phase coding receptors are called T-type electroreceptors as their discharge is phase-locked to the EOD cycle. Similar to Knollenorgans, these T-type receptors are used in electrocommunication as they were found to be crucial in the jamming avoidance response (Heiligenberg and Partridge, 1981).

Contrary to these time-coding electroreceptors, amplitude coding electroreceptors are sensitive to changes of the EOD amplitude. In Mormyrid fish these are the A- and B-cells of the so-called Mormyromasts. Both respond to increases of the EOD amplitude with a drop of their latency and vice versa (Sawtell et al., 2006). The B-cells are in addition sensitive to the waveform of the EOD, adding a second channel of information to the active electrosensory world (von der Emde and Bleckmann, 1997). Amplitude coders of the wave-type Gymnotiformes fish are called P-type electroreceptors as their discharge rate is proportional to the EOD amplitude: larger EOD amplitudes will increase the firing rate and vice-versa. Despite the above differences, electroreception in all cases has a short working range (Caputi et al., 2013; Chen et al., 2005), sometimes referred to as the *pre-haptic* or *pre-touch* range. The active electric sense thus is typically used to explore the sensory volume within a couple of centimeters to one body length around the animal.



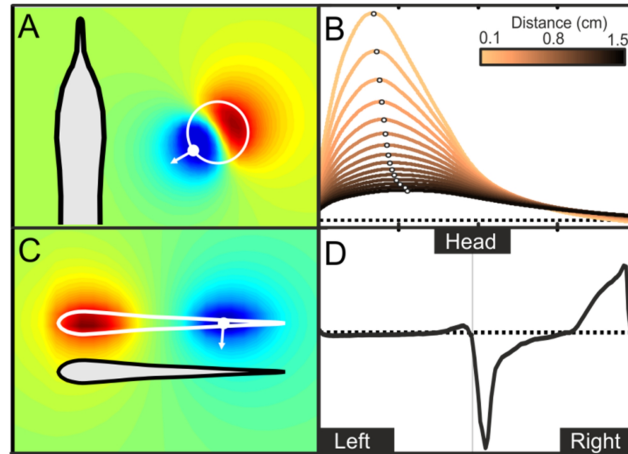
**Figure 1.2:** **A.** In passive electroreception, externally generated currents are detected by ampullary electroreceptors in the skin, enabling fish to detect and localize visually hidden prey (modified from Kalmijn, 1971). **B.** Communication is one of the main functions of the electrosense. Global modulations of the electric field amplitude (color lines represent the potential map and inset shows an example of amplitude modulation), which affect large parts of the sensory surface, are used as communication signals (from Krahe and Gabbiani, 2004). **C.** The carrier for active electrolocation in weakly electric fishes is generated by the discharge of an electric organ that produces an electric field surrounding the fish's body (here shown for *G. petersii*). Black lines represent the flow of the electric current while the color gradient indicates the gradient of the voltage (negative values in blue, positive values in red) (from Pedraja et al., 2018). **D.** Phylogenetic tree showing that active electroreception evolved independently in Gymnotiformes (blue) and Mormyriiformes (red). The species shown represent pulse type (*Gymnotus* and *Gnathonemus*) and wave type (*Eigenmannia*, *Apteronotus* and *Gymnarchus*) species (modified from Nelson, 2011 and Gallant et al., 2014). **E.** Electroreceptors: ampullary receptors (left) respond to low-frequency external stimuli. They contain electroreceptor cells (orange) at the base of a mucous-filled duct (blue) that opens to the surface. Tuberous organs (right) respond to high-frequency stimuli. The electroreceptor cells (orange) are generally located within an intra-epidermal cavity plugged by epidermal cells. Both types of Mormyrid tuberous organs (Knollenorgan and Mormyromast) and Gymnotids tuberous organs P and T (P/T both with similar morphology) are shown (modified from Baker et al., 2013).

In case of the passive electric sense, this range may extend up to about one meter (Pedraja et al., 2014; Pereira et al., 2012; Push and Moller, 1979; Toerring and Moller, 1984; Toerring and Belbenoit, 1979; von der Emde and Schwarz, 2002). Within this sensory volume both passively and actively generated information is accessible to the fish and used in a variety of behaviors. To understand how tasks can be successfully solved using electroreception, it is necessary then to know how electric images are generated.

### **1.3 Electrolocation tasks and their sensory-motor consequences**

Electrolocation, defined as the ability to **detect**, **localize** and **characterize** objects in the environment, does depend on the properties of the electric images (Bullock et al., 2006). The electrical current generated by the electric organ extends from the skin of the animal into the environment. This has different consequences for active and passive electroreception and the electric images. In the case of active electroreception the source is predictable, i.e., the fish knows where, when and at which amplitude the current is generated. However, the impedance of the external environment typically is inhomogeneous due to the presence of objects (Figure 1.3A). When the spatial and temporal profile of the transcutaneous currents is modulated by the environment, a so-called *active electric image* is generated (Figure 1.3B). In the case of high frequency passive electroreception the source is unpredictable in space and time as it is generated external to the receiver (Figure 1.3C). The resulting modulation

of the transcutaneous current at the side of the receiver then is called the *passive electric image* (Figure 1.3D).



**Figure 1.3:** **A.** Active electrolocation is based on the modulation of the self-generated current by the environment (from Pedraja et al., 2018). This image shows the perturbing field, calculated as the difference between the unperturbed and perturbed field. The perturbing field thus represents a virtual source mimicking the modulation of the field by the object (color map). For a simple object like the metal sphere used here (white circle), the virtual object resembles a simple dipole where the direction of the current goes towards the fish body (white arrow). **B.** A simple object like the one shown in A results in a spatio-temporal modulation of the transcutaneous current, called the “active electric image”. Data represents the modeled electric images calculated for a patch of skin while keeping the x and z coordinates of the sphere constant while increasing its distance from the sensory surface. Images become weaker, wider and also show a systematic shift of their peak location (see grey dots) with distance. **C.** High frequency passive electrolocation is based on the external current generated by an electric fish. Similar to A the perturbing field (color map) and the direction of the current (white arrow) are being shown here. Note that in this case the perturbing field is represented by the perturbed field only. **D.** Calculated electric image along a transect of the fish midline from head to tail for the fish shown in grey in panel C. The EOD of the conspecific (white fish in C) generates a spatio-temporal modulation of the transcutaneous current, called the “passive electric image”.

In both cases the properties of the electric images are influenced by movements, either of the receiving fish, or those in the environment. These movements result in spatio-temporal patterns of the electric images. These



modulations can be both, friend or foe in active electrolocation. While detrimental effects of movements are well investigated (Bell et al., 1997; Kennedy et al., 2014), my thesis will focus on the less researched possibility of animals to use movement to improve perception. The rich repertoire of electromotor behaviors commonly reported for weakly electric suggest that they can actively position and align their body in order to shape the re-afferent sensory input, potentially making additional use of different parts of their sensory mosaic (reorientation of the sensory surface) for the extraction of different features from the sensory flow. A particularly striking example for this comes from a wave-type weakly electric Gymnotiform fish that engages in energetically inefficient foraging in order to enlarge the electrosensory range (Biswas et al., 2018; MacIver et al., 2010; Snyder et al., 2007). Furthermore, in the same species a modeling study has suggested that when the signal-to-noise ratio is unfavorable, as is the case of prey capture in cluttered environments, active sensorimotor strategies could be relevant in improving electrolocation (Babineau et al., 2007).

My thesis will address the interactions of electromotor behavior and the information an animal can obtain in both active electrolocation and communication. The individual research aspects are introduced in the following, by considering electrolocation as a three-stage process that involves detection, localization and characterization.

### **1.3.1 Detection in electric sensing: motor learning to enhance sensory information**

Detection requires determining whether an item is present or not. In the late 1950s Lissmann and Machin (1958) demonstrated for the first time that weakly electric fish, specifically *Gymnarchus niloticus*, are able to detect

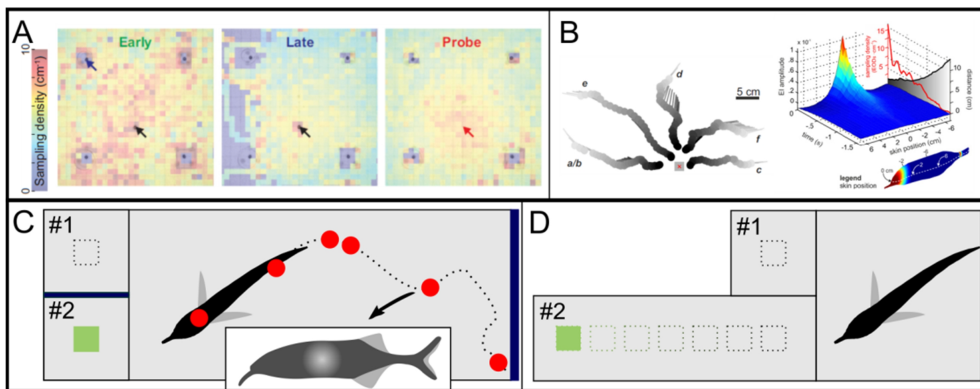
objects based on their electrical properties. Since this pioneering study, several works focused on the detection of different elements, as preys (Babineau et al., 2007; Nelson and Maciver, 1999), conspecifics (Heiligenberg et al., 1991; Naruse and Kawasaki, 1998) or inanimate objects in the environment (von der Emde, 2006, 1999). Superficially, detection appears to be a simple binary decision based on the sensory input. Despite this apparent simplicity, even simple detection tasks require learning (Wolpert et al., 2011). In active sensory systems this implicates both motor and sensory learning, as the corollaries of the behavior need to be incorporated into the analysis of the sensory input. Learning then is reflected in the iterative improvement of the performance. This will converge to a steady-state that will depend on the information acquired, the motor efficiency and energetic costs, as well as other limiting factors.

What weakly electric fish can learn using their active sensory system and how this is integrated with other senses has attracted a lot of research (Dangelmayer et al., 2016; Hofmann et al., 2013; Jun et al., 2016; Schumacher et al., 2017b, 2016; Walton and Moller, 2010). Several studies also analyzed how the motor system may interact with the ability to electrolocate (MacIver et al., 2010; Nelson et al., 2002; Nelson and Maciver, 1999). However, to which extent electrosensory learning also involves motor and electromotor learning, is largely unknown. A recent study indicates that sensory learning is paralleled by altered motor and electromotor behaviors. In this study *Gymnotus sp.* was shown to increase its information intake by reducing its swim speed while increasing its EOD rate during a spatial learning task (Jun et al., 2016)(Figure 1.4A). Other experiments that did not focus on learning revealed that weakly electric fish perform several stereotyped electromotor patterns. These probing motor

acts (Toerring and Moller, 1984) are considered to be used by the animals to actively exploit sensorimotor dependencies and obtain sensory input that otherwise would not be available. While preliminary evidence for this hypothesis was published recently, showing that depth information may be obtained by the use of a specific motor pattern (Hofmann et al., 2017) (Figure 1.4B), it remains to be shown if such information is truly used by the fish. **Chapters 2-3** of my thesis thus focus on the question how electromotor behaviors shape sensory information. Furthermore, I address if and how animals can actively exploit the ability to shape the sensory flow both in spontaneous behavior and in a task involving electrosensory learning. Both studies used the weakly electric Mormyrid fish *Gnathonemus petersii*, the species for which we have the best knowledge of its behavioral, anatomical and physiological data.

**Chapter 2** specifically focuses on the question how learning affects electromotor behaviors by testing the ability of fish to detect and localize an object in a reinforced conditioning paradigm. In these experiments, the fish must extract the relevant spatial information from the sensory input that is generated by the ongoing electromotor behavior (Figure 1.4C). Notably, fish did not modulate the timing of the EOD, but the improved performance depended on incremental changes of the motor pattern with learning. These mainly were based on the versatile manner in which fish changed the spatial and temporal allocation of otherwise stable motor components. These adaptations significantly improved the quality of the sensory information, as quantified using a computational approach. The altered behavior also led to a shift of the animals' attention. In line with previous studies that considered electromotor behavior as overt displays of attention-modulated cognitive processes (Jun et al., 2016; Walton and

Moller, 2010), weakly electric fish hence emerge as promising model organisms to study how attention can shape behavior and learning in vertebrates lacking an orbitofrontal cortex, a key structure in guiding mammalian attention (Padoa-Schioppa, 2011).



**Figure 1.4:** **A.** While learning a detection task the sampling density (product of swim speed and EOD rate, color-coded) of *Gymnotus* spec. is initially increased near salient objects (left panel, blue squares), decreases with learning (middle panel) and is again increased when the previously acquired motor strategy failed (right panel). The arrow indicates where a food-reward was obtained in the arena (figure modified from Jun et al., 2016). **B.** Weakly electric fish (*G. petersii*) show a stereotyped electromotor pattern when they approach novel objects (left). This approach strategy results in a fixed change of the sensory information (electric images) that potentially could be used by the fish to dynamically determine the distance to their target (right) (figure modified after Hofmann et al., 2017). **C.** Schematic of the behavioral task used in the experiments of chapter 2. Fish were trained to enter an arena (gate: blue vertical bar) where they had to swim to the compartment marked by a metal cube. The cube was randomly altered between both compartments (#1: possible position. #2: actual position). A schematic trajectory with individual sampling events (EODs, red dots) is shown. **D.** Same set-up as in C, but in the paradigm presented in chapter 3 the fish now had to detect the metal cube from gradually increasing distances (#1 vs #2).

**Chapter 3** extends upon these findings by exploring how versatile fish are in altering their previously learned electromotor behavior. For this I challenged the animals after having acquired the detection task used in chapter 2 by making the sensory cue indicating where to swim less salient

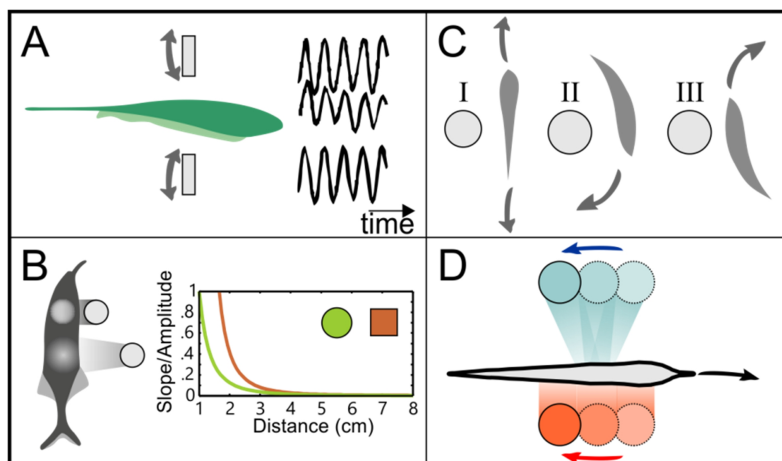
(Figure 1.4D). This resulted in a drop of the animals' performance to chance levels when the cue became too weak to be detected. At intermediate levels, however, the animals switched to a new motor strategy by incorporating a previously non-informative cue into their behavior. This cue had no value for the detection task itself, but enabled the fish to navigate to the part of the arena from where they could compare the two possible behavioral options at once. It thus appears that detection in active electrolocation is a dynamic process where the current sensory input is used to shape the upcoming behavior. When this information is insufficient, the fish can shift their attention to an intermediate solution that here depended on relational knowledge to facilitate the sensation-based choice of the next step in behavior.

### **1.3.2 Distance estimation in the electric sense: motion parallax as a mechanism for distance estimation**

Object localization requires obtaining information about the direction of an object with respect to the own position. Secondly, it involves to obtain an estimate of the distance between oneself and the object (Abrams and Landgraf, 1990). How weakly electric fish can localize objects to for example successfully capture their prey has been studied intensely (Babineau et al., 2007; Caputi and Budelli, 2006; Nelson and Maciver, 1999; Rasnow, 1996). In 1973, Heiligenberg was the first to show that weakly electric fish can in fact determine distances with their electric sense (Heiligenberg, 1973a, 1973b). He found that the South American species *Eigenmannia* can control its distance to two oscillating conductive objects and center itself between them (Figure 1.5A). The experimentally imposed

object-tracking behavior mimics the natural propensity of these fish to seek shelter and is known as the shelter-tracking experiment. While these early studies revealed that weakly electric fish can dynamically determine the distance to objects, the first study that proposed a mechanism by which electrosensory distance estimation may be possible focused on the geometric properties of electric images. This measure, as worked out by von der Emde and co-workers (von der Emde et al., 1998), requires fish to obtain a normalized measure of the width of electric images (Figure 1.5B). Electric images produced by purely resistive objects depend on the distance to the object, its size and resistance. Objects of varying resistance can thus produce electric images of the same amplitude at different distances. Therefore, distance information not only depends on the amplitude, but also on the width of the electric image profile. To resolve this size-distance ambiguity, the authors proposed a normalization of the electric images by their blurriness. Indeed, fish trained to discriminate distances were found to use this metric (Caputi et al., 1998; Lewis and Maler, 2001; von der Emde et al., 1998). This mechanism does not include movement and are not spontaneously used by the fish as they needed to learn to apply this metric.

Hence it remained unclear by which mechanism fish were able to determine the distance in the shelter-tracking experiments. The back-and-forth movements that fish show in these experiments are comparable to the stereotyped *va-et-vient* motor patterns described to occur in electrosensory guided behaviors (Toerring and Moller, 1984; Toerring and Belbenoit, 1979). The presence of such stereotyped motor patterns has led to the hypothesis that fish may use the spatiotemporal sensory input generated by these motor movements for electrolocation (Figure 1.5C).



**Figure 1.5:** **A.** Shelter-tracking experiment in *Eigenmannia virescense* can control its distance from two moving conductive objects (top and bottom black sine-waves) and centers between them (middle sine-wave; from Heiligenberg, 1973a, 1973b). **B.** In 1998 von der Emde and colleagues demonstrated that *Gnathonemus petersii* estimate distance to an object by comparing the slope and the amplitude of the electric images, a mechanism comparable to visual distance estimation by contrast and blur (Mather, 1997; Mather and Smith, 2002; Schwarz et al., 2001; von der Emde et al., 1998). As shown by the inset, this metric depends on the shape of the objects. **C.** Schematic representation of motor patterns occurring in prey-catching behavior (Toerring and Moller, 1984; Toerring and Belbenoit, 1979). These motor patterns led to the hypothesis that their spatiotemporal sensory patterns could aid in electrolocation. **D.** Sketch showing the hypothesis that electrical motion parallax might provide distance information generated by the fish's own movement. Here a fish swims along two identical objects at different distances, leading to a difference in the apparent speed potentially indicative of object distance.

Indeed many of the stereotyped probing motor acts may induce relative motion cues and hence are regarded as an active sensing strategy to enhance electroreception (Hofmann et al., 2013). The *va-et-vient* movement detailed above is suggestive of peering movements used by insects to exploit and generate visual parallax for visual depth estimation (Shaffer et al., 1987). However, there is no direct evidence that weakly electric fish use motion-related cues or electric parallax for distance estimation.

In **chapter 4** I hence first addressed if the electric field can provide a dynamic depth cue comparable to the nonlinear image formation properties in visual parallax. I found that the dipole-like electric field geometry coupled to motion provides the physical basis for non-visual parallax (Figure 1.5D). Extending on this, I then explored if this information can be used in electrolocation, documenting that electric parallax is used for electrosensory distance perception across phylogenetically distant taxa of weakly electric fish. Notably, these species electrically sample the environment in temporally distinct ways (using discrete pulses or quasi-sinusoidal waves), suggesting a ubiquitous role for parallax in electric sensing. These results demonstrated for the first time that electrosensory information is extracted from sensory flow and used in a behaviorally relevant context.

### **1.3.3 Discrimination in the electric sense: Electric image formation from conspecifics**

In detection and localization the features an animal needs to determine are well defined (i.e., presence, distance and position of a target). This is less clear when we consider the characterization, since the features used for this may vary along a continuum. A characterization that weakly electric fish must solve is the discrimination of living and non-living items, or the discrimination between prey and predator and/or conspecifics. Only few studies have addressed electrosensory characterization in social interactions (Gómez-Sena et al., 2014). Similar to the interactions with objects, social interactions require to detect and localize other fish and to assess their attributes. Mate-finding, agonistic encounters and the formation of social hierarchies can thus be regarded as natural situations, where electrosensory



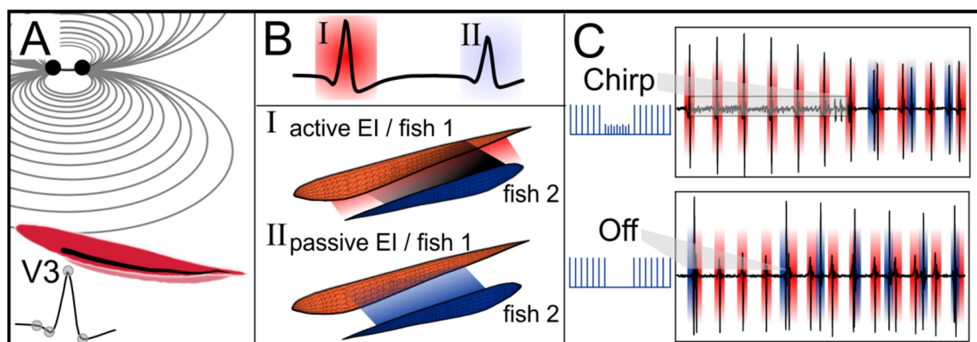
mediated detection, localization and characterization are crucial. The last two chapters of my thesis thus aim to further our understanding of how basic sensory capabilities are integrated in more complex behaviors. For this, I turn to potentially aggressive interactions in *Gymnotus omarorum*.

It is well documented that changes in amplitude or frequency of the EOD waveform convey social information, for example in mate or species recognition of both wave-type and pulsatile species (Arnegard et al., 2010; Arnegard and Carlson, 2005; Fotowat et al., 2013; Henninger et al., 2018). When this exchange of information is reciprocal and active, it is termed electrocommunication (see above). However, socially relevant information may also be conveyed in an undirected or even unintended way: fish may gather information of their peers through the analysis of their passive and active electric images.

In **chapter 5**, I thus study the agonistic encounters in intra- and intersexual dyads of the South-American weakly electric fish *G. omarorum*. While it is known that the EODs of other fish can be used to localize them by passive electrolocation (Hopkins, 2005)(Figure 1.6A), it remains unknown if either passive or active electric images, and thus the active electric sense, are also used to obtain information about the characteristics of the contender (e.g. size, shape)(Gómez-Sena et al., 2014). By reconstructing the sensory images during different phases of interactions between dyads of fish (figure 1.6B), I showed that passive electric images are suitable for the evaluation of a contender when pairs are relatively far from each other. At very short distances however, the information extracted from active electric images appears to outweigh that of passive images.

Together this shows that passive and active electric images are fundamental in characterization of a contender and the decision to approach it.

In the **final chapter** of this thesis, I evaluate the consequences of the agonistic behaviors from chapter 5. Agonistic interactions are associated with the resolution of conflicts between members of the same species that compete for resources (King, 1973; Lorenz, 1963). As resources are often spatially distributed, conflict resolution can lead to territoriality, where the territory of a dominant animal is the area from which subordinates are excluded. As an outcome of the dyadic interactions in a small arena, a sex-independent dominant-subordinate separation emerged after highly aggressive contests (Batista et al., 2012). Subordinates were found to signal submission by retreating and emitting characteristic submissive electric signals (chirps and offs figure 1.6C). In large territories as the studied in chapter 5 a similar segregation in dominant and subordinate animals could be observed after less aggressive interactions where electric displays of submission were rare. Importantly, once dominance was established, the rank persisted over time, including marked territoriality of the dominant animal. Although the territorial behavior of *Gymnotus* has been recognized since the first reports on this species in small territories (Batista et al., 2012), this is the first study to show how agonistic encounters mediate territoriality in this genus.



**Figure 1.6:** **A.** Electrodes mimicking the EOD of a conspecific (black dots) produce an electric field that can be used by electric fish to detect and localize this source. (Hopkins, 2005). The species used in this study is *Gymnotus omarorum*, a pulse-type South American weakly electric fish. The sketch on the bottom of this figure shows the distributed electric organ (black on top of fish body in red) and the head to tail EOD waveform showing the positive peak V3 (used for the EI modeling). **B.** For each EOD produced by two nearby *Gymnotus omarorum* (top, red fish 1 and blue fish 2), active and passive electric images are generated (middle and bottom). The red halo indicates the self-generated EOD carrier from fish 1, the black halo the modulation of this carrier by the presence of fish 2 and the blue halo the EOD carrier generated by fish 2. **C.** In the agonistic behavior studied in chapters 5-6 physical as well as electric behaviors were elicited. Chirps (increase in frequency and decrease in amplitude of the EOD) and offs (turn off of the EOD) signals are used by the fish that lost the contest as submissive signals (blue color), leading to long-term dominant-subordinate hierarchy as a resolution of the conflict.

The electrosensory system of weakly electric fish presents several advantages that have facilitated the research of diverse general problems in neuroscience, in particular of sensory systems. This includes peripheral coding (Sawtell et al., 2005; Stamper et al., 2013), the representation and central processing of sensory signals (Caputi, 2004; Hollmann et al., 2016; Rose et al., 1999; Sawtell and Williams, 2008), sensory-motor and multi-sensory integration (Dangelmayr et al., 2016; Hofmann et al., 2017, 2013; Schumacher et al., 2017a, 2016), social interactions (Arnegard and Carlson, 2005; Batista et al., 2012; Perrone et al., 2009; Silva et al., 2007; Zakon et al., 2002; Zubizarreta et al., 2015), as well as research of the development of sensory systems and the role of electric signals in evolution (M. E. Arnegard

et al., 2010; Gallant et al., 2014; Stoddard, 1999). These studies relied on multiple experimental and theoretical approaches and demonstrated that neuroethological research on apparently alien senses can reveal mechanisms of general relevance. At least in part, the apparent (sensory) specialties of electroreceptive fish as well as the unique accessibility of the carrier of sensory information have been instrumental in revealing general mechanisms.

In this spirit, my thesis aims to provide an in-depth analysis of the rich behavioral repertoire to elucidate how sensorimotor mechanisms contribute to the detection, localization and characterization of different features of the external world. These challenges are shared by all animals, but the ability to model the corollaries of sensorimotor behavior with respect to the sensory input makes weakly electric fish useful models for the intended research. Each of the following chapters includes a specific introduction, a detailed description of the experimental design, the results and their discussion.

## **1.4 Bibliography**

- Abrams RA, Landgraf JZ. 1990. Differential use of distance and location information for spatial localization. *Percept Psychophys* 47:349–359.
- Arnegard ME, Carlson BA. 2005. Electric organ discharge patterns during group hunting by a mormyrid fish. *Proceedings Biol Sci* 272:1305–1314.
- Arnegard ME., McIntyre PB, Harmon LJ, Zelditch ML, Crampton WGR, Davis JK, Sullivan JP, Lavoué S, Hopkins CD. 2010. Sexual Signal Evolution Outpaces Ecological Divergence during Electric Fish Species Radiation. *Am Nat* 176:335–356.
- Arnegard ME., Zwickl DJ, Lu Y, Zakon HH. 2010. Old gene duplication facilitates origin and diversification of an innovative communication system--twice. *Proc Natl Acad Sci*.

- Assad C, Rasnow B, Stoddard PK. 1999. Electric organ discharges and electric images during electrolocation. *J Exp Biol* 202:1185–93.
- Babineau D, Lewis JE, Longtin A. 2007. Spatial acuity and prey detection in weakly electric fish. *PLoS Comput Biol* 3:e38.
- Baker CVH, Modrell MS, Gillis JA. 2013. The evolution and development of vertebrate lateral line electroreceptors. *J Exp Biol* 216:2515–2522
- Batista G, Zubizarreta L, Perrone R, Silva AC. 2012. Non-sex-biased Dominance in a Sexually Monomorphic Electric Fish: Fight Structure and Submissive Electric Signalling. *Ethology* 118.
- Bell C, Bodznick D, Montgomery J, Bastian J. 1997. The generation and subtraction of sensory expectations within cerebellum-like structures. *Brain Behav Evol* 50:17–31.
- Bell CC, Szabo T. 1986. Electroreception in mormyrid fish: Central anatomy In: Bullock TH, Heiligenberg W, editors. *Electroreception*. New York: Wiley. pp. 319–322.
- Biswas D, Arend LA, Stamper SA, Vágvölgyi BP, Fortune ES, Cowan NJ. 2018. Closed-loop control of active sensing movements regulates sensory slip. *Curr Biol* 28:4029-4036.e4.
- Boyle KS, Colley O, Parmentier E. 2014. Sound production to electric discharge: sonic muscle evolution in progress in *Synodontis* spp. catfishes (Mochokidae). *Proc R Soc B Biol Sci* 281:20141197.
- Bullock TH, Bodznick DA, Northcutt RG. 1993. The phylogenetic distribution of electroreception: evidence for convergent evolution of a primitive vertebrate sense modality. *How Do Brains Work?* Springer. pp. 581–602.
- Bullock TH, Chichibu S. 1965. Further analysis of sensory coding in electroreceptors of electric fish. *Proc Natl Acad Sci U S A* 54:422–429.
- Bullock TH, Hopkins CD, Fay RR. 2006. *Electroreception*. Springer Science & Business Media.
- Caputi AA., Budelli R. 2006. Peripheral electrosensory imaging by weakly electric fish. *J Comp Physiol A* 192:587–600.
- Caputi AA. 2004. Contributions of electric fish to the understanding of sensory processing by reafferent systems. *J Physiol Paris* 98:81–97.
- Caputi A, Budelli R, Grant K, Bell C. 1998. The electric image in weakly electric fish: II. Physical images of resistive objects in *Gnathonemus petersii*. *J Exp Biol* 201:2115–2128.
- Caputi AA, Aguilera PA, Carolina Pereira A, Rodríguez-Cattáneo A. 2013. On the haptic nature of the active electric sense of fish. *Brain Res*

- 1536:27–43.
- Chen L, House JL, Krahe R, Nelson ME. 2005. Modeling signal and background components of electrosensory scenes. *J Comp Physiol A* 191:331–345.
- Coombs S, Montgomery JC. 2005. Comparing octavolateralis sensory systems: What can we learn? *Electroreception*. pp. 318–359.
- Crapse TB, Sommer MA. 2008. Corollary discharge across the animal kingdom. *Nat Rev Neurosci* 9:587.
- Dangelmayer S, Benda J, Grewe J. 2016. Weakly electric fish learn both visual and electrosensory cues in a multisensory object discrimination task. *J Physiol* 110:182–189.
- Fotowat H, Harrison RR, Krahe R. 2013. Statistics of the electrosensory input in the freely swimming weakly electric fish *Apteronotus leptorhynchus*. *J Neurosci* 33:13758–13772.
- Fulton JF. 1946. *Howell's Textbook of Physiology*. Philadelphia.
- Gallant JR, Traeger LL, Volkening JD, Moffett H, Chen P-H, Novina CD, Phillips GN, Anand R, Wells GB, Pinch M, Guth R, Unguez GA, Albert JS, Zakon HH, Samanta MP, Sussman MR. 2014. Genomic basis for the convergent evolution of electric organs. *Science* 344:1522–1525.
- Gómez-Sena L, Pedraja F, Sanguinetti-Scheck JI, Budelli R. 2014. Computational modeling of electric imaging in weakly electric fish: Insights for physiology, behavior and evolution. *J Physiol Paris* 108:112–128.
- Gordon G, Kaplan DM, Lankow B, Little DY-J, Sherwin J, Suter B a, Thaler L. 2011. Toward an integrated approach to perception and action: conference report and future directions. *Front Syst Neurosci* 5:20.
- Greggers U, Koch G, Schmidt V, Dürr A, Floriou-Servou A, Piepenbrock D, Göpfert MC, Menzel R, Durr A, Floriou-Servou A, Piepenbrock D, Gopfert MC, Menzel R. 2013. Reception and learning of electric fields in bees. *Proc R Soc B Biol Sci* 280:20130528.
- Heiligenberg W. 1973a. “Electromotor” response in the electric fish *Eigenmannia* (Rhamphichthyidae, Gymnotoidei). *Nature* 243:301–302.
- Heiligenberg W. 1973b. Electrolocation of objects in the electric fish *Eigenmannia* (Rhamphichthyidae, Gymnotoidei). *J Comp Physiol* 87:137–164.
- Heiligenberg W, Keller CH, Metzner W, Kawasaki M. 1991. Structure and

- function of neurons in the complex of the nucleus electrosensorius of the gymnotiform fish *Eigenmannia*: detection and processing of electric signals in social communication. *J Comp Physiol [A]* 169:151–164.
- Heiligenberg W, Partridge BL. 1981. How electroreceptors encode JAR-eliciting stimulus regimes: Reading trajectories in a phase-amplitude plane. *J Comp Physiol* 142:295–308.
- Henninger J, Krahe R, Kirschbaum F, Grewe J, Benda J. 2018. Statistics of natural communication signals observed in the wild identify important yet neglected stimulus regimes in weakly electric fish. *J Neurosci* 38:5456–5465.
- Hofmann V, Sanguinetti-Scheck JI, Gómez-Sena L, Engelmann J. 2017. Sensory flow as a basis for a novel distance cue in freely behaving Electric Fish. *J Neurosci* 37:302–312.
- Hofmann V, Sanguinetti-Scheck JI, Künzel S, Geurten B, Gómez-Sena L, Engelmann J, Kunzel S, Geurten B, Gomez-Sena L, Engelmann J. 2013. Sensory flow shaped by active sensing: sensorimotor strategies in electric fish. *J Exp Biol* 216:2487–2500.
- Hollmann V, Hofmann V, Engelmann J. 2016. Somatotopic map of the active electrosensory sense in the midbrain of the mormyrid *Gnathonemus petersii*. *J Comp Neurol* 524:2479–2491.
- Hopkins CD. 2005. Passive electrolocation and the sensory guidance of oriented behavior. *Electroreception*. pp. 264–289.
- Hopkins CD. 1980. Evolution of electric communication channels of mormyrids. *Behav Ecol Sociobiol* 7:1–13.
- Hudspeth A, Logothetis NK. 2000. Sensory systems. *Curr Opin Neurobiol*. 5:631-641
- Jun JJ, Longtin A, Maler L. 2016. Active sensing associated with spatial learning reveals memory-based attention in an electric fish. *J Neurophysiol* 115:2577–2592.
- Kalmijn AJ. 1974. The detection of electric fields from inanimate and animate sources other than electric organs. *Electroreceptors and other specialized receptors in lower vertebrates*. Springer. pp. 147–200.
- Kalmijn AJ. 1971. The electric sense of sharks and rays. *J Exp Biol* 55:371 LP – 383.
- Kennedy A, Wayne G, Kaifosh P, Alviña K, Abbott LF, Sawtell NB. 2014. A temporal basis for predicting the sensory consequences of motor commands in an electric fish. *Nat Neurosci*. 17(3):416-22
- King JA. 1973. The ecology of aggressive behavior. *Annu Rev Ecol Syst*

- 4:117–138.
- Krahe R, Gabbiani F. 2004. Burst firing in sensory systems. *Nat Rev Neurosci* 5:13-23.
- Lewis JE. 2014. Active electroreception: signals, sensing, and behavior. The physiology of fishes, Fourth Edition. pp. 375–390.
- Lewis JE, Maler L. 2001. Neuronal population codes and the perception of object distance in weakly electric fish. *J Neurosci* 21:2842–2850.
- Lissmann HW. 1958. On the function and evolution of electric organs in fish. *J Exp Biol* 35:156–191.
- Lissmann HW, Machin KE. 1958. The mechanism of object location in *Gymnarchus niloticus* and similar fish. *J Exp Biol* 35:457–486.
- Lorenz K. 1963. On aggression London: Methuen.
- MacIver MA, Patankar NA, Shirgaonkar AA. 2010. Energy-information trade-offs between movement and sensing. *PLoS Comput Biol* 6:e1000769.
- Mather G. 1997. The use of image blur as a depth cue. *Perception* 26:1147–1158.
- Mather G, Smith DRR. 2002. Blur discrimination and its relation to blur-mediated depth perception. *Perception* 31:1211–1219.
- McGurk H, MacDonald J. 1976. Hearing lips and seeing voices. *Nature* 264:746.
- Meredith MA, Stein BE. 1986. Visual, auditory, and somatosensory convergence on cells in superior colliculus results in multisensory integration. *J Neurophysiol* 56:640–662.
- Migliaro A, Budelli R. 2006. Generación de la imagen eléctrica en peces eléctricos de descarga debil . Montevideo: UdelaR.
- Migliaro A, Caputi AA., Budelli R. 2005. Theoretical analysis of pre-receptor image conditioning in weakly electric fish. *PLoS Comput Biol* 1:e16.
- Moller P. 1995. Electric fishes: history and behavior. London: Chapman & Hall London.
- Naruse M, Kawasaki M. 1998. Possible involvement of the ampullary electroreceptor system in detection of frequency-modulated electrocommunication signals in *Eigenmannia*. *J Comp Physiol [A]* 183:543–552.
- Nelson ME. 2011. Electric fish. *Curr Biol* 21(14):R528-9.
- Nelson ME, Maciver MA. 1999. Prey capture in the weakly electric fish



- Apteronotus albifrons*: sensory acquisition strategies and electrosensory consequences. *J Exp Biol* 202:1195–203.
- Nelson ME, MacIver MA, Coombs S. 2002. Modeling electrosensory and mechanosensory images during the predatory behavior of weakly electric fish. *Brain Behav Evol* 59:199–210.
- Noë A. 2004. Action in perception. MIT press.
- Ol'shanskii VM, Soldatova OA, Nga NT. 2011. Episodic electric discharges in the course of social interactions: an example of Asian Clariidae catfish. *Biol Bull Rev* 1:458.
- Orlov AA, Baron VD. 2005. Responses of the electrogeneration system of *Synodontis* (Mochokidae, Siluriformes) to weak electric fields. *Doklady Biological Sciences*. pp. 284–287.
- Orlov AA, Baron VD, Olshansky VM. 1993. Electrogenative activity of *Synodontis* and its changes under action of weak electric-fields. *Doklady Akademii Nauk*. pp. 108–111.
- Padoa-Schioppa C. 2011. Neurobiology of economic choice: a good-based model. *Annu Rev Neurosci* 34:333–359.
- Pedraja F, Aguilera P, Caputi AA., Budelli R. 2014. Electric imaging through evolution, a modeling study of commonalities and differences. *PLoS Comput Biol* 10:e1003722.
- Pedraja F, Hofmann V, Lucas KM, Young C, Engelmann J, Lewis JE. 2018. Motion parallax in electric sensing. *Proc Natl Acad Sci* 115:573–577.
- Pereira AC, Aguilera P, Caputi AA. 2012. The active electrosensory range of *Gymnotus omarorum*. *J Exp Biol* 215:3266–3280.
- Perrone R, Macadar O, Silva A. 2009. Social electric signals in freely moving dyads of *Brachyhypopomus pinnicaudatus*. *J Comp Physiol A Neuroethol Sens Neural Behav Physiol* 195:501–514.
- Push S, Moller P. 1979. Spatial aspects of electrolocation in the mormyrid fish, *Gnathonemus petersii*. *J Physiol (Paris)* 75:355–7.
- Rasnow B. 1996. The effects of simple objects on the electric field of *Apteronotus Leptorhynchus*. *J Comp Physiol A* 178:397–411.
- Rose GJ, Fortune ES, Gabbiani F, Metzner W, Turner RW, Maler L, Berman NJ, Maler L, Caputi AA. 1999. Mechanisms for generating temporal filters in the electrosensory system. *J Exp Biol* 202:1281–1289.
- Sanguinetti-Scheck JI, Pedraja EF, Cilleruelo E, Migliaro A, Aguilera P, Caputi AA, Budelli R. 2011. Fish geometry and electric organ

- discharge determine functional organization of the electrosensory epithelium. *PLoS One* 6:e27470.
- Sawtell NB, Williams A. 2008. Transformations of electrosensory encoding associated with an adaptive filter. *J Neurosci* 28:1598–1612.
- Sawtell NB, Williams A, Bell CC. 2005. From sparks to spikes: information processing in the electrosensory systems of fish. *Curr Opin Neurobiol* 15:437–443.
- Sawtell NB, Williams A, Roberts PD, von der Emde G, Bell CC. 2006. Effects of sensing behavior on a latency code. *J Neurosci* 26:8221–8234.
- Scheich H, Langner G, Tidemann C, Coles RB, Guppy A. 1986. Electroreception and electrolocation in platypus. *Nature* 319:401–402.
- Schumacher S, Burt de Perera T, Thenert J, von der Emde G. 2016. Cross-modal object recognition and dynamic weighting of sensory inputs in a fish. *Proc Natl Acad Sci* 113:7638–7643.
- Schumacher S, Burt de Perera T, von der Emde G. 2017a. Electrosensory capture during multisensory discrimination of nearby objects in the weakly electric fish *Gnathonemus petersii*. *Sci Rep* 7:43665.
- Schumacher S, von der Emde G, Burt de Perera T. 2017b. Sensory influence on navigation in the weakly electric fish *Gnathonemus petersii*. *Anim Behav*.
- Schwarz S, von der Emde G, von der EG, von der Emde G. 2001. Distance discrimination during active electrolocation in the weakly electric fish *Gnathonemus petersii*. *J Comp Physiol [A]* 186:1185–1197.
- Shaffer DR, Ogden JK, Wu C. 1987. Effects of self-monitoring and prospect of future interaction on self-disclosure reciprocity during the acquaintance process. *J Pers* 55:75–96.
- Silva A, Perrone R, Macadar O. 2007. Environmental, seasonal, and social modulations of basal activity in a weakly electric fish. *Physiol Behav* 90:525–536.
- Snyder JB, Nelson ME, Burdick JW, MacIver MA. 2007. Omnidirectional Sensory and Motor Volumes in Electric Fish. *PLoS Biol* 5:e301.
- Sperry RW. 1950. Neural basis of the spontaneous optokinetic response produced by visual inversion. *J Comp Physiol Psychol* 43:482–489.
- Stamper SA, Fortune ES, Chacron MJ. 2013. Perception and coding of envelopes in weakly electric fishes. *J Exp Biol* 216:2393–2402.
- Stein BE, Stanford TR. 2008. Multisensory integration: current issues from the perspective of the single neuron. *Nat Rev Neurosci* 9:255.
- Stoddard PK. 1999. Predation enhances complexity in the evolution of

- electric fish signals. *Nature* 400:254–256.
- Straka H, Simmers J, Chagnaud BP. 2018. A new perspective on predictive motor signaling. *Curr Biol* 28:R232–R243.
- Toerring M-J, Moller P. 1984. Locomotor and electric displays associated with electrolocation during exploratory behavior in mormyrid fish. *Behav Brain Res* 12:291–306.
- Toerring MJ, Belbenoit P. 1979. Motor programmes and electroreception in mormyrid fish. *Behav Ecol Sociobiol* 4:369–379.
- von der Emde G. 2006. Non-visual environmental imaging and object detection through active electrolocation in weakly electric fish. *J Comp Physiol A* 192:601–612.
- von der Emde G. 1999. Active electrolocation of objects in weakly electric fish. *J Exp Biol.* 202:1205-15
- von der Emde G, Bleckmann H. 1997. Waveform tuning of electroreceptor cells in the weakly electric fish, *Gnathonemus petersii*. *J Comp Physiol A* 181:511–524.
- von der Emde G, Schwarz S. 2002. Imaging of objects through active electrolocation in *Gnathonemus petersii*. *J Physiol* 96:431–444.
- von der Emde G, Schwarz S, Gomez L, Budelli R, Grant K. 1998. Electric fish measure distance in the dark. *Nature* 395:890–894.
- von Holst E, Mittelstaedt H., 1950. Das reafferenzprinzip wechselwirkungen zwischen zentralnervensystem und peripherie. *Naturwissenschaften* 37:464–476.
- Walton AG, Moller P. 2010. Maze learning and recall in a weakly electric fish, *Mormyrus rume probosciostris* Boulenger (Mormyridae, Teleostei) 1. *Ethology* 116:904–919.
- Waxman SG, Pappas GD, Bennett MVL. 1972. Morphological correlates of functional differentiation of nodes of Ranvier along single fibers in the neurogenic electric organ of the knife fish *Sternarchus*. *J Cell Biol* 53:210–224.
- Wilkins LA, Hofmann MH, Wojtenek W. 2002. The electric sense of the paddlefish: a passive system for the detection and capture of zooplankton prey. *J Physiol* 96:363–377.
- Wolpert DM, Diedrichsen J, Flanagan JR. 2011. Principles of sensorimotor learning. *Nat Rev Neurosci* 12:739–751.
- Zakon H, Oestreich J, Tallarovic S, Triefenbach F. 2002. EOD modulations of brown ghost electric fish: JARs, chirps, rises, and dips. *J Physiol*

*Paris* 96:451–458.

Zubizarreta L, Stoddard PK, Silva A. 2015. Aggression levels affect social interaction in the non-breeding territorial aggression of the weakly electric fish, *Gymnotus omarorum*. *Ethology* 121:8–16.

Zupanc GKH, Bullock TH. 2005. From electrogenesis to electroreception: an overview. *Electroreception*. pp. 5–46.

# Task related sensorimotor adjustments increase the sensory range in electrolocation

## 2



A version of this chapter is under review:

**Pedraja F.**; Hofmann V.; Goulet J.; Engelmann J.; *Task related sensorimotor adjustments increase the sensory range in electrolocation*. J. Neuroscience.

*Perception and motor control traditionally are studied separately. More recently, the idea that motor activity serves as a scaffold to shape the sensory flow has been put forward. According to this view, motor-guided sensation and perception are not detached, an aspect which is of particular importance in active sensory systems. Here, we investigate how the weakly electric mormyrid fish *G. petersii* restructures sensing and motor behavior while learning a perceptual task. We find systematic adjustments of the motor behavior that correlate with increased sensory performance. Using a model to compute the electrosensory input, we find that these behavioral adaptations increase the sensory range. As our recordings of single unit activity from medullary electrosensory neurons reveal poor neuronal detection thresholds, it seems that such behavior-driven improvement of detection is highly suitable to overcome this limitation.*

*Our study shows that understanding seemingly simple behaviors requires an appreciation of the impact of motor control onto sensory flow to be able to explain how both can mediate perception.*

## **2.1 Introduction**

Exploratory behavior is a crucial substrate for learning (Loewenstein, 1994). Learning a sensory task requires an animal to find a solution that makes its behavior more robust and efficient. As the animals' movements influence the sensory input, re-organizing the motor patterns with respect to recent experiences may contribute to learning or improving a behavior. Analyzing these modifications can thus reveal how motor action contributes to learning (Wolpert and Landy, 2012; O'Hara et al., 2013) and may also

reveal decision making through action selection (Charlesworth et al., 2011; O’Hora et al., 2013; Zgonnikov et al., 2017).

While the variability of motor behavior may facilitate motor learning by widening the search space from which behaviors are instantiated (Brainard and Doupe, 2013; Wu et al., 2014), the same variability can set bounds on the task-optimization of motor control (van Beers et al., 2002). This is particularly evident in active sensory systems, where the sensory input directly depends on the motor output. Here the strong sensorimotor dependencies may be exploited by an animal to adjust motor behavior in order to not only improve the motor but also the sensing efficiency (Friston, 2010; Little and Sommer, 2013; Gordon et al., 2014).

We here investigated how sensorimotor behavior changes while *Gnathonemus petersii*, a pulse type weakly electric fish, learned a detection task. During active electro-location these fish obtain sensory information through brief discharges of a specialized electric organ in their tail. The discharge rate of this electric organ (electric organ discharge, EOD) is under top-down control and changes in a context-dependent manner (Post and von der Emde, 1999; Caputi et al., 2003). Each emitted EOD creates a 3-dimensional electric field around the fish which is perturbed by nearby objects (Lissmann and Machin, 1958). Also motion of the animal can create modulations of this electric field (e.g., tail movement (Sawtell et al., 2006)), both of which are perceived by electroreceptors in the skin of the fish. To discriminate between the predictable (*re-afferent*) and unpredictable (*ex-afferent*) components of the sensory input, weakly electric fish are known to rely on a sophisticated neuronal circuitry (Sawtell et al., 2005; Bell et al., 2008) which enables them to analyze their nearby environment.

Not all (re-afferent) sensory consequences of behavior must be unfavorable however: similar to other organisms (Poteser and Kral, 1995; Kern et al., 2001), weakly electric fish exhibit a variety of stereotyped behaviors (Toerring and Belbenoit, 1979; Toerring and Moller, 1984; Nelson and Maciver, 1999; Hofmann et al., 2014). Recent studies have revealed that behaviorally relevant sensory information can emerge from such strongly patterned sensorimotor behaviors, i.e. weakly electric fish actively exploit these sensorimotor dependencies (Hofmann et al., 2017; Pedraja et al., 2018).

The ability to actively control the timing of sensory sampling while at the same time being able to shape the properties of the sensory input through their motor behavior, makes weakly electric fish particularly suitable to study how changes in exploratory behaviors can guide sensory-driven learning efficiently.

We here focussed on a reinforced object detection task and found that performance was progressively enhanced by consistent changes of the motor patterns. These changes resulted in an increased sensory range. Our results add further support to the idea that weakly electric fish actively improve sensing capabilities by selecting purposeful components from their motor repertoire and focus their electric attention in a goal-directed manner. Such behavioral control of the sensory input might contribute to improving neuronal stimulus detection and encoding, as we found neuronal performance to be relatively poor at the level of the medulla.



## 2.2 Methods

### 2.2.1 Animals

Wild-caught *Gnathonemus petersii* were obtained from a commercial fish dealer (Aquarium Glaser, Rodgau, Germany) and housed in communal 400L aquaria. The water temperature in these aquaria and the setup was  $25 \pm 1$  °C at a conductivity of  $100 \pm 5$   $\mu\text{S cm}^{-1}$  and a 12L:12D photoperiod. Fish were fed with bloodworms. All procedures for animal maintenance and preparations comply with the current animal protection law of the Federal Republic of Germany and have been approved by the local authorities (Landesamt für Natur, Umwelt und Verbraucherschutz Nordrheinwestfalen: 87-51- 04.2010.A202).

### 2.2.2 Behavior

**Training setup.** Five fish (10 – 12 cm in length) were used and housed in separate experimental tanks and fed with bloodworms to satiation three times per week before the beginning of the experiments. The experimental tanks (120 · 50 · 50 cm) were comprised of the living area (60 · 50 · 30 cm, water level) and an experimental area (60 · 50 · 10 cm, water level) separated by a plastic gate. A plastic plate divided the proximal end (20 cm) of the experimental arena in two target compartments. Perpendicular to this plate a 1 cm wide plastic stripe marked the entry to the compartments on the floor. Crossing of this *decision line* was scored at the end of each trial. A metal cube (2 · 2 · 2 cm) served as a cue to the rewarded compartment (S+) and was placed on the floor at the decision

line, centered in front of the cued compartment. Experiments were performed in darkness ( $< 0.1$  lux measured above the water level) and videotaped from the top (60 fps; AVT Marlin F-131 & F-033) using IR-illumination (880 nm) from below. This wavelength is beyond the perceptual range of this species (Cialli et al., 1997). EODs were recorded differentially (custom-built electrode array, 0.6 – 40 kHz band pass) and stored as events (PC audio card, 12 bit, 10 kHz) alongside the video acquisition.

**Training procedure.** Animals first learned to swim through the opened gate to receive some food by swimming to the opposite end of the experimental area. Once fish did this reliably, training commenced and videos of each trial were acquired. Each trial started by opening the gate. At the end of the trial (i.e., after either the food reward was obtained or after having entered the wrong compartment), fish swam back to the living area and the gate was closed prior to the next trial. The metal cube cueing the rewarded compartment was placed to either of the two compartments in a pseudo-random fashion (Gellermann, 1933). The cube was removed from the tank and re-positioned after each trial, even when the same compartment was cued in consecutive sessions. Training was done for six days a week with one session of 20 - 30 trials per day. When fish reached 80% correct trials in six consecutive sessions, we considered learning to be completed. For data analysis, we then segregated the data of each fish into three learning stages: stage I contained the first six sessions where performance was below 60% (511 trials from 5 animals); stage II the consecutive six sessions (530 trials) where performance was  $>60\%$  and  $<80\%$

and stage III comprises the first six session after the fish exceeded 80% performance (592 trials).

**Video tracking.** Using a background subtraction approach the animals' center of mass was determined off-line (custom written Matlab routines). The posture of the animal was obtained by applying a 3<sup>rd</sup> order polynomial fit through the midline of the body. This fit was restricted in length to the size of each individual. Head and tail positions were determined based on the spindle-like shape of the fish's body with the head being closer to the body's center of mass. The position of the object was tracked similarly. From the change of the animals position between consecutive frames we determined the 2D kinematics (i.e. thrust, slip and yaw velocity) which we used for the behavioral classification (see Hofmann et al. (2014) for more information).

**Data analysis and statistical tests.** To quantify the spatial distribution of behaviors the arena was binned (1 · 1 cm bin size). Distance to the cube was measured as the Euclidean distance between the fish's head and the object. In trials where the fish choose the wrong compartment distance was calculated with respect to the virtual object position (i.e., we assume the object to be present in the compartment the fish had erroneously chosen). To illustrate the average trajectories per fish and learning stage, we obtained the mean direction in which fish passed from one spatial bin to the next and the vector strength ( $r^2 \cdot N$  with N being the number of elements in the bin and  $r^2$  Rayleigh's coefficient of angular dispersion). Based on these values the average gradient of the trajectories was visualized using the *streamline*-function in Matlab. This was used for visualization only, while

all analysis are based on single trajectories. Sampling density (SD) was calculated as the number of EODs emitted per cm traveled (EOD count  $\cdot$  cm<sup>-1</sup>). For this we used swim speed and the EOD rate per frame. To calculate attractors, spatial maps were generated from all trajectories. From each trajectory, the first coordinate received a weight of +1 and the last coordinate of -1. Weights for in between coordinates were linearly interpolated based on the travel time and distance. For each session, we superimposed all weighted trajectories, resulting in cumulative 2D maps. The attractor area was defined as the area in which all values fell below a threshold of two standard deviations from the trough value of the cumulative 2D map.

Transient increases in EOD rate (E-scans) were detected from the z-transformed first derivative of the EOD intervals. The variance and mean for the z-transform were based on pooled data of a given training session. Accelerations exceeding a z-value of 1.5 were defined as E-scans and their location was defined by the position at which the E-scan began.

For statistics we assessed the normality of the data (Shapiro-Wilk test), and homogeneity of variance were appropriate (Levene's test). The appropriate parametric or non-parametric tests were used accordingly and are indicated in the results section and captions throughout. Data used for multiple comparisons was post-hoc corrected where necessary.

**Behavioral classification.** We classified the behavior based on clustering algorithms as done previously (Braun et al., 2010; Geurten et al., 2010; Hofmann et al., 2014). Kinematics were clustered with a hierarchical approach (Ward's criterion) and their quality and stability was assessed to determine the number of clusters within the data. Next, data was clustered

(10 clusters) using k-means algorithm. The values of the resulting centroid of each cluster (thrust, slip and yaw) were used to express the kinematic properties of this specific cluster termed *prototypical movements* (PM). These PMs resemble the basic motor components of the recorded behavior on a frame-by-frame basis.

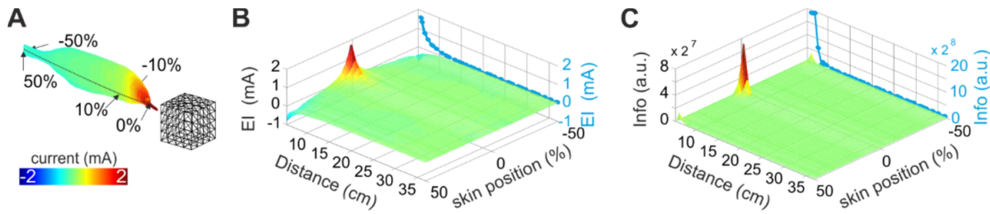
To characterize behavior on larger timescales, we calculated the transition probabilities between PMs. This was based on the transition probabilities between PMs. The probabilities were used in a hidden Markov Model to calculate the most frequent sequences of four consecutive PMs, termed *super-prototypical movements* (SPMs). The spatial distribution of SPMs was analyzed based on the x and y coordinates of the first PM in each SPM sequence. This was accumulated and fitted with a 2-D Gaussian. For visualization, the shown ellipses indicate the area for which SPM probability is above 0.1%. On average 89% of the individual data falls within this contour (range: 77-96%).

**Electric image model.** Electric images were computed with software developed by Rother (Rother, 2003) as verified and utilized in previous studies (Rother et al., 2003; Migliaro et al., 2005; Sanguinetti-Scheck et al., 2011; Hofmann et al., 2013, 2017; Pedraja et al., 2014). This model has two parts, a geometric reconstruction of the fish's body and a calculation of the transcutaneous field by solving the Poisson equation for the fish boundary using the Boundary Element Method (BEM). Briefly, this method determines the boundary electrical distributions solving a linear system of  $M \cdot N$  equations for  $M$  poles and  $N$  nodes, with the unknown variables being the trans-epithelial current density and potential at each node (Pedraja et al., 2014). The trans-epithelial current density and potential is

calculated for each node and linearly interpolated for the triangles defined by the nodes, forming the geometry of fish and objects. From this the electric images for each trajectory were calculated as the difference between amplitude of positive EOD peak in presence and absence of the object.

**Fisher information analysis.** To calculate the information about the location of the object between consecutive EODs, we used the electric image obtained along an equatorial line of the fish’s body (Figure 2.1A-B).

With this we calculated the Fisher information as  $I(\theta, x) = \left( \frac{\partial E(\theta, x)}{\partial \theta} \cdot \frac{1}{\sigma} \right)^2$ , where  $x$  is the location from the goal,  $\theta$  is the direction of motion (calculated as finite derivative between the EODs) and  $\sigma$  is the variance of the noise.



**Figure 2.1: Electric image analysis.** **A.** View of the modelled fish at the end of an approach to the cube. The stippled black line spanning the fish’s body along the midline shows the “cut” used for the electric image and Fisher information analysis. The color code represents the magnitude of the calculated current distribution over the fish’s skin. The relative skin position (0 at the front) is shown to enable a better orientation in the following panels. **B.** Temporal sequence of the electric images calculated along the fish’s midline for a complete approach sequence. The blue line represents the EI-maxima as a function of distance to the object. **C.** As in B but for the Fisher information. The blue line shows the Fisher information calculated for the whole image as a function of distance.

The Fisher information in our case can be thought of as the amount of information a measurement provides at location  $x$  for a given  $EI_n$  using the ratio of the derivative of the expected signal ( $EI_n$  and  $EI_{n+1}$ ) to the variance of the noise (furthest EIs measured) (Silverman et al., 2013; Miller et al., 2016) (Figure 2.1C).

### **2.2.3 Physiology**

**Surgery.** Electrophysiological experiments were performed in 16 *Gnathonemus petersii* (BL  $11 \pm 2$  cm). Prior to experiments fish were anesthetized in buffered 3-aminobenzoic acid ethyl ester methanesulfonate salt (MS-222  $0.1 \text{ g} \cdot \text{L}^{-1}$ , Sigma-Aldrich), immobilized with an intramuscular injection of  $20 \text{ } \mu\text{l}$  Pancuronium bromide (1:100 in Ringer, Braun-Melsungen) and transferred to a holder in the experimental tank ( $60 \cdot 40 \cdot 15$  cm). During surgical procedures, fish were respired with MS-222 solution for anesthesia ( $0.05 \text{ g} \cdot \text{L}^{-1}$ ). In addition, the surgery site was treated with a local anesthetic (Xylocaine 2%, Astra Zeneca). Afterwards the skin at the dorsal part of the cranium was removed and the head fixed to a plastic rod (Formatray, Kerr). Then craniotomy was carried out above the caudal end of the cerebellum.

After surgery fish were respired with freshwater and the tank-water was exchanged to remove any MS-222 residuals. Spinal cord activity (see below) resumed typically within 10 - 15 minutes following the end of anesthesia. In all cases, water conductivity was  $100 \pm 5 \text{ } \mu\text{S}$  and respiration rate was  $40 \text{ ml} \cdot \text{min}^{-1}$ .

**EOD playback.** Paralysis blocks the myogenic electric organ, but the descending command signal of the pacemaker nucleus persists and can be used to trigger a synthetic EOD at the time and amplitude of the natural EOD. Amplitude and timing of the EOD of each individual was measured before the surgery by sedating the fish with Etomidate (Etomidat-Lipuro,  $400 \mu\text{g} \cdot \text{L}^{-1}$ , Braun Melsungen, Melsungen) and recording the command signal and the EOD. Timing of the command signal was measured with a hook-shaped electrode around the electric organ (amplification x500, MA 103, Electronic Workshop University Cologne, band-pass filtering 1 Hz – 1 kHz). The natural EOD was measured (amplification x50, MA 103, Electronic Workshop University Cologne, band-pass filtering 10 Hz - 30 kHz) with a dipole electrode placed in the water close to the left eye and oriented perpendicular to the fish's main body axis. As a playback a pre-recorded EOD (DG1000 waveform generator, RIGOL technologies, Beijing, China; A385 Stimulus isolator, WPI, Sarasota, FL USA) was issued via two silver-wires, one of which was implanted into the EO and the other was placed caudal to the fish's tail. The playback was triggered by the command signal with the pre-determined delay and set to match the natural EOD's amplitude.

**Electrophysiological recording.** Tungsten electrodes ( $3 \pm 2.5 \text{ M}\Omega$ , Eckhorn 7 electrode Microdrive & SUA amplifier, 1000x, MTREC Thomas recording, Giessen, Germany) were inserted through the posterior part of the cerebellum towards the medial zone of the electrosensory lateral line lobe (ELL). Electrode depth and the local field potential (LPF, 10 Hz) was monitored until the plexiform layer of the ELL was reached. Then filter settings were adjusted (band pass: 100 - 3000 Hz) and electrodes were



carefully advanced to isolate single unit activity. Recordings were digitized (25 kHz sampling rate, 12 bit resolution, Spike 2 v6 & CED Micro 1401-MKII, CED, Cambridge, UK) and stored for offline analysis.

**Stimulation.** We recorded from principal cells of the medial zone of the ELL. These cells show either an excitatory response to an increase in local EOD amplitude (E-cells) or an inhibitory response (I-cells). Receptive fields are heterogeneous in size and location on the body (Metzen et al., 2008) and the center was determined with a small dipole electrode over which a local playback of the EOD was issued while moving it alongside the animal. For stimulation cubes (metal or plastic,  $2 \cdot 2 \cdot 2$  cm) were presented in the center of the receptive field. For later analysis, the object causing the strongest response was used. The object was presented for 1 minute during which typically 30 - 70 EODs were registered. The distance of the object surface relative to the skin surface was randomly varied between 1 and 35 mm using a micromanipulator and in-between each stimulus presentation we recorded 1 minute of ongoing activity without the object being present.

**Analysis.** Spikes were extracted and sorted using a wavelet separation with following PCA and cluster analysis (Spike 2, CED). Further analysis included only well isolated single units and was carried out with custom written routines in MATLAB (R2016b 64 bit, MathWorks, Natick, MA USA). ELL units fire a burst of spikes following each EOD with changes in the burst parameters encoding for electrosensory stimuli. We characterized the mean firing rate, maximum firing rate and latency of each burst. Mean firing rate was determined as the number of spikes following the EOD within a 150 ms window. Maximum firing rate was determined as the peak

of the convolved firing rate (15 ms boxcar convolution). Burst latency was determined as the latency of the 1<sup>st</sup> elicited spike relative to the EOD time. We used a receiver-operating-characteristic (ROC) analysis to quantify if and at which distance neuronal activity would enable the detection of the object. For this, we used the probability distributions of the burst parameters as determined for stimulated and ongoing activity to calculate the probability of true positive and false positive hits. The area under the ROC-curve (AUC) was used as a sensitivity measure at a given distance of the cube. This measure was plotted as a function of distance and fitted (sigmoidal function). The detection limit was determined as the point where the fit fell below a sensitivity of 0.7. The population average was assessed through calculating a sliding bin (bin width 2 cm) of the raw sensitivity data.

## **2.3 Results**

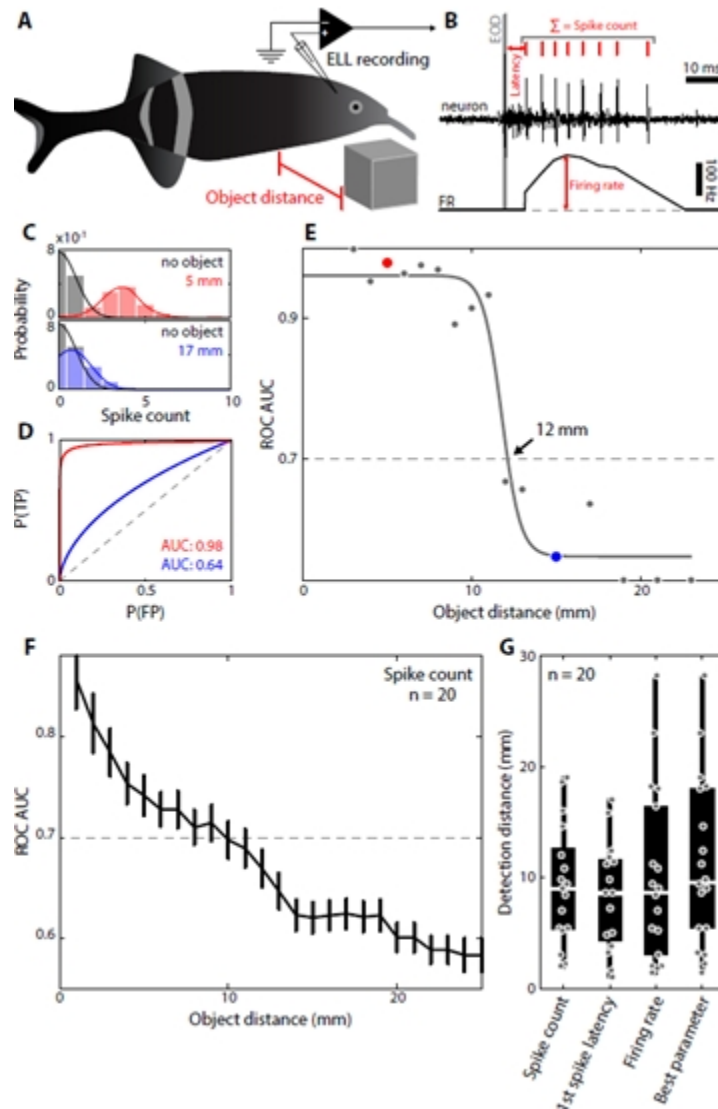
In the current study, we investigated the object detection performance of the weakly electric fish *Gnathonemus petersii*. First, we will present results from single unit recordings of medullary electrosensory principal neurons. Based on these recordings, we establish the distances at which physical objects were detected neuronally. We then contrast the neuronal results with the behavioral performance levels, emphasising the often-underestimated contribution of sensorimotor interactions for perception.

### **2.3.1 Detection limits based on neuronal recordings in ELL**

The electrosensory lateral line lobe (ELL) is the 1<sup>st</sup> central nucleus of the ascending electrosensory pathway and receives converging input from electroreceptor afferents (Bell et al., 1989, 2005; Hollmann et al., 2016).

Afferent responses are directly related to the local amplitude modulation of the EOD, however even large conductive objects modulate afferent activity only within a range of about 10 mm (Szabo and Hagiwara, 1967; Gomez et al., 2004). It is known that ELL principal cells can have large and complex receptive fields (Metzen et al., 2018), their detection threshold for physical object distance however, has not been established.

We recorded the responses of 20 isolated ELL principal cells in immobilized animals ( $n = 16$ ) to objects (metal & plastic cube, edge length 2 cm) presented within the receptive fields center (RF) at varying distances up to 40 mm from the skin of the fish (Figure 2.2A). ELL principal cells typically issued a short burst of spikes following each EOD (Figure 2.2B). We characterized these burst in terms of their latency, their maximum firing rate and the mean firing rate (see also methods), which are the parameters that typically change in response to a presented stimulus. To evaluate object detection, we analyzed responses using a receiver operating characteristic (ROC). For this, response distributions were obtained over several instances of EOD emission and compared to ongoing activity (Figure 2.2C; top: object at 5 mm (red) vs. ongoing activity (black), bottom: object at 17 mm (blue) vs. ongoing activity (black)). ROC sensitivity, quantified by the area under the ROC curve (Figure 2.2D), decreased in a sigmoidal fashion (Figure 2.2E, solid line).



**Figure 2.1:** (*Cont. next page*). **Object detection capabilities of hindbrain neurons.** **A.** The activity of ELL principal neurons ( $n = 20$ ) was recorded in immobilized *Gnathonemus petersii*. Ongoing activity was recorded prior to each stimulus presentation (metal or plastic cube, 2 cm side length). **B.** Neuronal activity (middle, black) typically consists of a burst of action potentials following the EODs (gray vertical line). For each burst we measured the number of spikes within 150 ms after each EOD (top red), the latency of the 1st spike (red arrow) and the peak of the convolved firing rate (bottom, black trace & red arrow). **C.** Probability distributions (solid lines) for the measured parameters (here spike count) of the responses of an example E-unit stimulated with a metal object at 17 mm (blue) and 5 mm (red) as well as ongoing activity (black). **D.** Receiver operating characteristics (ROC, see Methods) obtained for the data shown in C. For each stimulation distance the probability of true positive ( $P(TP)$ ) was calculated as a function of the probability of false

positive (P(FP)) classification. The area under the curve (AUC) was assessed. **E.** Area under the ROC curve as a function of distance of the object for an exemplary E-unit. The detection distance of all units was determined as the point where a sigmoidal fit to the data exceeded an AUC of 0.7. For the shown example detection distance is 12 mm. Red and blue dots correspond to the data shown in C and D. **F.** Average ROC data for 20 single units based on spike count probability. **G.** Distribution of the best detection distances of all units. While some neurons had detection distances up to 28 mm, the average detection threshold was below 10 mm for all parameters. Gray dots show the detection distances of individual neurons.

Detection distance was defined as the point where the sigmoidal fit fell below 0.7 (Figure 2.2E, see arrow). On average, this distance was within the range of 10 mm (Figure 2.2F, population average  $n = 20$  neurons analyzed with spike counts), irrespective of the parameter used to analyse responses (Figure 2.2G; mean  $\pm$  std: spike count:  $9.3 \pm 5.4$  mm; latency:  $8.3 \pm 4.8$  mm; firing rate:  $10.0 \pm 7.9$  mm). Threshold in these groups (different parameters analyzed) were not significantly different (Kruskal Wallis,  $p = 0.90$ ). Also the detection distance did not increase significantly when the best parameter per cell were pooled (Kruskal Wallis,  $p = 0.76$ ). While the responses of some individual neurons allowed for object detection up to a distance of 28 mm, the average detection threshold across the recorded population was poor and roughly within a range of 10 mm.

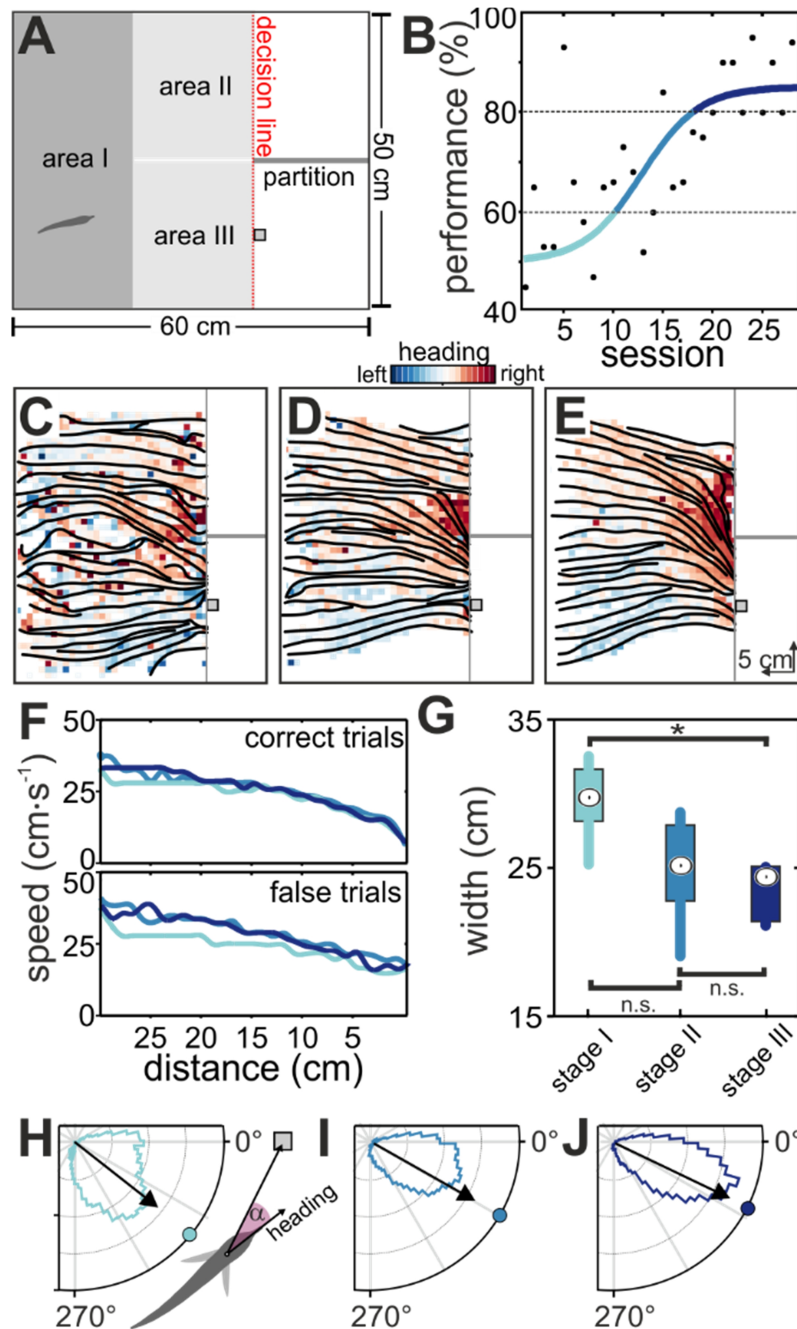
The physiological detection limits determined here were well below the behavioral detection range of *G. petersii*. Depending on the methodology, it falls between  $\frac{1}{4}$  to  $\frac{1}{2}$  body length (Push and Moller, 1979; Toerring and Belbenoit, 1979; Hofmann et al., 2017).

### **2.3.2 Task learning is paralleled by sensorimotor alterations**

We trained five fish to detect a metal cube of the same size as used in physiology (Figure 3A and methods). All fish reached a stable performance

within  $22.8 \pm 3.8$  sessions (Figure 2.3B and Figure S2.1). Based on performance the data was split for further analyses (Figure 2.3B, stage I < 60% (light cyan), stage II 60 - 80 % (dark cyan), stage III > 80% (violet)). Figure 2.3C depicts the average movements (black lines) of one fish during the three different stages. The mean heading direction within each spatial bin ( $1 \text{ cm}^2$ ) is shown as a color code (left to right as blue to red) indicating that trajectories in phase I (Figure 2.3C) were mainly straight, corresponding to the chance-level performance in this stage (Figure 2.3B, light cyan). With learning, trajectories became more directed towards the object, with a characteristic increase of right-turns (red) in area II (Figure 2.3D-E). While traversing the arena, fish gradually decreased their speed (Figure 2.3F) with swim speeds being slightly higher close to the target in incorrect trials (Figure 2.3F). In addition, the dispersion of the trajectories (distribution along the shorter axis of the arena) decreased with learning, showing that fish preferentially swam along the middle of the arena in later learning stages (Figure 2.3G). This led to a better alignment of the fish's heading with the object (Figure 2.3H-J, mean direction:  $321^\circ$ ,  $330^\circ$  and  $333^\circ$  for stage I-III; William-Watson test for difference in orientation,  $p < 0.001$ ; mean vector strength: 0.72, 0.79 and 0.86 for stages I-III, respectively). Note that fish were rewarded at the end of the arena, i.e., only after having passed the object. As such they were not forced to target the object.

These results, centered on the general motor behaviour, already show that improved performance went along with adjustments of the motor behavior.



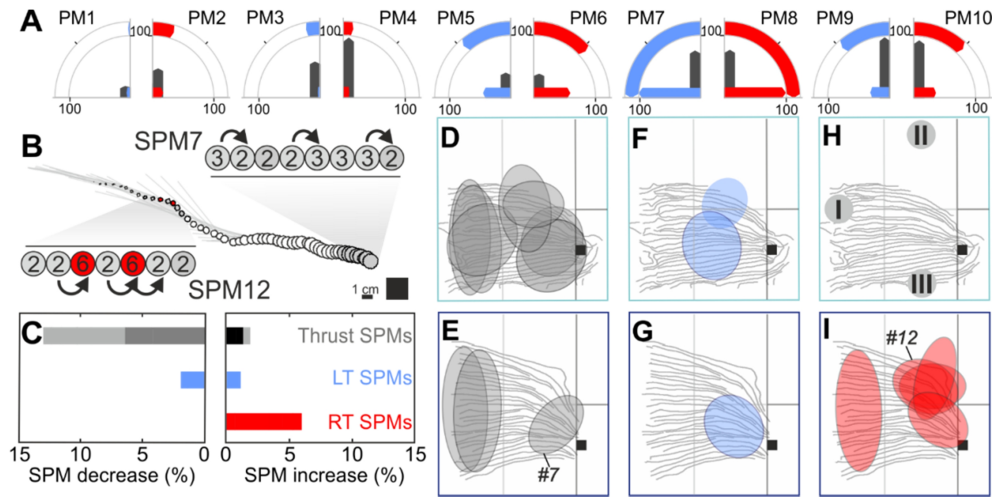
**Figure 2.3:** (*Cont. next page*). **Performance and motor behavior change with learning.** **A.** Top-view on the experimental arena. Upon lowering the gate that separated area I from the living compartment (to the left, not shown in figure), fish entered the arena at any position. The task was to swim into the compartment marked with the metal cube (gray square). When passing the decision line, the session was scored and a food-reward was given at the end of the compartment in correct trials. The behavior was filmed under IR-illumination

(880 nm). Here and in all following figures, the data is presented with the target (square) on the right side of the arena (from the view of the fish entering). During experiments, the position was altered pseudo-randomly. The arena was partitioned in the three areas (I-III) for the later data analysis. **B.** Psychometric functions fitted to the performance of one exemplary fish. The data was separated by performance based on these fits (learning stage I: < 60% of correct decision, light cyan; II: > 60 to 80%, dark cyan; III: > 80%, violet). **C-E.** Top view on the average movements (black lines) during the three stages for the same fish as shown in panel B. The color code indicates mean heading direction (see sketch in H). **F.** Median swim speed ( $N = 5$  fish) with respect to the distance to the object in correct trials (top;  $n = 1119$ ) and incorrect trials (bottom;  $n = 514$ ). **G.** Box-plots showing the width of the distribution of the fish along the width of the arena (in total 50 cm) for all trials ( $n = 1633$  trials,  $N = 5$ ). Width was quantified as the range including 90 and 10 percentile of the data of each individual fish. This measure shows that with learning fish transitioned from exploring the whole width of arena to a more refined use of the arena that brought them more towards the middle of the arena (Kruskal-Wallis test with Bonferroni post hoc; test stage I vs. III:  $p = 0.03$ ). **H-J.** With learning fish aligned better with the object, as shown here by the mean alignment vector (black arrows, see  $\alpha$  in sketch). Colored lines are circular histograms of the raw data in the three stages. With learning the mean alignment was closer to  $0^\circ$  (towards the object).

### **2.3.3 Motor behavior changes through differential recruitment of basic kinematic components**

We next decomposed the kinematic data into ten prototypical movements (Geurten et al., 2010; Hofmann et al., 2014) (Fig 4A). These were either thrust-dominated (PMs 1-4), or could be grouped into right-turn (PMs 6, 8, 10) and left-turn dominated PMs (PMs 5, 7, 9). Notably, learning did not result in the formation of new PMs, and only weak changes of the PM frequencies. From the transition probabilities between PMs, we obtained behavioral sequences of PMs, also referred to as super-prototypical movements (SPM).





**Figure 2.4: The spatial recruitment of motor patterns (SPMs) shows pronounced changes in the different learning stages.** **A.** Composition of the 10 kinematic clusters and their relative frequency for the three learning stages. In each panel the relative centroid values of thrust slip and yaw are shown. Blue bars indicate slip and yaw components directed to the left, while red bars show the corresponding values for movements to the right. PMs 1-4 are thrust-dominated, while PMs 5-10 are turn-dominated. **B.** Exemplary trajectory showing the fish's head position by the circles and the orientation of its body by the grey lines, while time since the start of the trial is indicated by the size of the circles. Using the transition probabilities between PMs chains of consecutive motor behaviours are extracted (superprototypical movements, SPM). For two examples (SPM 7 and 12) the series of numbered circles shows the sequence of PMs that make up these SPMs in the trajectory depicted. **C.** Relative change of occurrence for the SPMs that showed the strongest difference in recruitment between learning stage I (left) and III (right) for correct trials. Note that low to medium thrust SPMs (light and darker gray) decreased, while high thrust SPMs (black) increased. Right turn (RT) dominated SPMs (red) were more frequent in stage III, while left turn (LT) dominated SPMs (blue) were less altered. **D-I.** Spatial distribution of the SPMs shown in C for learning stages I (top row, D, F and H) and III (bottom row, E, G and I). The colored ellipses are based on 2D-Gaussian fits to the spatial distribution of SPM with colors separating thrust (grey), right turn (red) and left turn (blue) dominated SPMs. The numbers in E and I refer to the two SPMs detailed in B.

Those SPMs with the highest frequency were further analyzed (Figure 2.4B and Figure S2.2 for details of the SPM composition). Contrary to PMs, the frequency of these SPMs changed with learning. While less thrust dominated SPMs occurred after learning than at the beginning (Figure

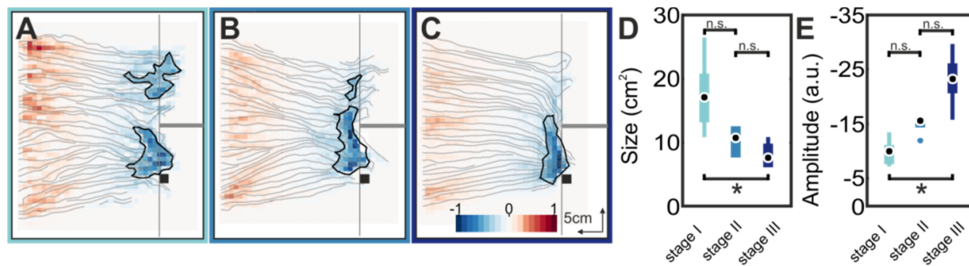
2.4C, shades of black), left turn dominated SPM frequencies were barely affected (Figure 2.4C, blue) and the occurrence of right-turn dominated SPMs increased (Figure 2.4C, red). These changes were spatially specific: Thrust dominated SPMs initially occurred throughout the arena (Figure 2.4D) whereas after learning they were confined to area I (high thrust speed; Figure 2.4E) and area III. The SPM in area III (SPM#7) had low thrust velocity and altered between left and right rotatory velocities (i.e. a kind of “zig-zagging” behavior, see Figure 2.4B). Left turn dominated SPMs were found close to the target both before and after learning (Figure 2.4F vs. G). The most prominent change is the emergence of right turn dominated SPMs after learning (Figure 2.4H vs. I). These SPMs were mainly found in area II and represent corrective movements that adjust the fish’s heading towards the object. Notably these SPMs occurred at distances where the fish should be able to detect the absence of the cube (Toerring and Belbenoit, 1979; von der Emde, 2010).

In summary the changes of the motor behavior with learning (Figure 2.3) are reflected in the temporal and spatial display of certain kinematic patterns (Figure 2.4).

#### **2.3.4 Altered behavior is reflected by the formation of an attractor**

Altered trajectories may represent overt actions reflecting the internal motor decision-making process necessary to improve the performance with learning. In this context trajectories leading to behavioral choices have been used to map how motor behavior may represent the formation of internal states like goals (O’Hora et al., 2013; Zgonnikov et al., 2017). Applying this approach to our data (see all fish in Figure S2.3) we found that two

attractors ("sink") are present at the start of learning, one on each of the target compartments entrance (Figure 2.5A). With learning, a single attractor emerged at the entry of the reinforced (S+) compartment (Figure 2.5B & C).

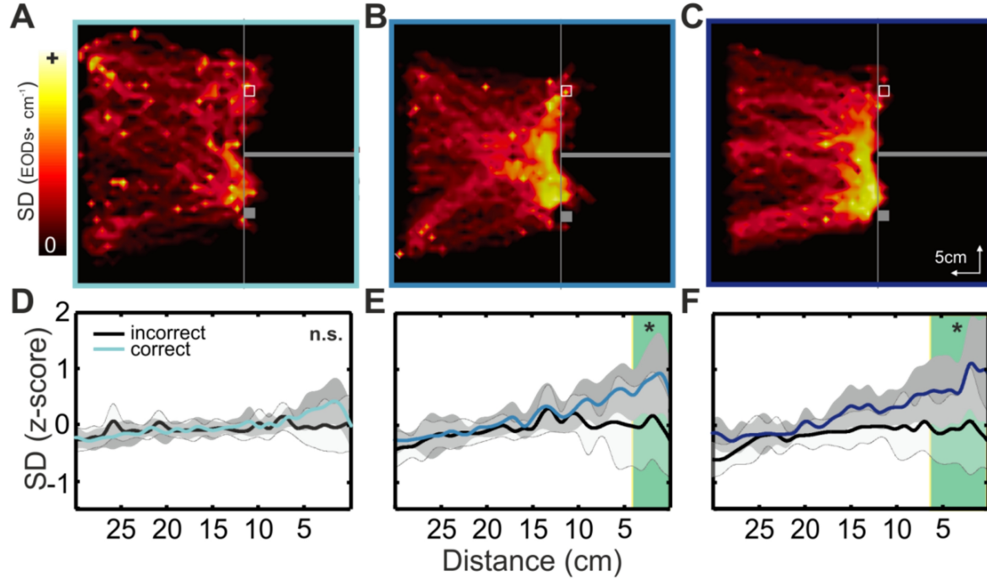


**Figure 2.5: Development of attractor states with learning.** **A.** Attractor landscape diagram from trajectories of one exemplary fish during learning stage I. Color code depicts the attractor values, light solid lines depict trajectories and black solid lines depict the area of the attractor. Initially two attractors of similar size were present. **B.** Same as A, but for learning stage II. The size of the two attractors changed, while the one in front of the reinforced compartment increased in size, the other one decreased. **C.** Same as A and B but for learning stage III. The attractor at the reinforced compartment became more distinct while the one on the other compartment has disappeared. **D.** Attractor size (see methods) for all fish and the three learning stages. Attractor size significantly decreased from stage I to stage III. (Mann-Whitney pairwise test with Bonferroni post hoc test: stages I-II  $p = 0.13$ , stages I-III  $p = 0.04$  and stages II-III  $p = 0.49$ ). **E.** Attractor peak amplitude. Peak amplitude increased significantly from stage I to stage III (Mann-Whitney pairwise test with Bonferroni post hoc test: stages I-II  $p = 0.13$ , stages I-II  $p = 0.06$ , stages I-III  $p = 0.03$  and stages II-III  $p = 0.1$ ). In all panels, asterisks indicate statistical significance ( $p < 0.05$ ).

This attractor became more distinct with learning, i.e. its size decreased (Mann-Whitney pairwise test with Bonferroni post hoc test: stages I - II  $p = 0.13$ , stages I - III  $p = 0.04$  and stages II - III  $p = 0.49$ ; Figure 2.5D) and its peak amplitude increased (Mann-Whitney pairwise test with Bonferroni post hoc test: stages I - II  $p = 0.06$ , stages I - III  $p = 0.03$  and stages II-III  $p = 0.11$ ; absolute values; Figure 2.5E). Overall, these results show that the fish learned to focus their behavioral attention from an initially bimodal to a unimodal attractor.

### **2.3.5 Electromotor behavior adapts alongside kinematics**

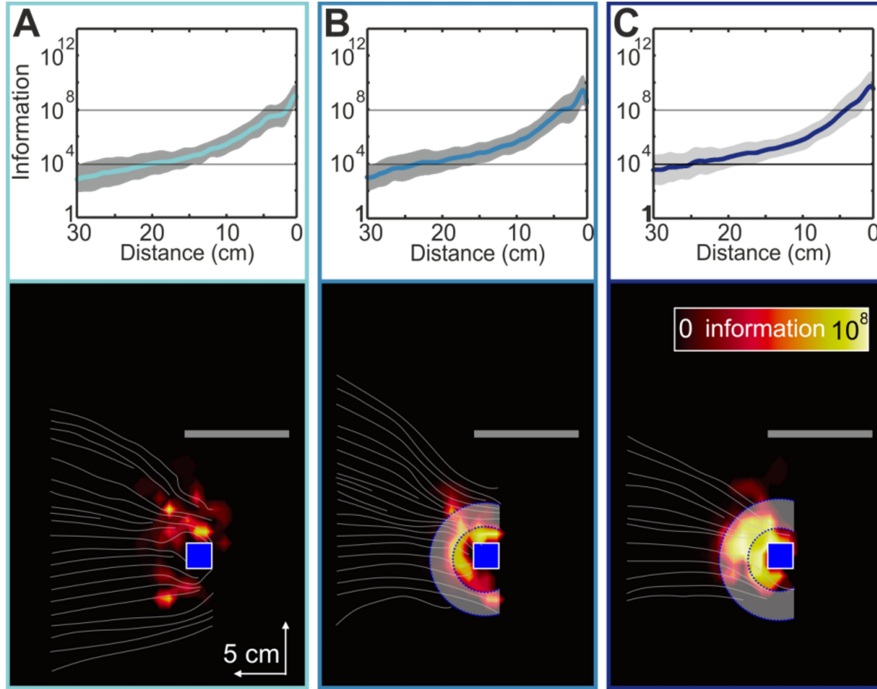
The emergence of a single attractor indicates that the animals learned to attend to and use the object cue in their motor planning. To understand if and how this affected the sensory sampling behavior, we calculated the sampling density (SD, number of EODs emitted per distance traveled,  $\text{EOD} \cdot \text{cm}^{-1}$ ). SD increased towards the object, with the peak getting more prominent during later learning stages (Figure 2.5A–C, data for an exemplary fish; Figure S2.4 for all fish). During stage I, SD was similar between correct and incorrect trials as a function of distance to the object (Figure 2.6D cyan vs. black line). In the later stages however, SD was significantly increased for correct versus incorrect trials close to the object (Figure 2.6E dark cyan vs. black; Wilcoxon-signed-rank test  $p \leq 0.0495$  for stage II; Figure 2.6F violet vs. black,  $p \leq 0.02$  for stage III). The distance to the cube over which the SD was significantly higher in correct vs. incorrect trials (green shading & asterisk in Figure 2.6E & F) increased from stage II (4 cm) to stage III (6 cm). The EOD rate (mean  $\pm$  std:  $35.8 \pm 2.9 \text{ EODs} \cdot \text{s}^{-1}$ ) remained unchanged with distance to the object and learning (Figure S2.5). Thus, the changes of the sampling density mainly reflect a reduction in swim velocity between correct and incorrect trials. This pattern lead to a selective increase of the sensory update rate around the cue marking the rewarded compartment. This confirms that the region of the attractor (determined above based on motor behavior only), also recruited the highest information seeking electromotor behavior.



**Figure 2.6: Change of the sampling density with learning.** A-C. Distribution of the normalized sampling density (SD) for the three stages of learning (data from 1 fish). Arena is shown like in Figure 2.3A, open square shows position of absent cube (S- compartment). D-F. SD (z-scored) as a function of distance to the object (correct trials,  $n = 1119$ ; colored lines and shaded area depict median and MAD) and the virtual object (incorrect trials,  $n = 514$ ; black lines and light gray outlines show median and MAD). The distances over which SD was significantly increased in correct vs. incorrect trials are indicated by green shaded areas (Wilcoxon-signed-rank test  $p = 2e^{-4} - 0.0495$  and  $7e^{-7} - 0.02$  for stages II and III respectively).

### 2.3.6 Sensory consequences of behavioral adaptations

To understand how the spatial changes in SD translate to sensory information, we used a biophysical model to calculate the electric images (EI, the afferent sensory input) (Pedraja et al., 2016; Hofmann et al., 2017). From these, we calculated the Fisher information (FI) between successive electric images of any given trajectory (see methods and Figure 2.1). FI can be regarded as a linear decoder of the information that a given EI provides at location  $x$  about the position of the cube. As expected, FI increased with proximity to the cube (Figure 2.7A–C, top graphs).



**Figure 2.7: Fisher information increases with object proximity and learning. A-C.** *Top:* Fisher information as a function of distance to the cube for the three learning stages (left to right). Colored lines show median, shaded areas MAD. Note the log-scale of the y-axis. *Bottom:* spatial representation of the same data. Color code depicts values of FI, light gray lines show average trajectories superimposed. White semicircles depict the range over which FI was significantly higher in successive learning stages (Kruskal-Wallis test with Bonferroni post hoc test:  $p < 0.05$ ). This data confirms that the behavioral adaptations that were observed during learning in fact impact the available information to the fish.

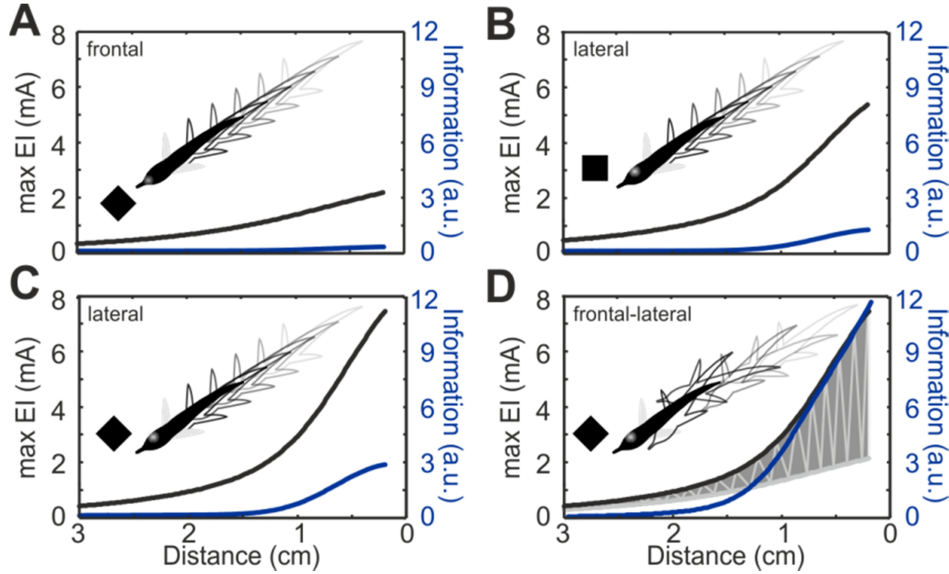
Interestingly the increase was significantly stronger in later learning stages (median FI: stage I:  $1.90 \cdot 10^4$ , stage II:  $1.64 \cdot 10^5$  and stage III:  $3.32 \cdot 10^5$ ; Kruskal-Wallis test with Bonferroni post hoc test,  $p < 0.001$  for all comparisons). The distance over which FI was significantly increased between learning stages also progressively increased (Figure 7A – C, white arc indicates significant areas; stage I vs. II: 5 cm; stage I vs. III: 6 cm; Kruskal-Wallis test with Bonferroni post hoc test, p values between  $1 \cdot 10^{-5}$

<sup>4</sup> - 0.049). These results were similar to what we found for SD (Figure 2.6D – F) and confirmed our hypothesis that the sensory information is enhanced by the sensorimotor adjustments.

To further understand the means by which behavioral adjustments can increase sensory information we turned to a simple theoretical abstraction. Figure 8 shows the amplitude of the electric images of a fish approaching a metal cube for different scenarios: Once for the fish approaching the cube frontally with the EI being focussed on the head (Figure 2.8A), once for an angled approach to the edge of the cube that places the EI more laterally (Figure 2.8B) and once for a straight approach to the side of the cube that again places the EI laterally (Figure 2.8C). The increase in electric image amplitude is higher in the later cases (black lines). This translates into higher FI (blue lines) between successive sampling events (assuming a constant SD). The EI gradient is less steep when an object is frontally approached (see Figure 2.8 and Fig. 4 in Hofmann et al. 2017). Thus, by moving the electric image over the head region between EODs, fish could potentially exploit the heterogeneity of the electric field geometry and pre-receptor mechanisms, to increase the gradient and thereby the sensory information. To explore this we modeled EIs and calculated FI for a virtual scanning behavior, in which the EI is moved repetitively from the frontal to the lateral side of the body side (Figure 2.8D).

This behaviour results in a strongly increased FI. This further demonstrates that the recruitment of SPM #7 (Figure 2.4C), characterized by a slow approach to the cube with consecutive small left and right turns that will shift the EI in a manner comparable to the virtual approach analyzed here, can be crucial for the performance improvement observed.

As already mentioned, this SPM is increasingly recruited close to the object with learning.

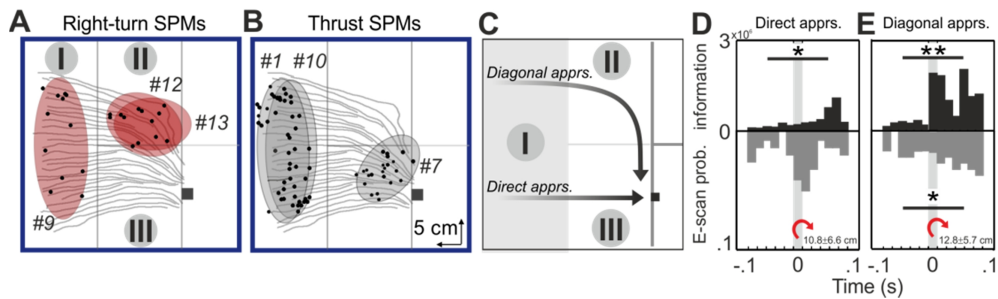


**Figure 2.8: Changes in electric image positioning and motor behaviour modify Fisher information.** **A-C.** Relation of the electric image amplitude and the Fisher information modelled for different approaches of a fish to a metal cube; **A.** straight approach; **B.** approach to the side of the cube and **C.** Off cube rotation. For the same distance to the cube, the amplitude and gradient between successive distances is higher for the more lateral position, translating into a higher Fisher information rate. Amplitude further depends on the orientation between the cube and the sensory surface, being highest when both are parallel to each other (B vs. C). **D.** The electric image amplitude of the lateral (black line) and frontal position (light grey line) are superimposed. The lines alternating between both represent a hypothetical motor pattern in which a fish gradually reduces the distance to the cube and moves to alternate the electric image between both positions. This virtual zig-zagging induces an additional gradient between electric images and thus leads to higher Fisher information rates. Note that fisher information is given in arbitrary units as the calculation is based on modelled data for which sigma (the noise level) cannot be used.

We further wanted to know if particular behavioral patterns displayed throughout the trajectories could serve as specific actions that increase sensory information. For this, we calculated the electromotor behavior and



the sensory information (FI) surrounding the occurrence of a specific SPM. We found that the SPMs characteristic for the late learning stage and occurred close to the compartments II and III were associated with transient rises of EOD frequency (Figure 2.9A, SPMs #12 & #13, occurrence: 20%, 14%; Figure 2.9B, SPM #7, occurrence 25%).



**Figure 2.9: Target-directed turns increased sensory information and result in transient increases of sampling rates.** **A-B.** Spatial distributions of the SPMs (see methods) with the strongest change between learning stages I and III that also showed an elevated E-scan probability (range: 14 - 30%, 25% for #7). **A:** Right-turn dominated SPMs (red), **B:** thrust dominated SPMs (gray). In both plots dots indicate positions of E-scans. Light gray lines are average trajectories. **C.** Schematic of the experimental arena with the sketched trajectories (arrows) indicating the two forms of object-approaches (direct vs. diagonal). **D.** Fisher information (top) and E-scan probability (bottom) triggered on right-turns (PM based, PM occurrence at time 0) during direct approaches (see C). FI was significantly increased after the right turn (positive time values, Kruskal-Wallis test with Bonferroni post hoc test; direct  $p = 0.02$ ). **E.** Same as E but for diagonal trajectories (see C). FI and E-scan probability was significantly increased after the right turn (Kruskal-Wallis test with Bonferroni post hoc test; FI:  $p = 0.005$ ; E-scan probability:  $p = 0.02$ ). In both panels, light gray numbers indicate the distance at which turns were observed on average (mean  $\pm$  SD).

These electromotor displays, known as novelty responses (Post and von der Emde, 1999) or E-scans (Jun et al., 2016), occur when the electrosensory input deviates from the recent baseline (Caputi et al., 2003) and also have been considered overt displays of sensory expectations

(Moller, 1995). We investigated whether these kinematic patterns had an impact on the FI and found that right turns caused transient peaks in the FI. Such right turns occur predominantly in area II and orient the fish towards the correct compartment (Figure 2.9A, SPMs #12 and #13). Indeed, during both direct and diagonal approaches (Figure 2.9C), right turns resulted in a significant increase of the Fisher information (Figure 2.9D & E, top; Kruskal-Wallis test with Bonferroni post hoc test; direct:  $p = 0.02$ ; diagonal:  $p = 0.005$ ). During diagonal approaches this behavioral pattern also coincided with a significantly increased probability of E-scans after the turn (Figure 2.9E, bottom; Kruskal-Wallis test with Bonferroni post hoc test:  $p = 0.02$ ).

## **2.4 Discussion**

To which degree sensing depends on the mutual interactions of sensory and motor processes is a fundamental question (Gordon et al., 2011). Examples for the contribution of motor behavior include situations where movements stabilize sensory input, or directly enhance or generate sensory information. In either case, movement is an integral part of sensing. Motor behaviors may thus be regarded as a way in which animals can probe internal models of their environment in light of current sensory input (Der and Martius, 2015). This is particularly evident in active sensory systems, where motor control and planning are directly connected (Ahissar and Assa, 2016).

We found the electrosensory range of ELL units to be similar to those reported for the electroreceptor afferents (Szabo and Hagiwara, 1967;

Gomez et al., 2004) and thus lower than the behavioral detection limits. However, we probably underestimated the sensitivity of ELL units, as it likely depends on feedback (Chacron, 2005; Sawtell and Bell, 2008; Clarke and Maler, 2017; Enikolopov et al., 2018; Metzen et al., 2018) as well as feedforward mechanism in natural behaviour. It was also shown that changes in the EOD rate influences the sensitivity of afferents (Grant et al., 1998; Sawtell et al., 2006), however in our experiments EOD rate was regularized due to immobilization of the animal. Furthermore, population activity is a better determinant of perception and behavior than the activity of single neurons (Pitkow and Angelaki, 2017; Runyan et al., 2017; Ni et al., 2018) and decoding ELL population activity with more naturalistic decoders is likely to be influenced by neural correlations (Hofmann and Chacron, 2018). It is also possible that stimulus detection is encoded in a parallel pathway (McGillivray et al., 2012; Huang and Chacron, 2016), where the selective decoding of information of ELL efferents with high detection ranges could improve the perceptual range. While selective decoding would likely happen at the level of the midbrain, there is no indication for a functional clustering of ELL efferents at the level of the torus to date (Bell and Szabo, 1986; Hollmann et al., 2016). Future studies will need to assess both, ELL population activity as well as the connectivity and the decoding in upstream areas.

Despite these possible mechanisms to improve the neuronal detection range under natural conditions, our results posit that systematic and task related behavioural adjustments may also improve the physiological detection thresholds. In line with this, we demonstrate that the adaption of sensorimotor behavior substantially enhances the obtained information. Indeed, using the EI amplitudes at the detection limit, we would predict

that the physiological range is increased 2fold between naïve and experienced animals.

In our experiments fish learned to find and swim to the compartment marked by a metal cube. Apart from slight variations in the time fish took to acquire this task, they all learned to solve it and further did so using very similar sensorimotor patterns. This involved a refined use of the arena, emergence of targeted turn patterns and an increase of the sampling density in vicinity to the object. This is comparable to the kinematic data published for this species (Hofmann et al., 2017) for spontaneous approaches towards novel objects where alterations of the sensorimotor behavior were found to contribute to the shaping of the sensory input, leading to the emergence of depth information. Notably, in the present study, changes of the motor patterns occurred both within and outside of the detection range of the electric system, suggesting that they are driven by sensory information (i.e. reactive control) as well as internalized predictions. Together this resulted in changes of the animals' spatial attention with learning.

Wave-type weakly electric fish position themselves with a preferred distance to transversely moving objects, where the slope of the signal is highest, corresponding to the Fisher-optimal distance (Clarke et al., 2015). Similarly, echolocating bats track targets by aiming their acoustic beam to hit the target *off center*, i.e., where the slope in the acoustic beam amplitude is the highest (Yovel et al., 2010). In addition, unconditioned approaches to objects of *G. petersii* were shown to be oriented along the field gradient in a manner that may enable fish to determine the distance to their target (Hofmann et al., 2017). These examples show that in active

sensing animals, the most informative aspects of the sensory input often are linked to the highest gradient in the carrier signal.

We found that the behavior that fish used to approach the object after they had learned the task resulted in an increased distance over which FI was increased. One option to achieve this consists in positioning the electric images on the head, which has the highest receptor density (von der Emde and Schwarz, 2002; Caputi and Budelli, 2006). Such a strategy should be particularly helpful to optimize neuronal representation and resolution of the electric images and thus may be favored to discriminate finer sensory parameters. The second strategy is bringing the electric image onto the part of the sensory surface where it causes the strongest change in EI amplitude, thus increasing the gradient in the temporal afferent signal (Figure 2.8A-C) (Babineau, 2006). We here offer a third option in which fish actively move the sensory input over their foveal head region, a strategy that will significantly increase information about a target (Figure 2.8D). Fish did focus the input to the head, but not to the front. They further recruited a motor prototype consisting of a slow zig-zagging towards the object. This indicates that this third option may indeed be used to enhance sensory input. Future studies, using refined videography, should thus address if the positioning of the electric images on the foveal head region is different in tasks that demand the fish to detect an object versus one where object features need to be discriminated. Likewise, electrophysiological studies on freely behaving fish are required to directly address the predicted improvement of the neuronal detection limits through specific learned motor behaviors.

The ability to actively regulate the sensory input is emerging as a general research question. A particularly striking example for this comes from a wave-type weakly electric Gymnotiformes fish, that engages in energetically inefficient foraging in order to enlarge the electrosensory range (Snyder et al., 2007; MacIver et al., 2010; Biswas et al., 2018). An alternative strategy, increase of the signal's amplitude, seems to be common in echolocating toothed whales and bats (Madsen and Surlykke, 2013). Contrary to these species, weakly electric fish, likely due to the energetic costs of maintaining the EOD (Markham et al., 2016) and the spherical dissipation of the energy (Nelson and Maciver, 1999), appear to have favoured motor adjustments as a means to increase the sensory range.

A second modification that paralleled learning were turns when fish approached the wrong compartment. These predominantly occurred outside of the neuronal detection range of the object and were followed by elevated E-scans rates. Similar to head scans of rodents (Monaco et al., 2014), transient rises of the sampling frequency have been considered to serve special functions in the formation of spatial memories (Jun et al., 2016) and have further been implicated as overt displays of sensory expectations (Moller, 1995). Indeed, startle responses of the EOD were amongst the first evidence for the hypothesis (Heiligenberg, 1980, 1988) that weakly electric fish can compare current afferent input against an internal reference or memory of the past afference (Hall et al., 1995). One explanation of the turn-associated E-scans is that the animals seek to maintain the sensory change between successive sampling events within a preferred range. The transient increase of the EOD rate may thus serve to compensate the steep change of the sensory input that follows the turns. Further studies that allow clamping the level of sensory change in freely behaving fish are

required to investigate this hypothesis. Evidence for an active balancing of the level of sensory input has recently been shown for a different sensorimotor behavior in a wave-type weakly electric fish (Biswas et al., 2018). The finding that the motor behaviours likely relevant in regulating the sensory flow are fairly stereotyped, will also enable direct studies of their role in neuronal processing, as these motor behaviors easily can be quantified in the ongoing behavior and thus allow to directly connect them with neuronal data (Kern et al., 2001).

Active sensing in its most common form involves the generation of movements. Whether and how these are controlled with respect to their sensory corollaries is mostly unknown. Our results show that motor control can be an active component of sensory learning. Similar effects are to be expected in other sensory systems, particularly near-range and active sensory systems. A better understanding of the strategies guiding sensory learning thus will likely lead to a better understanding of sensorimotor integration, variation of behavior in natural contexts and learning in general. Active shaping of the sensory flow in general, may further be of interest in technical systems, where acoustic beam forming or field shaping can be used to acquire different information using different sensorimotor configurations when required.

## **2.5 Bibliography**

- Ahissar E, Assa E. 2016. Perception as a closed-loop convergence process. *Elife* 5:1–26.
- Babineau D. 2006. Modeling the electric field of weakly electric fish. *J Exp Biol* 209:3636–3651.
- Bell CC, Han V, Sawtell NB. 2008. Cerebellum-like structures and their implications for cerebellar function. *Annu Rev Neurosci* 31:1–24.

- Bell CC, Meek J, Yang JY. 2005. Immunocytochemical identification of cell types in the mormyrid electrosensory lobe. *J Comp Neurol* 483:124–142.
- Bell CC, Szabo T. 1986. Electroreception in mormyrid fish: Central anatomy: Electroreception. pp. 319–322.
- Bell CC, Zakon H, Finger TE. 1989. Mormyromast electroreceptor organs and their afferent fibers in mormyrid fish: I. Morphology. *J Comp Neurol* 286:391–407.
- Biswas D, Arend LA, Stamper SA, Vágvölgyi BP, Fortune ES, Cowan NJ. 2018. Closed-Loop Control of active sensing movements regulates sensory slip. *Curr Biol* 28:4029–4036.e4.
- Brainard MS, Doupe AJ. 2013. Translating Birdsong: Songbirds as a Model for Basic and Applied Medical Research. *Annu Rev Neurosci* 36:489–517.
- Braun E, Geurten B, Egelhaaf M. 2010. Identifying Prototypical Components in Behaviour Using Clustering Algorithms. *PLoS One* 5:e9361.
- Caputi AA., Budelli R. 2006. Peripheral electrosensory imaging by weakly electric fish. *J Comp Physiol A* 192:587–600.
- Caputi AA, Aguilera PA, Castelló ME. 2003. Probability and amplitude of novelty responses as a function of the change in contrast of the reafferent image in *G. carapo*. *J Exp Biol* 206:999–1010.
- Chacron MJ. 2005. Feedback and Feedforward Control of Frequency Tuning to Naturalistic Stimuli. *J Neurosci* 25:5521–5532.
- Charlesworth JD, Tumer EC, Warren TL, Brainard MS. 2011. Learning the microstructure of successful behavior. *Nat Neurosci* 14:373–380.
- Ciali S, Gordon J, Moller P. 1997. Spectral sensitivity of the weakly discharging electric fish *Gnathonemus petersi* using its electric organ discharges as the response measure. *J Fish Biol* 50:1074–1087.
- Clarke SE, Longtin A, Maler L. 2015. The neural dynamics of sensory focus. *Nat Commun* 6:8764.
- Clarke SE, Maler L. 2017. Feedback Synthesizes Neural Codes for Motion. *Curr Biol* 27:1356–1361.
- Der R, Martius G. 2015. Novel plasticity rule can explain the development



- of sensorimotor intelligence. *Proc Natl Acad Sci* 112:E6224–E6232.
- Enikolopov AG, Abbott LF, Sawtell NB. 2018. Internally Generated Predictions Enhance Neural and Behavioral Detection of Sensory Stimuli in an Electric Fish. *Neuron* 99:135-146.e3.
- Friston K. 2010. The free-energy principle: a unified brain theory? *Nat Rev Neurosci* 11:127–138.
- Gellermann LW. 1933. Chance orders of alternating stimuli in visual discrimination experiments. *Pedagog Semin J Genet Psychol* 42:206–208.
- Geurten BRH, Kern R, Braun E, Egelhaaf M. 2010. A syntax of hoverfly flight prototypes. *J Exp Biol* 213:2461–2475.
- Gomez L, Budelli R, Grant K, Caputi AA. 2004. Pre-receptor profile of sensory images and primary afferent neuronal representation in the mormyrid electrosensory system. *J Exp Biol* 207:2443–2453.
- Gordon G, Fonio E, Ahissar E. 2014. Emergent Exploration via Novelty Management. *J Neurosci* 34:12646–12661.
- Gordon G, Kaplan DM, Lankow B, Little DY-J, Sherwin J, Suter BA, Thaler L. 2011. Toward an Integrated Approach to Perception and Action: Conference Report and Future Directions. *Front Syst Neurosci* 5:20.
- Grant K, Sugawara Y, Gómez L, Z. Han V, Bell CC. 1998. The Mormyrid Electrosensory Lobe In Vitro: Physiology and Pharmacology of Cells and Circuits. *J Neurosci* 18:6009–6025.
- Hall C, Bell C, Zelik R. 1995. Behavioral evidence of a latency code for stimulus intensity in mormyrid electric fish. *J Comp Physiol A* 177:29–39.
- Heiligenberg W. 1988. Electrosensory Maps Form a Substrate for the Distributed and Parallel Control of Behavioral Responses in Weakly Electric Fish. *Brain Behav Evol* 31:6–16.
- Heiligenberg W. 1980. The jamming avoidance response in the weakly electric fish *Eigenmannia*. *Naturwissenschaften* 67:499–507.
- Hofmann V, Chacron MJ. 2018. Population coding and correlated variability in electrosensory pathways. *Front Integr Neurosci* 12:56.
- Hofmann V, Geurten BRH, Sanguinetti-Scheck JI, Gómez-Sena L,

- Engelmann J. 2014. Motor patterns during active electrosensory acquisition. *Front Behav Neurosci* 8.
- Hofmann V, Sanguinetti-Scheck JI, Gómez-Sena L, Engelmann J. 2017. Sensory flow as a basis for a novel distance cue in freely behaving electric fish. *J Neurosci* 37:302–312.
- Hofmann V, Sanguinetti-Scheck JI, Gómez-Sena L, Engelmann J. 2013. From static electric images to electric flow: Towards dynamic perceptual cues in active electroreception. *J Physiol* 107:95–106.
- Hollmann V, Engelmann J, Gómez-Sena L. 2016. A quest for excitation: Theoretical arguments and immunohistochemical evidence of excitatory granular cells in the ELL of *Gnathonemus petersii*. *J Physiol* 110:190–199.
- Huang CG, Chacron MJ. 2016. Optimized Parallel Coding of Second-Order Stimulus Features by Heterogeneous Neural Populations. *J Neurosci* 36:9859–9872.
- Jun JJ, Longtin A, Maler L. 2016. Active sensing associated with spatial learning reveals memory-based attention in an electric fish. *J Neurophysiol* 115:2577–2592.
- Kern R, Petereit C, Egelhaaf M. 2001. Neural Processing of Naturalistic Optic Flow. *J Neurosci* 21:RC139–RC139.
- Lissmann HW, Machin KE. 1958. The mechanism of object location in *Gymnarchus niloticus* and similar fish. *J Exp Biol.* 35: 451-486
- Little DY, Sommer FT. 2013. Learning and exploration in action-perception loops. *Front Neural Circuits* 7:1–19.
- Loewenstein G. 1994. The psychology of curiosity: A review and reinterpretation. *Psychol Bull* 116:75–98.
- MacIver MA, Patankar NA, Shirgaonkar AA. 2010. Energy-Information Trade-Offs between Movement and Sensing. *PLoS Comput Biol* 6:e1000769.
- Madsen PT, Surlykke A. 2013. Functional Convergence in Bat and Toothed Whale Biosonars. *Physiology* 28:276–283.
- Markham MR, Ban Y, McCauley AG, Maltby R. 2016. Energetics of Sensing and Communication in Electric Fish: A Blessing and a Curse in the Anthropocene? *Integr Comp Biol* 56:889–900.

- McGillivray P, Vonderschen K, Fortune ES, Chacron MJ. 2012. Parallel coding of first- and second-order stimulus attributes by midbrain electrosensory neurons. *J Neurosci* 32:5510–5524.
- Metzen MG, Engelmann J, Bacelo J, Grant K, von der Emde G. 2008. Receptive field properties of neurons in the electrosensory lateral line lobe of the weakly electric fish, *Gnathonemus petersii*. *J Comp Physiol A* 194:1063–1075.
- Metzen MG, Huang CG, Chacron MJ. 2018. Descending pathways generate perception of and neural responses to weak sensory input. *PLOS Biol* 16:e2005239.
- Migliaro A, Caputi AA., Budelli R. 2005. Theoretical analysis of pre-receptor image conditioning in weakly electric fish. *PLoS Comput Biol* 1:e16.
- Miller LM, Silverman Y, MacIver MA, Murphey TD. 2016. Ergodic exploration of distributed information. *IEEE Trans Robot* 32:36–52.
- Moller P. 1995. Electric fishes: history and behavior. London: Chapman & Hall London.
- Monaco JD, Rao G, Roth ED, Knierim JJ. 2014. Attentive scanning behavior drives one-trial potentiation of hippocampal place fields. *Nat Neurosci* 17:725–731.
- Nelson ME, Maciver MA. 1999. Prey capture in the weakly electric fish *Apteronotus albifrons*: sensory acquisition strategies and electrosensory consequences. *J Exp Biol* 202:1195–203.
- Ni AM, Ruff DA, Alberts JJ, Symmonds J, Cohen MR. 2018. Learning and attention reveal a general relationship between population activity and behavior. *Science* 359:463–465.
- O’Hora D, Dale R, Piironen PT, Connolly F. 2013. Local dynamics in decision making: The evolution of preference within and across decisions. *Sci Rep* 3:2210.
- Pedraja F, Aguilera P, Caputi AA., Budelli R. 2014. Electric imaging through evolution, a modeling study of commonalities and differences. *PLoS Comput Biol* 10:e1003722.
- Pedraja F, Hofmann V, Lucas KM, Young C, Engelmann J, Lewis JE. 2018. Motion parallax in electric sensing. *Proc Natl Acad Sci* 115:573–577.
- Pedraja F, Perrone R, Silva A, Budelli R. 2016. Passive and active

- electroreception during agonistic encounters in the weakly electric fish *Gymnotus omarorum*. *Bioinspir Biomim* 11:065002.
- Pitkow X, Angelaki DE. 2017. Inference in the Brain: Statistics Flowing in Redundant Population Codes. *Neuron* 94:943–953.
- Post N, von der Emde G. 1999. The “novelty response” in an electric fishresponse properties and habituation. *Physiol Behav* 68:115–128.
- Poteser M, Kral K. 1995. Visual distance discrimination between stationary targets in praying mantis: an index of the use of motion parallax. *J Exp Biol* 198:2127–2137.
- Push S, Moller P. 1979. Spatial aspects of electrolocation in the mormyrid fish, *Gnathonemus petersii*. *J Physiol (Paris)* 75:355–7.
- Rother D. 2003. Simulación de imágenes eléctricas en peces eléctricos de descarga débil. *Imágenes Eléctricas en Peces Eléctricos Descarga*. Universidad de la Republica. Master thesis
- Rother D, Migliaro A, Canetti R, Gómez L, Caputi A, Budelli R, Gomez L, Caputi A, Budelli R, Gómez L, Caputi A, Budelli R. 2003. Electric images of two low resistance objects in weakly electric fish. *Biosystems* 71:169–177.
- Runyan CA, Piasini E, Panzeri S, Harvey CD. 2017. Distinct timescales of population coding across cortex. *Nature* 548:92–96.
- Sanguinetti-Scheck JI, Pedraja EF, Cilleruelo E, Migliaro A, Aguilera P, Caputi AA, Budelli R. 2011. Fish geometry and electric organ discharge determine functional organization of the electrosensory epithelium. *PLoS One* 6:e27470.
- Sawtell NB, Bell CC. 2008. Adaptive processing in electrosensory systems: Links to cerebellar plasticity and learning. *J Physiol* 102:223–232.
- Sawtell NB, Williams A, Bell CC. 2005. From sparks to spikes: information processing in the electrosensory systems of fish. *Curr Opin Neurobiol* 15:437–443.
- Sawtell NB, Williams A, Roberts PD, von der Emde G, Bell CC. 2006. Effects of sensing behavior on a latency code. *J Neurosci* 26:8221–8234.
- Silverman Y, Miller LM, MacIver MA, Murphey TD. 2013. Optimal planning for information acquisition2013 IEEE/RSJ International Conference on Intelligent Robots and Systems. IEEE. pp. 5974–5980.

- Snyder JB, Nelson ME, Burdick JW, MacIver MA. 2007. Omnidirectional sensory and motor volumes in electric fish. *PLoS Biol* 5:e301.
- Szabo T, Hagiwara S. 1967. A latency-change mechanism involved in sensory coding of electric fish (Mormyrids). *Physiol Behav* 2:331–335.
- Toerring M-J, Moller P. 1984. Locomotor and electric displays associated with electrolocation during exploratory behavior in mormyrid fish. *Behav Brain Res* 12:291–306.
- Toerring MJ, Belbenoit P. 1979. Motor programmes and electroreception in mormyrid fish. *Behav Ecol Sociobiol* 4:369–379.
- van Beers RJ, Baraduc P, Wolpert DM. 2002. Role of uncertainty in sensorimotor control. *Philos Trans R Soc London Ser B Biol Sci* 357:1137–1145.
- von der Emde G. 2010. Active electroreception: Vertebrates. *Encycl Anmial Behav* 1:16–23.
- von der Emde G, Schwarz S. 2002. Imaging of objects through active electrolocation in *Gnathonemus petersii*. *J Physiol* 96:431–444.
- Wolpert DM, Landy MS. 2012. Motor control is decision-making. *Curr Opin Neurobiol* 22:996–1003.
- Wu HG, Miyamoto YR, Castro LNG, Ölveczky BP, Smith MA. 2014. Temporal structure of motor variability is dynamically regulated and predicts motor learning ability. *Nat Neurosci* 17:312–321.
- Yovel Y, Falk B, Moss CF, Ulanovsky N. 2010. Optimal localization by pointing off axis. *Science* 327:701–704.
- Zgonnikov A, Aleni A, Piiroinen PT, O’Hora D, di Bernardo M. 2017. Decision landscapes: visualizing mouse-tracking data. *R Soc Open Sci*

*Task related sensorimotor adjustments increase the sensory range*

---

# Shaping sensorimotor behavior in response to changes of cue saliency in active electrolocation

## 3



A version of this chapter is in preparation for publication:

**Pedraja F.;** Engelmann J.; *Shaping sensorimotor behavior in response to changes of cue saliency in active electrolocation.*

*Being able to recruit behavioral sequences and connect them in a directed manner can be a flexible and efficient way to respond to variable sensorimotor demands. Such demands are already present in apparently simple behavioral situations like foraging, where an animal needs to detect, localize and characterize variable properties in its environment. In the previous chapter, I could show that the active sensory system of the weakly electric Mormyrid fish *Gnathonemus petersii* is particularly suitable to study how animals can shape their sensory input in a task-dependent manner to optimize the sensory information required to solve a localization task. Here I extend on this study by addressing how the saliency of the electrosensory cue that is required to solve the task influenced behavior.*

*In line with results from chapter 2, fish performed stereotyped approaches to the object when it was within the sensory detection range of the active electrosensory system. Decreasing the saliency of the object to the limit of active electro-detection resulted in a consistent switch of the behavioral strategy. While fish initially followed the previously acquired strategy to reach a single electrically salient point in their environment, they switched to a strategy that incorporated a spatial landmark from where a direct (sensory) comparison of the two choices was feasible. Importantly, the landmark itself did not provide task-relevant information. This indicates that weakly electric fish are able to acquire relational knowledge of their environment and use it when purely sensory-guided orientation fails. As a consequence of the flexible transition to a new strategy, fish now searched for two attractors in their environment. Fish thus showed a flexible, spontaneous and task-dependent response, allowing them to cope with the altered condition.*



### **3.1 Introduction**

The efficiency of behaviors to some extent depends on the quality of the sensory information available to guide them. Which behavior to perform when and where, depends on a disambiguation of the environment. This not only requires a dynamic update of the sensory percept through constant acquisition of sensory information, but also depends on internal mechanisms like memories and forward models of the sensory consequences of the current behavior (Verwey et al., 2015; Wilson et al., 2010). Thus, sensing is tightly intertwined with the planning and execution of movements. Understanding how animals seamlessly coordinate sensing and motor behavior is a current challenge in sensory neuroscience.

For a fixed sensorimotor task, it seems adequate that animals internalize a viable motor solution. For example, bats adopt stereotyped flight paths when flying in confined spaces. Once they have *mapped* the space, they reduce their acoustic call rate and appear to rely on an internalized map acting in an open loop condition where the motor behavior is independent from the present sensory information (Barchi et al., 2013). Under less stable conditions, flexible adjustments of sensorimotor behaviors are required and behavior is modified in an open loop condition that relies on sensory input. We hence speculated that sensorimotor behaviors should be altered flexibly depending on the requirements. This hypothesis will be tested here using weakly electric fish.

Weakly electric Mormyrid fish, here *Gnathonemus petersii*, generate a 3-dimensional electric field around their body. This field is generated through the voluntarily timed discharge of an electric organ (EOD) (Assad et al.,

1999; Caputi and Budelli, 2006; Lissmann, 1958; Lissmann and Machin, 1958). Objects in the field induce local and object-specific perturbations that result in a 2-dimensional pattern of currents at the animal's skin. This pattern is referred to as the *electric image* (EI). It is sensed by an array of several thousand electroreceptors that together constitute the sensory mosaic of the active electric sense (Caputi and Budelli, 2006; Caputi et al., 1998; Engelmann et al., 2008). Weakly electric fish make use of various spatial and temporal features of these electric images to disambiguate their environment to orient and even forage in complete darkness (Nelson and MacIver, 2006; Rasnow, 1996; Rasnow and Bower, 1997; Sicardi et al., 2000; von der Emde et al., 1998; von der Emde and Fetz, 2007). The range over that active electrolocation can be used depends on different factors like the size and conductivity of the object as well as the conductivity of the water and the inherent electrical properties of the fish itself (von der Emde et al. 1998; Pedraja et al. 2014; Migliaro et al. 2005; Sanguinetti-Scheck et al. 2011). For *Gnathonemus petersii* small objects can be detected within  $\frac{1}{4}$  to  $\frac{1}{2}$  body length (Hofmann et al., 2017; Push and Moller, 1979; Toerring and Belbenoit, 1979), for bigger objects, this range might be larger, but active electrolocation clearly is a near-range sensory modality. Within the detection range, electric images of physically distinct objects can superimpose to a single electric image (Engelmann et al., 2008) and objects of very different electric properties may aid electrolocation by resulting in an electrical pop-out effect (Fechler et al., 2012; Gómez-Sena et al., 2014). In this study, we make use of the reduced detection range of active electrolocation in order to systematically change the reliability of the sensory input that is required for the animal to solve a detection-localization task.

A notable advantage of using this animal model is that the timing and content of the sensory input is uniquely accessible, as we can measure when and calculate what an animal samples. Hence, this system provides the possibility to directly study the relationship between motor behavior, the sensory input generated by it and how both shape motor planning and attentive scanning. This idea that adjustments of motor activity are actively exploited by animals as a scaffold to shape the sensory flow has recently been investigated in very different sensorimotor systems (Baird et al., 2006; Hofmann et al., 2017, 2014, 2013b; Pedraja et al., 2018; Srinivasan, 2011). We here extend on this by investigating how motor and electrosensory patterns of the weakly electric fish *Gnathonemus petersii* are changed when a previously successful routine fails. Initially fish were found to follow a stereotyped sensorimotor routine when they had to localize and approach a salient object placed in one of two possible compartments (see chapter 3). Reducing the saliency of this object resulted in a switch to a new motor strategy. Rather than following a sensory-guided routine, fish now first sought a position within the experimental arena from which they could simultaneously evaluate the sensory evidence from either compartment equally well. For this they now used the partition between both compartments as a cue to reach this position. The cue itself had no value for the detection itself. It thus appears that detection based on active electrolocation is a dynamic process where the current sensory input is used to shape the upcoming behavior. When this information is insufficient to directly solve the task, fish flexibly resort to a strategy that relies on relational knowledge of the environment to aid in overcoming the limited sensory information.

## **3.2 Methods**

### **3.2.1 Animals**

Wild-caught *Gnathonemus petersii* (n=5, 10-12cm in length) were obtained from a commercial fish dealer (Aquarium Glaser, Rodgau, Germany) and housed in groups of 5-10 in aerated tanks. Water temperature was 24-29°C and water conductivity between 100-300  $\mu\text{S}\cdot\text{cm}^{-1}$  with a light-dark cycle of 12L:12D. Fish were fed with blood worms to satiation three times per week before the beginning of the experiments. For the experiments reported here, individuals were kept in separate tanks (120 · 48 · 50 cm, water temperature was  $25 \pm 1^\circ\text{C}$ , conductivity  $100\pm 5 \mu\text{S}\cdot\text{cm}^{-1}$ ). All procedures comply with the current animal protection law of the Federal Republic of Germany, approved by the local authorities LANUV NRW: 87-51.04.2010.A202 and 84-02.04.2017.A151.

### **3.2.2 Training setup**

The experimental tanks were divided into a living area (60 · 48 · 30 cm, water level) and a test area (60 · 48 · 10 cm, water level) that could be separated by a plastic gate. The test area was further split in a left and right compartment by a plastic partition. This partition started 40 cm from the gate and ended at the wall opposing the gate (i.e., the partition divided that last third of the test area in two compartments of 20 · 24 cm each). All procedures were done in darkness, video-taped from above at 60fps (AVT Marlin F-131 & F-033) using infrared illumination (880 nm). The EODs were captured simultaneously with the videos (custom-built amplifier, E-

workshop, Bielefeld University), and digitized at 10 kHz and stored for off-line analysis.

### **3.2.3 Training procedure**

To become familiar with the set-up, animals learned to first swim through the open gate to receive some food at the end of the test area. Once fish readily entered the test area, training started. In this two-alternative forced-choice paradigm the fish had to choose the compartment containing a metal cube ( $2 \cdot 2$  cm). Trials started by opening the gate after a cube was placed in the middle of the compartment at the decision line (distance = 0 cm). The cube was altered between the two compartments following a pseudo-random table (Gellermann, 1933). To avoid indirect cues, the cube was removed from the tank after every trial. The choice of the area was scored and rewarded by a single blood-worm offered at the end of the test area once the fish passed the decision line. After eating the reward, the fish had to swim back into the living area, and the gate was closed to prepare the next trial. Training was done for 6 days a week with one session of 20-30 trials per day. Acquisition of the task was considered to be stable once a fish performed at or above 80% correct choices per session for at least six consecutive sessions.

**Object detection at different distances.** When the fish had acquired the task, we began the testing level by placing the object at different distances. The distances were increased in steps of 1 cm until the performance fell to chance level (11 or 12 cm distance). Every test trial was followed by two control trials where the object was at the initial training distance (0 cm). At each distance, 20-40 test trials were conducted before increasing the test

distances. Similar to the training procedure, sessions were done for 6 days a week with 30 trials per session.

### **3.2.4 Video tracking**

Position, orientation and posture of the animals were analyzed offline. Using a background subtraction approach with subsequent thresholding, the animal's center of mass was determined and the animal's posture was obtained by applying a 3rd order polynomial fit through the midline of the detected body. This fit was restricted in length to match the size of each individual. Head and tail points were determined based on the spindle-like shape of the fish's body with the head being closer to the body's center of mass. The object was tracked similarly to the animal in each single frame of the videos. From the tracked positions of the animals, we determined the frame wise 2D kinematics (i.e. thrust, slip and yaw velocity) which we used for the behavioral classification.

### **3.2.5 Data analysis and statistical tests**

To quantify the spatial distribution of behaviors the arena was separated in  $1 \text{ cm}^2$  bins. The Euclidean distance between the fish's head and the object was calculated. In trials where the fish choose the wrong compartment distance was calculated with respect to the virtual object position (i.e., we assume the object to be present in the compartment the fish had erroneously chosen). Sampling density (SD) was calculated as the number of EODs emitted per cm traveled ( $\text{EOD count} \cdot \text{cm}^{-1}$ ). For this, we used swim speed and the EOD rate per frame. To illustrate the average trajectories per fish and learning stage, we obtained the mean direction in

which fish passed from one spatial bin to the next and the vector strength ( $r^2 \cdot N$  with  $N$  being the number of elements in the bin and  $r^2$  Rayleigh's coefficient of angular dispersion). Based on these values the average gradient of the trajectories was visualized using the function "*streamline*" in Matlab. This was used for visualization only, while all analyses are based on single trajectories. To calculate attractors, spatial maps were generated from all trajectories. From each trajectory, the first coordinate received a weight of +1 and the last coordinate of -1. Weights for in between coordinates were linearly interpolated based on the travel time and distance. For each session, we superimposed all weighted trajectories, resulting in cumulative 2D maps. The attractor area was defined as the area in which all values fell below a threshold of two standard deviations from the trough value of the cumulative 2D map. Transient increases in EOD rate (E-scans) were detected from the z-transformed first derivative of the EOD intervals. The variance and mean for the z-transform was based on pooled data of a given training session. Accelerations exceeding a z-value of 1.5 were defined as E-scans and their location was defined by the position that this E-scan began. To calculate the spatial correlation of Fisher information, alignment of the electric images, sampling density and the E-scan probability, each the spatially binned maps of each measure were normalized individually (range 0 - 1). The correlation map was generated by multiplying the four normalized maps. In this correlation map perfect spatial correlation of the four parameters will yield a value of 1, while the absence of spatial correlation will have a value of 0.

For statistics we assessed the normality of the data (Shapiro-Wilk test), and homogeneity of variance were appropriate (Levene's test). The

appropriate parametric or non-parametric tests were used accordingly and are indicated in the results section and captions throughout. Data used for multiple comparisons was post-hoc corrected where necessary.

### **3.2.6 Electric images models**

Electric images were computed with software developed by Rother (Rother, 2003) as verified and utilized in previous studies (Hofmann et al., 2013a, 2017; Migliaro et al., 2005; Pedraja et al., 2014; Rother et al., 2003; Sanguinetti-Scheck et al., 2011). This model has two parts, a geometric reconstruction of the fish's body and a calculation of the transcutaneous field by solving the Poisson equation for the fish boundary using the Boundary Element Method (BEM). Briefly, this method determines the boundary electrical distributions solving a linear system of  $M \cdot N$  equations for  $M$  poles and  $N$  nodes, with the unknown variables being the trans-epithelial current density and potential at each node (Pedraja et al., 2014). The trans-epithelial current density and potential is calculated for each node and linearly interpolated for the triangles defined by the nodes, forming the geometry of fish and objects. From this the electric images for each trajectory were calculated as the difference between amplitude of positive EOD peak in presence and absence of the object.

### **3.2.7 Fisher information analysis**

To calculate the information about the location of the object between consecutive EODs, we used the electric image obtained along a section of the fish's midline. With this we calculated the Fisher information as  $(\theta, x) = \left( \frac{\partial E(\theta, x)}{\partial \theta} \cdot \frac{1}{\sigma} \right)$ , where  $x$  is the location from the goal,  $\theta$  is the direction

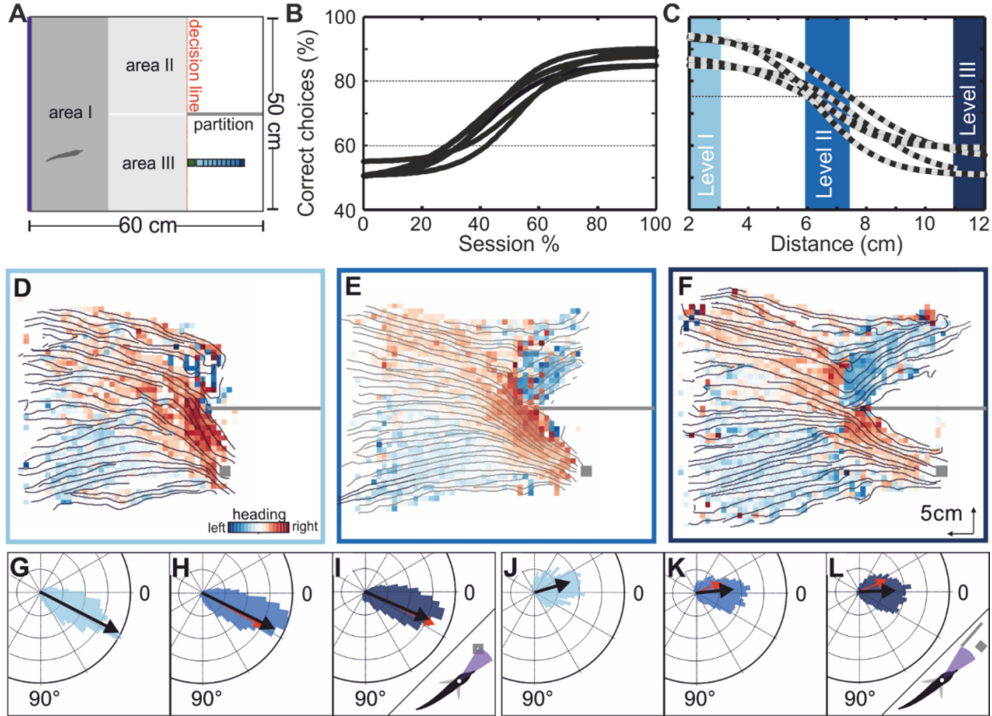


of motion (calculated as finite derivative between the EODs) and  $\sigma$  is the variance of the noise. The Fisher information in our case can be thought of as the amount of information a measurement provides at location  $x$  for a given  $EI_n$  using the ratio of the derivative of the expected signal ( $EI_n$  and  $EI_{n+1}$ ) to the variance of the noise (furthest EIs measured) (Miller et al., 2016; Silverman et al., 2013).

### **3.3 Results**

#### **3.3.1 Performance and motor behavior change with object distance**

Five weakly electric fish (*Gnathonemus petersii*) were trained to enter one of the two compartments of the test arena that was set apart from the alternative compartment by the presence of a meal cube directly at the decision line (0 cm distance, Figure 3.1A, B). After animals had learned this, we tested their performance by gradually increasing the distance between the object and the decision line. With increased distance, the performance of all fish decreased (Figure 3.1C). Using a performance level of 75%, the individual threshold to detect the object was between 6 and 7.5 cm, while it approached chance level at 11 - 12 cm (Figure 3.1C). To investigate if and how the increased difficulty in detecting the object led to altered electromotor behaviors, we pooled the data into near, threshold and chance level distances (see shaded areas in Figure 3.1C).



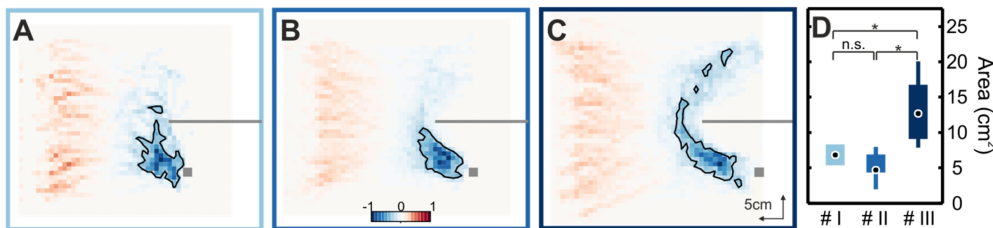
**Figure 3.1:** **A.** Schematic top view of the experimental setup. Experiments started by opening a gate (blue line), fish then had to swim towards the compartment where the metal cube was placed at the decisions line (training and control trials). In test trials the object was positioned at increasingly larger distance from the decision line (see color gradient). **B.** Psychometric functions of all 5 fish for the learning phase where the object was directly at the decision line. **C.** Psychometric function obtained for the test trials of the 5 fish after learning. For later analysis the data is compared for three distances according to performance levels: 2 cm (high performance level; level I), the distance where performance fell until 75% (limit range 5-6 cm; level II) and the furthest distance tested (11 or 12cm; level III). In the following figures, the data for these decreasing levels of performance are shown in light to dark blue, with high performance corresponding to light blue and chance performance to dark blue. **D-F.** Top view on the average trajectories (black lines) found during the three performance levels for all fish ( $n = 5$ ). The color-coded map represents the mean heading direction. Here and in all following figures, the data is presented with the metal cube (grey square) on the right side of the arena. The horizontal grey bar shows the plastic partition between compartments. **G-L.** Mean heading vector (black arrow) based on all trials shown with the circular histogram of the heading angles. While panels G-I show the heading with respect to the object, panels J-L show the heading with respect to the partition. The red arrows show the mean heading vectors calculated for the for control trials.

As reported before (Pedraja et al. submitted, see Chapter 2), fish followed a rather stereotyped motor pattern when the object was close. As shown in Figure 3.1D for the object at 2 cm distance (see also Figure S3.1 for controls at 0 cm for levels II-III), fish veered rightwards when approaching from the left half of the test area while they mainly swam straight otherwise. Note that for the visualization of pooled data we artificially flipped the data of trials where the object was on the left side. As can be seen in the individual example in Figure 3.1D-F as well as the pooled orientation data in Figure 3.1G-L, fish used a different approach strategy when the object distance was around the detection limit. In these cases they started to orient towards the tip of the partition, as can already be seen in the average trajectories in Figures 3.1D-F. While this did not affect the fish's alignment with respect to the object (Figure 3.1G-I;  $28^\circ$ ,  $27^\circ$  and  $24^\circ$  for levels I-III; William-Watson test for difference in orientation,  $p > 0.05$ ), it resulted in an enhanced alignment to the partition (Figures 3.1J-L;  $-16^\circ$ ,  $-5^\circ$  and  $-1^\circ$  for levels I-III; William-Watson test for difference in orientation,  $p < 0.001$  for levels I-II and levels I-III,  $p=0.04$  for levels II-III). This improvement in the alignment towards the partition is distance specific, since the control data showed not change with respect to distances below 2 cm (red arrows in Figure 3.1H-I and K-L). Note that all alignment analysis is based on data up to the decision line.

Traversing through the arena and reaching the correct compartment relies on sensory input as well as continuous motor control and planning. Initially the goal of the task must be learned by the fish. For this it can be expected that the animals focus their sensory attention on specific zones of the arena that provide the most relevant information for task completion.

The trajectories can thus be interpreted as overt actions that reflect an internal sensorimotor decision-making process. Analyzing the trajectories can therefore reveal how internal states evolve within trials and with learning.

We here analyzed this by investigating if and how attractors developed (see methods). We found that the behavior for the conditions where sufficient sensory input was available to successfully solve the task (levels I and II and controls), was characterized by a single attractor extending from the object to the decision line (Figure 3.2A-B and Figure S3.2). This attractor was more distributed between both compartments and middle section in the cases where sensory information was not sufficient to complete the task (level III, Figure 3.2C). Using a value of one standard deviation from the mean of the attractor basin as a threshold to measure the attractor's size confirmed that it was less distinct and more distributed for increased object distances (Mann-Whitney pairwise test with Bonferroni post hoc test:  $p=0.53$  levels I-II;  $p=0.04$  levels I-III;  $p=0.03$  levels II-III; Figure 3.2D).



**Figure 3.2: Attractor states for different sensory saliency levels.** A-C. Mean Attractor landscape diagrams from all fish trajectories for the three performance levels (level I in A, level II in B and level III in C). D. Size of the attractors shown as a box-plot for all fish sorted by performance levels (I-III). The size became significantly larger when the object's saliency was lowest (Mann-Whitney pairwise test with Bonferroni post hoc test:  $p=0.53$  levels I-II;  $p=0.04^*$  levels I-III;  $p=0.03^*$  levels II-III).

Fish thus modified the focus of their behavioral attention switching from an object-centered approach to one that incorporated the sensory information from the object only after having attended a salient spatial cue in the arena.

### **3.3.2 Sensory consequences of decrease in object saliency**

In addition to the reduced performance and the switch in the behavior, we found that the electric images of the arena were less well positioned on the head region of the fish for the highest object distance. For this we analyzed the position of the peak of the electric images (see methods and Figure S3.3A-B for details), finding that the peak was less well centered onto the foveal head region (Bacelo et al., 2008) at larger distances (Figure 3A-C, level I:  $r = 0.78$ , mean orientation  $\pm$  std =  $-0.01 \pm 11.5\%$ ; level II:  $r = 0.66$ ,  $0.66 \pm 14.8\%$ ; level III:  $r = 0.53$ ,  $1.51 \pm 18.1\%$ , K test to determine whether two concentration parameters are different. Levels I-II:  $p=3.54^7$ ; Levels I-III:  $p=2.14^9$ ; Levels II-III:  $p=1.97^5$ ). The standard deviation of the EI-peak position increased as well. This increase was particularly high when fish approached the wrong compartment (compare Figure 3.3D-F). Together the observed motor changes and their effect on the electric image position indicate that the fish acquired a new strategy in order to cope with insufficient sensory information.

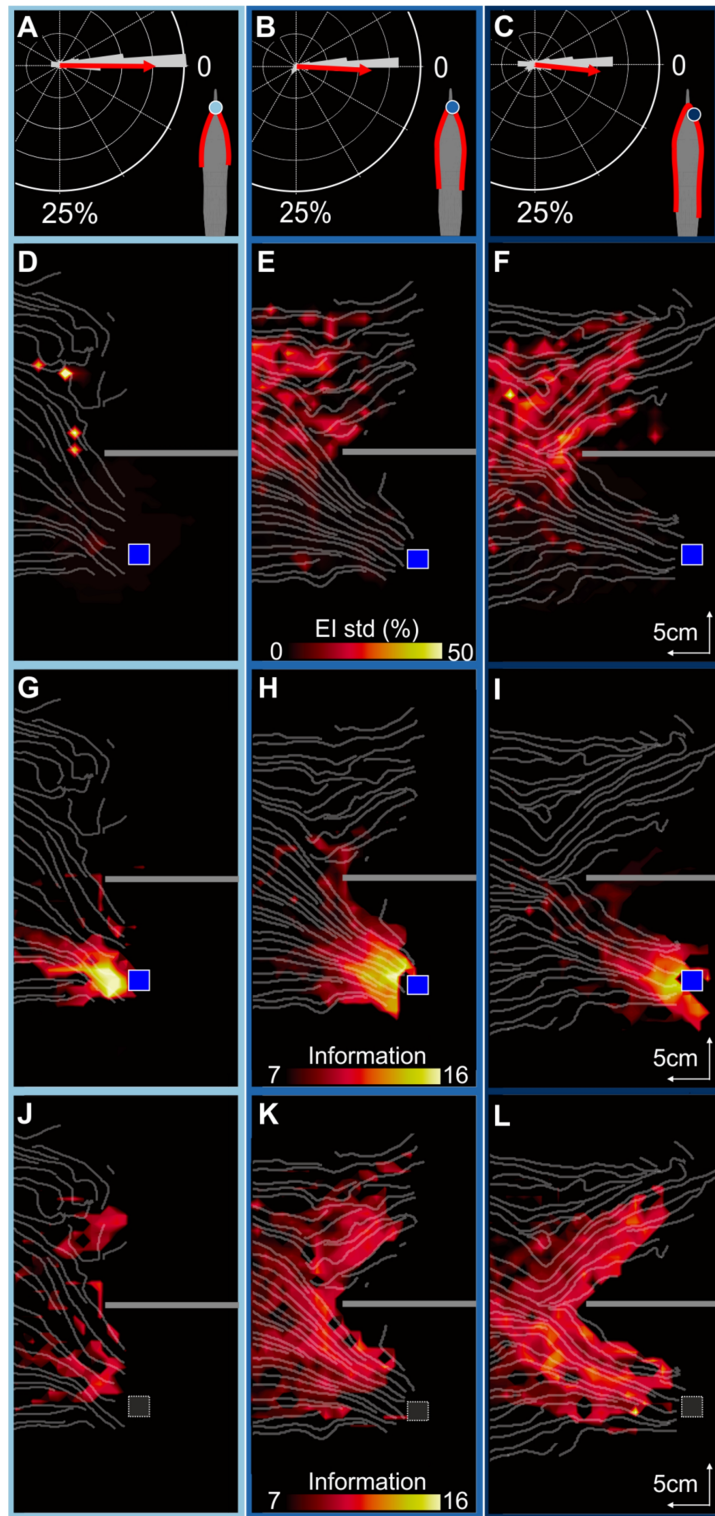
To quantify the sensory effect of the elevated variance in the electric images' position we calculated the Fisher information (FI, Figure S3.3C) between successive electric images in presence of the metal cube and the partition (see methods), providing an estimate of the information that each EOD provided about the location of the object. As expected, FI increase

proportional to the nearness to the object (Figure 3.3G-I). For the furthest object distance, FI was very low before the fish reached the decision line, adding support to the interpretation that at this distance a direct detection of the cube was impossible before passing the decision line. Interestingly, however, a slight increase in FI at the partition was observed for the conditions where the object was less salient.

To further understand the role of the partition, we calculated the FI of the partition alone (Figure 3.3J-L). This revealed two things: The electric images of the partition resulted in much weaker levels of Fisher information. However, the contribution of the information of the partition was found to increase with increased object distance (Figure 3.J-L). As the physical properties of the partition were constant, fish must have approached the partition and sampled more in its proximity when the object distance was large, whereas they directly targeted the object when it was within easy sensory reach.

---

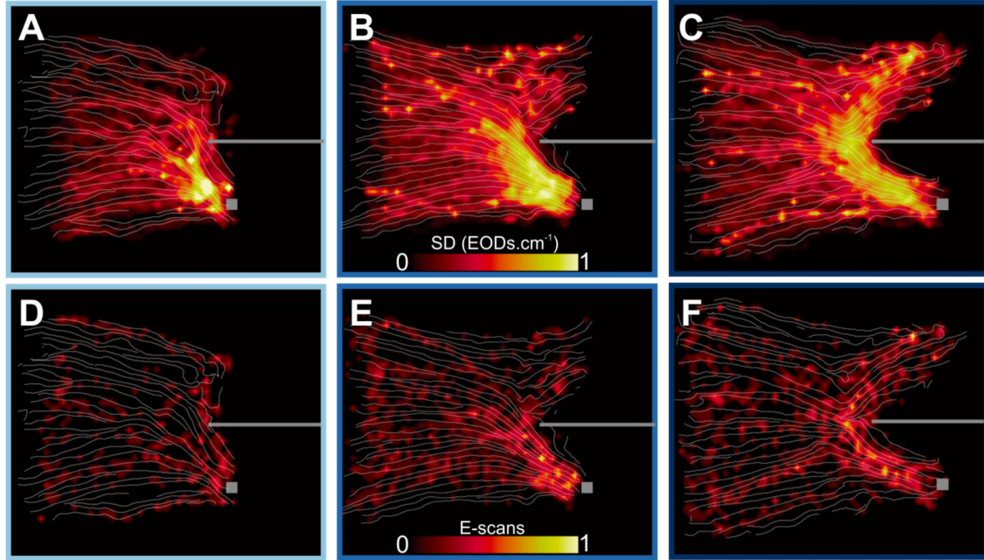
**Figure 3.3:** (*Opposite page*). **A-C.** Circular histograms of the alignment of the electric images over fish's body (0% corresponds to the fish's head while -50 and 50% to the tail from both sides) pooled for all fish and separated between the levels I-III. The red arrows represent the mean alignment, while the red outline covering the schematic fish silhouettes gives a visual representation of the variance of the data. Here the blue circles indicate the mean position of the EI peaks, corresponding to the mean orientation of the vector shown in the circular histograms. **D-F.** Top view of parts of the experimental arena. The averaged trajectories of all fish and all trials shown are shown by the white lines. Superimposed on that the color-coded map depicts the binned standard deviation of the alignment of the electric images. Note that the alignment became more variable for further object distances and was particularly elevated on the side of the wrong compartment. **G-I.** Fisher information distribution maps superimposed over the mean trajectories (white lines) of all fish and all trials, separated by the three performance levels. The data shown is based on computations that included the cube and the partition in the calculation of the electric images used to obtain the FI. **J-L.** As in in panels G-I, but for a computation that only considered the partition in the calculation of the electric images.



### **3.3.3 Modification of the electromotor behavior with the task**

The above results suggest that the partition could be flexibly incorporated into the behavior. To further investigate this hypothesis we analyzed how the sensorimotor patterns changed for the different levels of object saliency by calculating the sampling density (SD, number of EODs emitted per distance travelled,  $\text{EOD} \cdot \text{cm}^{-1}$ ). This provides an estimate of the joint contribution of the swim speed and the sampling frequency to the spatiotemporal structure of the sensory input. While the average EOD rate was independent of the fish's distance to the cube as well as the distance of the cube from the decision line (on average  $40.1 \pm 1.8$  EODs/s, Figure S3.4A), the time for visit density increased the closer the fish came to the cube (Figure S3.4B). Consequently, independent of the object distance from the decision line, the SD increased when fish approached the cube (Figure 3.4A-C). Similar results were obtained for the control trials where the object was at 0 cm distance (Figure S3.5A). In the two conditions where the object was less salient, the SD was also increased surrounding the partition (Figure 3.4B-C). This was not observed for the level I data (Figure 3.4A; level I vs. II: 2 - 7 cm around partition; level I vs. III: until 12.5 cm around partition; Kruskal-Wallis test with Bonferroni post hoc test, p values  $< 0.037$ ) or for the controls where the object was at 0 cm distance (Figure S3.5; controls vs. II: until 3cm around partition; controls vs. III: until 12 cm around partition; Kruskal-Wallis test with Bonferroni post hoc test, p values  $< 0.038$ ). Note that this difference can be explained by the fact that fish spent more time at the partition (see time for visit density in Figure S3.4B).



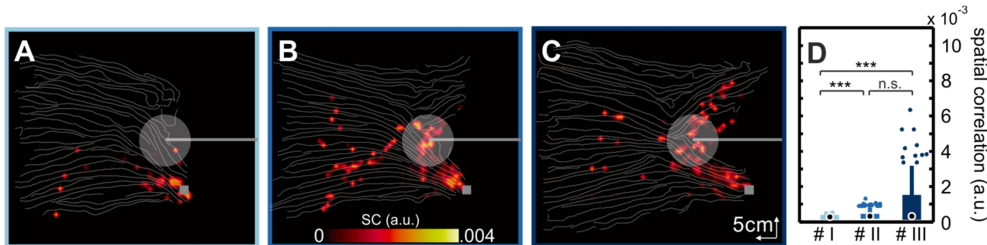


**Figure 3.4: A-F** Top view of parts of the experimental arena showing the averaged trajectories (white lines) of the fish performed for the three levels. The superimposed color code represents the binned normalized sampling density (A-C) and the binned normalized E-scan frequency (D-F). The partition and object are shown by the grey horizontal bar and the grey cube, respectively.

An electric sampling behavior that has received considerable attention are transient accelerations of the EOD rate, known as novelty responses (Post and von der Emde, 1999) or E-scans (Jun et al., 2016). These electromotor displays occur when the electrosensory input deviates from the recent baseline (Caputi et al., 2003) and also have been considered overt displays of sensory expectations (Moller, 1995). Here such E-scans most frequently occurred when the fish entered the arena (data not shown) and when the object was approached. Similar to the sampling density data, the E-scan probability was also elevated close to the partition when the object was placed further from the decision line (Figure 3.4D-F and Figure S3.5B for control trials).

### 3.3.4 Spatial correlation of sensorimotor behavior

The present results strongly support the hypothesis that the partition is incorporated in the behavior and decision making process in a flexible manner. Notably the partition was not only integrated in the behavior when performance approached chance level (level III), but it was already approached when the cube could be reliably detected (level II). Assuming that fish used the partition to enhance the detectability of the cube, we predicted that sensory information and electromotor patterns should reveal a spatially correlated increase close to the partition. To test this, we obtained the binned spatial correlation values of the Fisher information, the alignment of the electric images on the foveal head region; the sampling density and the E-scan probability (see methods). Figure 3.5 A-C shows the spatial correlation maps for the three levels.



**Figure 3.5: A-C.** Top view of parts of the experimental arena showing the averaged trajectories (white lines) of the fish performed for the three levels. The color code represents the spatial correlation of Finfo, EI alignment, SD and E-scans. To calculate this, each map was normalized by the range (values between 0 and 1) and then performed the product of the four variables at every bin. **D.** Spatial correlation 4cm radius around the partition. Kruskal-Wallis test with Bonferroni post hoc test were performed for comparison between levels (n.s.  $p > 0.05$ , \*\*\* $p < 0.001$ ).

As expected, these measures were elevated at the object, but also locally increased surrounding the partition once the object was placed further away

from the decision line (Figure 3.5 B-C). Evaluating the correlations around the partition (see white circle in Figure 3.5 A-C) confirmed that the spatial correlation was significantly higher for the two larger object distance conditions (Figure 3.5D: 4cm radius around the partition; Kruskal-Wallis test with Bonferroni posthoc test: levels I-II:  $p=6e^{-4}$ ; levels I-III:  $p=7e^{-4}$ , levels II-III:  $p=0.34$ ).

### **3.4 Discussion**

Behavior at very different levels of complexity can rely on internalized motor programs. Examples range from simple reflex behaviors with no or limited sensory control as well as more complex behaviors that depend on sensorimotor integration in closed-loop conditions like for example echo acoustic navigation in bats (Geva-Sagiv et al., 2015). Behaviors can also depend on sensory-controlled acquisition initially, like vocal motor learning in songbirds (Konishi, 2004), but then once acquired are executed in open-loop manner independent of sensory feedback. Arguably most behaviors fall between the extremes of feedback-controlled to open loop behavior, compromising speed for flexibility by the integration of real-time sensory feedback.

In weakly electric fish electrosensory information is likely the modality of major importance in the control of flexible behavior (Jun et al., 2016; MacIver et al., 2001; Schumacher et al., 2017; von der Emde et al., 1998). We here investigated if *Gnathonemus petersii* will change its sensorimotor pattern after having acquired a robust solution for a simple detection task, when the saliency of the detected cue was reduced. Importantly the animals

did not face constraints while solving the task, i.e., they were free to explore the arena as long as required, before passing the decision line to, in case of a correct choice, receive a food reward. Under these conditions, the value of the chosen behaviors likely is weighted by the success in securing the food reward. As we showed in a previous study (Pedraja et al submitted, see chapter 2), all fish learned to solve the task and did so by very similar electromotor patterns. This similarity already suggested that the solution on which animals converged is in some form optimal. Our analysis of the sensory information generated by these patterns suggested that a factor optimized by the behavior is the gained sensory information of the cue (the cube). This strategy here was found to be robust as long as the saliency of the cube was not decreased too much. This decrease was done by gradually moving the cube further away. As the amplitude of the electric images is inversely proportional to  $d^4$  (Chen et al., 2005), small changes in distance will already lead to big changes of the cues saliency. Up to distances of about 4 cm the initially acquired strategy was sufficient to reach a performance above 75% in all fish. Under these conditions, the fish learned to perform correcting turns to reach the metal cube when their initial approach was directed to the wrong compartment. We interpret this as evidence for a sensory-guided control of the electromotor behavior. However, when the cube's saliency was further reduced such that the success rate of the animals fell below 75%, a new sensorimotor strategy emerged.

This new behavior consisted in an approach to the partition separating the compartments. This strategy was preferentially chosen by the fish the more difficult the task was made (levels II & III) as can be seen by the increased alignment of the fish towards the partition in these conditions.

The possible object positions on either side of the arena are equidistant at the tip of the partition. With decreased saliency, the detection task gradually becomes more difficult and thus navigating to this point would allow to make a direct comparison. The alternative approach would require the animal to hover in front of the decision line halfway between the side of the arena and the partition for both compartments. While this would enable the fish to ensure it is acquiring sensory information at the shortest possible distance to the object, it requires detailed relational knowledge of the arena. We at present cannot determine if fish would resort to this latter strategy if the costs of wrong choices had been higher. From reports that used conditions where fish had to compare two objects placed behind separate gates (Schumacher et al., 2017, 2016; von der Emde, 2004; von der Emde and Fetz, 2007), we do know that *G. petersii* is capable to alternately sample two options in two-alternative forced-choice paradigms. In either case, future studies should further explore how these fish acquire sensory evidence to make decisions, as the unique pulsed sampling of this fish will allow to measure how much information is being accumulated before making a decision.

Animals appear to process value serially (Rich and Wallis, 2016a, 2016b). To optimize their decisions, the fish needs to maximize its certainty that the cube was present or absent. Thus it should seek to acquire enough sensory evidence to make its decision. Behavior that weights both options sequentially should gradually move the focus of attention to the correct compartment (Rich and Wallis, 2016a, 2016b). This agrees well with the high sampling density and E-scans occurrence near the object in level I. This behavior can be interpreted to represent a continuous integration of sensory evidence for the presence of the object along a trajectory. Once a

sufficient level certainty has been acquired, the trajectory is simply maintained, whereas in conditions where the certainty close to the decision line did not pass a threshold, the fish turned to evaluate the second option. It appears that with increased distance of the cube from the decision line the information required to make this serial decision is insufficient, resulting in a new strategy where both compartments are compared simultaneously from the partition. This interpretation corresponds well with the shift of the attention: From levels I to III the attractors shifted from the object to a wider attractor space including the partition. This shift was again sensory mediated, as the corresponding control trial maps (Figure 3.2 and Figure S3.2) were object-centered as well.

To address the sensory consequences of the observed behavior we used an established BEM (Gómez-Sena et al., 2014; Rother et al., 2003) approach to calculate the transepidermal currents that generate the electric images. With respect to the positioning of the electric images, we found that the variance of the position increased with increasing object distance, while electric images on average were shifted to the side of the head. This placed the EI outside of the foveal region (Castello et al., 2000; Castelló et al., 1998; von der Emde and Schwarz, 2001). However, the modulation of the electric field and the corresponding amplitude of the EI are highest at this position (Pedraja et al., 2014). This lateralization of the images may thus constitute an active strategy to increase the detection range (Pedraja et al submitted, see chapter 2). Support for a possible dual role of the frontal head region and the side or trunk of the fish has also been found in a modelling study that investigated the discriminability of two objects at

different parts of the trunk, suggesting that electro-acuity might be higher at the flanks than at the head region (Babineau et al., 2007).

The impact of the altered behavior was further investigated using the Fisher information measure. In a theoretically unbounded environment with a single object, the FI (and electric images) only depend on the object. However, in the actual experiments there were at least two objects, the cube and the partition. Nearby objects can produce nonlinear EIs. This superposition effect (Caputi and Budelli, 2006; Engelmann et al., 2008) is also relevant in our approach where the non-conductive partition between the compartments influenced the sensory input. To compare the net effect of the object with the partition present to the effect due only to the presence of the partition, we computed the electric images in two ways (metal cube and partition vs. fish in the scene: Figure 3G-I; and only partition vs. fish in the scene: Figure 3J-L). This showed that the information provided by the partition alone was less localized and weaker when compared to the combined condition. Moreover, information maps were very different when the object was positioned at 2 cm distance as opposed to the more distant placements of the object in levels II and III. This was even apparent before the fish passed the decision line, showing again that the partition was being attended more when the task became difficult. This was only found for the test trials, but not in the interspersed training trials. This indicates that the fish could flexibly alter their approach to the two compartments and this switch most likely depended on the amount of sensory information available prior to reaching the decision line. Rather than randomly choosing when insufficient evidence was accumulated up to the decision line, fish were found to shift their sensory focus. The evidence presented in the spatial correlation analysis (Figure 3.5)

supports this idea, since the localized increase in E-scan and sampling density (attentional evidence) at the partition correlated with the increased variance of the EI position (motor evidence) and the resulting information (FI) when the task was made more difficult only. To which extend performance based on this behavior might outperform the initially acquired performance is presently unclear. While it is obvious that the fish switched between strategies, we could not test if the performance is truly enhanced by this switch. This would require to compare the performance in experiments without any partition present to the data obtained here. Another interesting future approach concerns the quantification of the information leading up to a decision. A recent study of the somatosensory system of rats provided evidence that sensory information is accumulated in a touch-by-touch manner until a boundary for decision making is reached (Zuo and Diamond, 2019). Contrary to our study, rats had to remain stationed while actively palpating with their whiskers, and indicate a choice by moving to the left or right, enabling the authors to precisely quantify the sensory information accumulated prior to a decision. A similar approach could be used in weakly electric fish to test the hypothesis that a switch in behavior does depend on some certainty threshold that needed to be surpassed prior to make a decision. In agreement to this hypothesis we found that sampling density rose prior to the point where fish passed the decision line. This was mainly observed in correct trials in front of the decision line. Further work is required to investigate if similar to rats decisions of the fish were bounded by the quantity of sensory evidence for one of two choices.

Interestingly and in agreement with previous studies (Hofmann et al., 2017), this increase in sampling density was mainly due to a reduction of



the swim speed, and not based on an increased EOD rate. This is contrary to another well-studied pulsatile active sensory system, echolocation of bats. Here call rates typically are increased in phases where bats need to localize or discriminate precisely *terminal buzz*, (Amichai and Yovel, 2017; Ghose and Moss, 2006; Simmons et al., 1979). Contrary to bats, weakly electric fish thus appear to preferentially modulate their input through their motor behavior. If this difference reflects different energetic constraints of the signal production is presently unclear. The EOD frequencies in our experiments were on average high, probably indicating an alert state of the animals. Indeed previous studies (Jun et al., 2016) did find an increase of EOD frequency for freely behaving fish, when these approached an unknown object.

Perceptual exploration often is characterized by a move-dwell-move strategy (Ahissar and Assa, 2016) in which the sensory organs are moved from one region of interest to another, where information is acquired (often this local sampling includes smaller movements as well). The effects of the movements on the sensory input are often crucial for sensation. A well-established example are visual saccades. In animals incapable of true eye movements these are actually due to movements of the whole animal (Boeddeker et al., 2015; Helmer et al., 2017). A case report of a human incapable of eye movements even found that this person had developed a pattern of saccadic head movements (Gilchrist et al., 1997). These examples from the visual sense show that active sensing adds important information to perception. Examples for this also include recent studies of weakly electric fish that found that the temporal dynamics of the sensory input generated by movements can be exploited for depth analysis (Pedraja et al., 2018, see chapter 4). Similarly, we recently found that for the experimental

paradigm used in this study, weakly electric fish adjust their motor behavior to actively improve their detection performance. Motor learning thus may be an important aspect to structure motor behavior to extract specific sensory information optimally through motor learning. This agrees to theoretical considerations that view motor control as part of a decision-making problem (Wolpert and Landy, 2012).

### 3.5 Bibliography

- Ahissar E, Assa E. 2016. Perception as a closed-loop convergence process. *Elife* 5:1–26.
- Amichai E, Yovel Y. 2017. Bats pre-adapt sensory acquisition according to target distance prior to takeoff even in the presence of closer background objects. *Sci Rep* 7:467.
- Assad C, Rasnow B, Stoddard PK. 1999. Electric organ discharges and electric images during electrolocation. *J Exp Biol* 202:1185–93.
- Babineau D, Lewis JE, Longtin A. 2007. Spatial acuity and prey detection in weakly electric fish. *PLoS Comput Biol* 3:e38.
- Bacelo J, Engelmann J, Hollmann M, von der Emde G, Grant K. 2008. Functional foveae in an electrosensory system. *J Comp Neurol* 511:342–359.
- Baird E, Srinivasan M, Zhang S. 2006. Visual control of flight speed and height in the honeybee. *From Animals to animals 9*. Lecture Notes in Computer Science
- Barchi JRR, Knowles JMM, Simmons JAA. 2013. Spatial memory and stereotypy of flight paths by big brown bats in cluttered surroundings. *J Exp Biol* 216:1053–1063.
- Boeddeker N, Mertes M, Dittmar L, Egelhaaf M. 2015. Bumblebee homing: the fine structure of head turning movements. *PLoS One* 10:e0135020.
- Caputi AA., Budelli R. 2006. Peripheral electrosensory imaging by weakly electric fish. *J Comp Physiol A* 192:587–600.
- Caputi A, Budelli R, Grant K, Bell C. 1998. The electric image in weakly

- electric fish: II. Physical images of resistive objects in *Gnathonemus petersii*. *J Exp Biol* 201:2115–2128.
- Caputi AA, Aguilera PA, Castelló ME. 2003. Probability and amplitude of novelty responses as a function of the change in contrast of the reafferent image in *G. carapo*. *J Exp Biol* 206:999–1010.
- Castello ME, Aguilera PA, Trujillo-Cenoz O, Caputi AA. 2000. Electroreception in *Gymnotus carapo*: pre-receptor processing and the distribution of electroreceptor types. *J Exp Biol* 203 Pt 21:3279–3287.
- Castelló ME, Caputi A, Trujillo-Cenóz O. 1998. Structural and functional aspects of the fast electrosensory pathway in the electrosensory lateral line lobe of the pulse fish *Gymnotus carapo*. *J Comp Neurol* 401:549–563.
- Chen L, House JL, Krahe R, Nelson ME. 2005. Modeling signal and background components of electrosensory scenes. *J Comp Physiol A* 191:331–345.
- Engelmann J, Bacelo J, Metzen M, Pusch R, Bouton B, Migliaro A, Caputi A, Budelli R, Grant K, von der Emde G. 2008. Electric imaging through active electrolocation: Implication for the analysis of complex scenes. *Biol Cybern* 98:519–539.
- Fechler K, Holtkamp D, Neusel G, Sanguinetti-Scheck JI, Budelli R, von der Emde G. 2012. Mind the gap: the minimal detectable separation distance between two objects during active electrolocation. *J Fish Biol* 81:2255–2276.
- Gellermann LW. 1933. Chance Orders of Alternating Stimuli in Visual Discrimination Experiments. *Pedagog Semin J Genet Psychol* 42:206–208.
- Geva-Sagiv M, Las L, Yovel Y, Ulanovsky N. 2015. Spatial cognition in bats and rats: from sensory acquisition to multiscale maps and navigation. *Nat Rev Neurosci* 16:94–108.
- Ghose K, Moss CF. 2006. Steering by hearing: a bat's acoustic gaze is linked to its flight motor output by a delayed, adaptive linear law. *J Neurosci* 26:1704–1710.
- Gilchrist ID, Brown V, Findlay JM. 1997. Saccades without eye movements. *Nature* 390:130–131.
- Gómez-Sena L, Pedraja F, Sanguinetti-Scheck JI, Budelli R. 2014.

- Computational modeling of electric imaging in weakly electric fish: Insights for physiology, behavior and evolution. *J Physiol Paris* 108:112–128.
- Helmer D, Geurten BRH, Dehnhardt G, Hanke FD. 2017. Saccadic movement strategy in common cuttlefish (*Sepia officinalis*). *Front Physiol* 7:660.
- Hofmann V, Geurten BRH, Sanguinetti-Scheck JI, Gómez-Sena L, Engelmann J. 2014. Motor patterns during active electrosensory acquisition. *Front Behav Neurosci* 8.
- Hofmann V, Sanguinetti-Scheck JI, Gómez-Sena L, Engelmann J. 2017. Sensory Flow as a Basis for a Novel Distance Cue in Freely Behaving Electric Fish. *J Neurosci* 37:302–312.
- Hofmann V, Sanguinetti-Scheck JI, Gómez-Sena L, Engelmann J. 2013a. From static electric images to electric flow: Towards dynamic perceptual cues in active electroreception. *J Physiol* 107:95–106.
- Hofmann V, Sanguinetti-Scheck JI, Künzel S, Geurten B, Gómez-Sena L, Engelmann J. 2013b. Sensory flow shaped by active sensing: sensorimotor strategies in electric fish. *J Exp Biol* 216:2487–2500.
- Jun JJ, Longtin A, Maler L. 2016. Active sensing associated with spatial learning reveals memory-based attention in an electric fish. *J Neurophysiol* 115:2577–2592.
- Konishi M. 2004. The Role of Auditory Feedback in Birdsong. *Ann N Y Acad Sci* 1016:463–475.
- Lissmann HW. 1958. On the function and evolution of electric organs in fish. *J Exp Biol* 35:156–191.
- Lissmann HW, Machin KE. 1958. The mechanism of object location in *Gymnarchus niloticus* and similar fish. *J Exp Biol*. 35: 451-486
- MacIver M a, Sharabash NM, Nelson ME. 2001. Prey-capture behavior in gymnotid electric fish: motion analysis and effects of water conductivity. *J Exp Biol* 204:543–57.
- Migliaro A, Caputi AA., Budelli R. 2005. Theoretical Analysis of Pre-Receptor Image Conditioning in Weakly Electric Fish. *PLoS Comput Biol* 1:e16.
- Miller LM, Silverman Y, MacIver MA, Murphey TD. 2016. Ergodic Exploration of Distributed Information. *IEEE Trans Robot* 32:36–52.

- Moller P. 1995. Electric fishes: history and behavior. London: Chapman & Hall London.
- Nelson ME, MacIver MA. 2006. Sensory acquisition in active sensing systems. *J Comp Physiol A Neuroethol Sens Neural Behav Physiol* 192:573–586.
- Pedraja F, Aguilera P, Caputi AA., Budelli R. 2014. Electric imaging through evolution, a modeling study of commonalities and differences. *PLoS Comput Biol* 10:e1003722.
- Pedraja F, Hofmann V, Lucas KM, Young C, Engelmann J, Lewis JE. 2018. Motion parallax in electric sensing. *Proc Natl Acad Sci* 115:573–577.
- Post N, von der Emde G. 1999. The “novelty response” in an electric fishresponse properties and habituation. *Physiol Behav* 68:115–128.
- Push S, Moller P. 1979. Spatial aspects of electrolocation in the mormyrid fish, *Gnathonemus petersii*. *J Physiol (Paris)* 75:355–7.
- Rasnow B. 1996. The effects of simple objects on the electric field of *Apteronotus leptorhynchus*. *J Comp Physiol A* 178:397–411.
- Rasnow B, Bower JM. 1997. Imaging with electricity: How weakly electric fish might perceive objects. Proceedings of Computational Neuroscience: Trends in Research 1997. New York: Plenum press, London.
- Rich EL, Wallis JD. 2016a. Decoding subjective decisions from orbitofrontal cortex. *Nat Neurosci* 19:973–980.
- Rich EL, Wallis JD. 2016b. What stays the same in orbitofrontal cortex. *Nat Neurosci* 19:768–770.
- Rother D. 2003. Simulación de imágenes eléctricas en peces eléctricos de descarga débil. *Imágenes Eléctricas en Peces Eléctricos Descarga*. Universidad de la Republica. Master thesis
- Rother D, Migliaro A, Canetti R, Gómez L, Caputi A, Budelli R. 2003. Electric images of two low resistance objects in weakly electric fish. *Biosystems* 71:169–177.
- Sanguinetti-Scheck JI, Pedraja EF, Cilleruelo E, Migliaro A, Aguilera P, Caputi AA, Budelli R. 2011. Fish geometry and electric organ discharge determine functional organization of the electrosensory epithelium. *PLoS One* 6:e27470.

- Schumacher S, Burt de Perera T, Thenert J, von der Emde G. 2016. Cross-modal object recognition and dynamic weighting of sensory inputs in a fish. *Proc Natl Acad Sci* 113:7638–7643.
- Schumacher S, Burt de Perera T, von der Emde G. 2017. Electrosensory capture during multisensory discrimination of nearby objects in the weakly electric fish *Gnathonemus petersii*. *Sci Rep* 7:43665.
- Sicardi EA, Caputi A, Budelli R. 2000. Physical basis of distance discrimination in weakly electric fish. *Physica A* 283:86–93.
- Silverman Y, Miller LM, MacIver MA, Murphey TD. 2013. Optimal planning for information acquisition 2013 IEEE/RSJ International Conference on Intelligent Robots and Systems. IEEE. pp. 5974–5980.
- Simmons JA, Fenton MB, O'Farrell MJ. 1979. Echolocation and pursuit of prey by bats. *Science* 203:16–21.
- Srinivasan M V. 2011. Honeybees as a model for the study of visually guided flight, navigation, and biologically inspired robotics. *Physiol Rev*.
- Toerring MJ, Belbenoit P. 1979. Motor programmes and electroreception in mormyrid fish. *Behav Ecol Sociobiol* 4:369–379.
- Verwey WB, Shea CH, Wright DL. 2015. A cognitive framework for explaining serial processing and sequence execution strategies. *Psychon Bull Rev* 22:54–77.
- von der Emde G. 2004. Distance and shape: Perception of the 3-dimensional world by weakly electric fish. *J Physiol Paris*.
- von der Emde G, Fetz S. 2007. Distance, shape and more: recognition of object features during active electrolocation in a weakly electric fish. *J Exp Biol* 210:3082–3095.
- von der Emde G, Schwarz S. 2001. How the electric fish brain controls the production and analysis of electric signals during active electrolocation. *Zoology-Jena* 103:112–124.
- von der Emde G, Schwarz S, Gomez L, Budelli R, Grant K. 1998. Electric fish measure distance in the dark. *Nature* 395:890–894.
- Wilson AD, Snapp-Childs W, Bingham GP. 2010. Perceptual learning immediately yields new stable motor coordination. *J Exp Psychol Hum Percept Perform* 36:1508–1514.

Wolpert DM, Landy MS. 2012. Motor control is decision-making. *Curr Opin Neurobiol* 22:996–1003.

Zuo Y, Diamond MEE. 2019. Rats generate vibrissal sensory evidence until boundary crossing triggers a decision. *Curr Biol* 29:1415-1424.e5.





## Motion parallax in electric sensing

# 4



A version of this chapter has been published:

**Pedraja F.\***; Hofmann V.\*; Kathleen L.M.; Young C.; Engelmann J.; Lewis J.E.; 2017. *Motion parallax in electric sensing*. PNAS. 115(3):573-577.

*A crucial step in forming spatial representations of the environment involves the estimation of relative distance. Active sampling through specific movements is considered essential for optimizing the sensory flow that enables the extraction of distance cues. However, in electric sensing, direct evidence for the generation and exploitation of sensory flow is lacking. Weakly electric fish rely on a self-generated electric field to navigate and capture prey in the dark. This electric sense provides a blurred representation of the environment, making the exquisite sensory abilities of electric fish enigmatic. Stereotyped back-and-forth swimming patterns reminiscent of visual peering movements are suggestive of the active generation of sensory flow, but how motion contributes to the disambiguation of the electrosensory world remains unclear. Here, we show that a dipole-like electric field geometry coupled to motion provides the physical basis for a novel, non-visual parallax. We then show in a behavioral assay that this cue is used for electrosensory distance perception across phylogenetically distant taxa of weakly electric fish. Notably, these species electrically sample the environment in temporally distinct ways (using discrete pulses or quasi-sinusoidal waves), suggesting a ubiquitous role for parallax in electric sensing. Our results demonstrate for the first time that electrosensory information is extracted from sensory flow and used in a behaviorally relevant context. A better understanding of motion-based electric sensing will provide insight into the sensory-motor coordination required for active sensing in general, and may lead to improved electric-field based imaging applications in a variety of contexts.*

## **4.1 Introduction**

To form spatial representations, animals must estimate the relative distance of objects in their environment. Dynamic cues associated with

sensory flow can play a key role in this process. In vision, the motion parallax arising from changing viewpoints causes an object's image to move across a photoreceptor array with a speed that is inversely proportional to the object's distance (Kral, 2003; Ono and Wade, 2005). In this way, directed movement generates optic flow that provides important information for distance perception (Koenderink, 1986; Kral, 2003; Lee, 1980; Ono and Wade, 2005; Srinivasan, 2011). Here, we describe how a specific cue for distance perception arises from sensory flow during electric sensing by weakly electric fish.

The physics of electric sensing are similar across many species in the two independently-evolved families of electric fish (African Mormyrids and South American Gymnotiforms)(Lewis, 2014; Moller, 2005). These fish produce an electric organ discharge that is shaped by their body into an asymmetric dipole-like electric field (Figure 3.1A)(Assad et al., 1999; Caputi and Budelli, 2006; Pedraja et al., 2014). Environmental perturbations of the electric field modulate the spatial pattern of voltage across the fish's skin; this *electric image* provides a blurry representation of the environment but is nonetheless the sensory basis for object localization, prey capture and navigation in the dark (Nelson and MacIver, 2006; Rasnow, 1996; von der Emde and Fetz, 2007). A number of static cues related to the electric image have been linked to electrosensory distance perception (Lewis and Maler, 2002; Rasnow, 1996; von der Emde et al., 1998), but how fish use motion-based sensory flow is not clear. Indeed, the stereotyped *va-et-vient* swimming resembling visual peering movements (Lannoo and Lannoo, 1993; Snyder et al., 2007; Toerring and Belbenoit, 1979) strongly suggests that dynamic cues are extracted through the generation of sensory flow

(Hofmann et al., 2017, 2014, 2013; Stamper et al., 2012). In addition, electrosensory neurons encode a wide range of spatiotemporally-varying stimuli that could arise from sensory flow (Krahe and Maler, 2014; Metzen et al., 2016; Stamper et al., 2013). Interestingly, in the context of looming objects, these neurons have recently been shown to implement a focusing mechanism that correlates well with classic behavioral data (Clarke et al., 2013, 2015; Heiligenberg, 1973). However, it has not yet been possible to predictably manipulate electrosensory flow thereby testing the hypothesis that motion-generated cues are used for electric sensing.

In the following, we describe how the electric image is shaped by a dipole-like electric field geometry such that relative motion generates a cue similar to visual parallax. Then, by manipulating this electrosensory parallax cue in a behavioral assay, we show that both Mormyrid and Gymnotiform species exploit this cue for electrosensory distance perception.

## 4.2 Methods

### 4.2.1 Animals

Wild-caught *Gnathonemus petersii* (either sex, 10-15 cm body length (bl)) and *Eigenmannia virescens* (either sex, 8-15 cm bl) as well as captive-bred *Apteronotus albifrons* (either sex, 9-14 cm bl) were obtained from commercial fish dealers and housed in groups of 5-10 in aerated flow-through tanks. Water temperature was 24-29°C and water conductivity between 150-300  $\mu\text{S} \cdot \text{cm}^{-1}$  with a light-dark cycle of 12L:12D. Fish were fed blood worms to satiation three times per week. All procedures for animal maintenance and preparations comply with the current animal protection

law of the Federal Republic of Germany, approved by the local authorities LANUV NRW: 87-51- 04.2010.A202 and by the University of Ottawa Animal Care Committee (protocols BL-229 and BL-1773).

#### **4.2.2 Measuring the electric field and electric image**

To record and map the electric field (electric organ discharges, EODs; Figure S4.2), animals were initially anesthetized with Hypnomidate ( $2\text{mg} \cdot \text{L}^{-1}$ , Janssen-Cilag, Neuss, Germany) as in previous studies (Engelmann et al., 2006). Under this anesthesia, fish ventilate autonomously and show a reduced and regularized EOD rhythm while leaving EOD waveform and EOD amplitude unaltered. Following anesthesia, fish were moved to the experimental tank (Perspex tank  $30 \cdot 30 \cdot 15\text{cm}$ ;  $100\mu\text{S} \cdot \text{cm}^{-1} \pm 5 \mu\text{S} \cdot \text{cm}^{-1}$ ) and restrained in a holding apparatus, with anesthesia maintained at a lower dose ( $1\text{mg} \cdot \text{L}^{-1}$ ). At the end of the experiment, fish recovered quickly upon transfer to a recovery tank containing fresh water.

To record the electric field of *Gnathonemus* (N=5) a custom-built tetrode (X-Y-Z and reference; pairwise spacing of electrodes was 5mm) was moved in a plane alongside the fish's dorso-ventral axis by aid of a computer-controlled cantilever with a step motion profile (steps of 2.5 mm). At each position, at least 8 EODs were recorded for the rostro-caudal, medio-lateral and dorso-ventral planes. EODs were amplified (10x Gain Cyberamp, Axon Instruments), conditioned (band-pass filter 100Hz-10kHz, Cyberamp, Axon Instruments) and digitized (250kHz, PCIe-6341, National Instruments) using MatLab (Spike Hound v1.2, Gus Kbott III; for Matlab 2015a, The MathWorks Inc). The voltage gradient was determined by

calculating the average peak-to-peak amplitude of all EODs recorded at a given position.

To record electric images (EI; Figure S4.2) in *Gnathonemus* (N=5) a dipole electrode (spacing of 1 mm) oriented perpendicular to the fish's skin was used. The lateral distance of this electrode was fixed and adjusted to the closest possible distance between electrode and the animal's skin. The electrode was then moved along the rostral-caudal axis at this fixed lateral distance. The electrode's position was stored for every EOD recorded along the trajectory. From this we obtained the mean EOD peak-to-peak amplitude as a function of rostral-caudal position of the electrode, which was fitted using a smoothing spline (Matlab 2015a). This procedure was carried out without an object (unperturbed) and with an object (metal sphere,  $d = 2\text{cm}$ ) introduced at a defined rostral-caudal location and at different lateral distances (perturbed). From this, the EI was calculated as the ratio of the perturbed and the unperturbed EI profile. All distances (experimental and modeling results) refer to the distance between the mid-body axis of the fish and the surface of the object.

### **4.2.3 Modeling the electric field and electric image**

Two different approaches were used to model the electric fields and EIs. The results shown in Figures 4.1, S4.1 & S4.2 were calculated using the boundary element method, BEM (Hofmann et al., 2017; Pedraja et al., 2014; Rother et al., 2003); the electric images were calculated as described for the experimental data (modulation of perturbed vs unperturbed condition). To calculate the electric images produced by the Perspex shuttle (Figure S4.3), we used a previously described finite-element model (FEM)

for the electric field of *Apteronotus* (Babineau et al., 2007, 2006). The FEM approach is more suitable for complex heterogeneous geometries, such as those involved in the shuttle. However, since detailed FEM descriptions for *Gnathonemus* and *Eigenmannia* are not currently available, we used the BEM for all species comparisons.

#### 4.2.4 Behavioral experiments

Weakly electric fish track and center between pairs of moving vertical rods (Bastian, 1987), Perspex plates (Heiligenberg, 1973) and window gratings of a Perspex shuttle box (Stamper et al., 2012) using their electric sense. We took a hybrid approach, using two parallel (15 cm long and 8 cm high) Perspex plates with either a vertical cut-out (slit; 6 mm width) or a vertical aluminium stripe of similar dimensions (6 mm width, 1mm thick). As described in Figure S4.3, we found that a slit (or aluminium stripe) in such a plate mimics a vertical rod from an electrosensory point-of-view, but the Perspex plate had the advantage of increasing the reliability of centering.

Fish were moved to a test tank (61.4 · 31.8 · 31 cm for *Eigenmannia* and 49.6 · 29.6 · 20 cm for *Apteronotus* and *Gnathonemus*) with a water level of 10cm, temperature of 23-29°C and water conductivity of 185-230  $\mu\text{S}\cdot\text{cm}^{-1}$  (*Eigenmannia*) and 100-110  $\mu\text{S}\cdot\text{cm}^{-1}$  (*Gnathonemus* and *Apteronotus*). The two Perspex plates were positioned in the middle of the test tank, in parallel and 4cm apart (Figure 4.3A). In experiments with *Eigenmannia* the movement was generated with linear actuators and controlled with custom software (PROmech LP28, Parker.com with Labview, NI.com), while for *Apteronotus* and *Gnathonemus* plates were moved by aid of EPOS2 24/5

hardware and actuators (Maxon Motor GmbH, Munich, Germany) controlled with custom software (Matlab 2015a). In the control condition, both plates moved in phase with a speed of  $2 \text{ cm} \cdot \text{s}^{-1}$  and a cycle period of 6s (*Eigenmannia*) or 8s (*Apteronotus* and *Gnathonemus*), such that the range of movement was  $\pm 3\text{cm}$  or  $\pm 4\text{cm}$ . In the test conditions, one plate was moved at 90% or 70% of the control speed (i.e.  $1.8 \text{ cm} \cdot \text{s}^{-1}$  or  $1.4 \text{ cm} \cdot \text{s}^{-1}$ ); both plates remained in phase with the same cycle period, while the slower plate moved over a smaller range. Within a session, 12 trials (9 for *Eigenmannia*) were obtained per fish. Between trials, the plates remained stationary (50s or 30s for *Eigenmannia*). Parallax trials were randomly presented (70% or 90% speed condition) and alternated with both plates moving at 100% speed. To exclude side-biases, each parallax condition was presented on the left and on the right side of the shuttle in random order. All trials were video-recorded from above at 30 fps under infrared lighting using a Canon FS30 camcorder (Canon Canada Inc., Mississauga, ON, Canada) or an AVT Marlin F-131 (Allied Vision Technologies, Stadtroda, Germany).

#### **4.2.5 Behavioral Analyses**

Custom written Matlab routines and VideoPoint 2.5 analysis software were used to measure the lateral (right-left) and longitudinal (front-back) coordinates of the fish and moving plates every 33ms (30fps, *Apteronotus* and *Gnathonemus*) or 200ms (5fps, *Eigenmannia*). Data from repeated control trials for an individual fish were pooled. The variable of interest was the lateral position of the fish, which was defined as zero when centered between the two plates, and greater than zero when closer to the slow side



(or right side in the control condition; Figure 4.3A). Histograms of the lateral position were constructed (0.1 mm bins, interpolated to 0.02 mm for plotting; Figure 4.3B). We quantified the position change between control and parallax trials (i.e. the skew of the position distributions) as the change in position of 90% quantile of the position distribution; in other words, the fish was to the right of this position 10% of the time; Figure 4.3B, arrows). Choosing a different quantile (i.e. 50% or 95%) produced qualitatively similar results. Statistical analyses on the shifts in position (data in Figure 4.3C) were performed using multiple linear regression (species and speed condition as explanatory variables) and the Wilcoxon-signed-rank test for individual comparisons. The shift data for *Apteronotus* and *Gnathonemus* passed the Shapiro-Wilk normality test ( $p=0.76$  and  $p=0.44$  respectively), but that for *Eigenmannia* deviated slightly ( $p=0.04$ ), so data were log-transformed for the regression analysis. Head positions were used to calculate the speed of longitudinal motion (back-and-forth) over all fish for control and 70% parallax conditions. These were expressed as absolute speeds with the sign set to express the direction relative to the moving shuttle, i.e. positive speeds indicate movement of the fish in the same direction as the shuttle, while negative values indicate movement in the opposite direction (Figure 4.4).

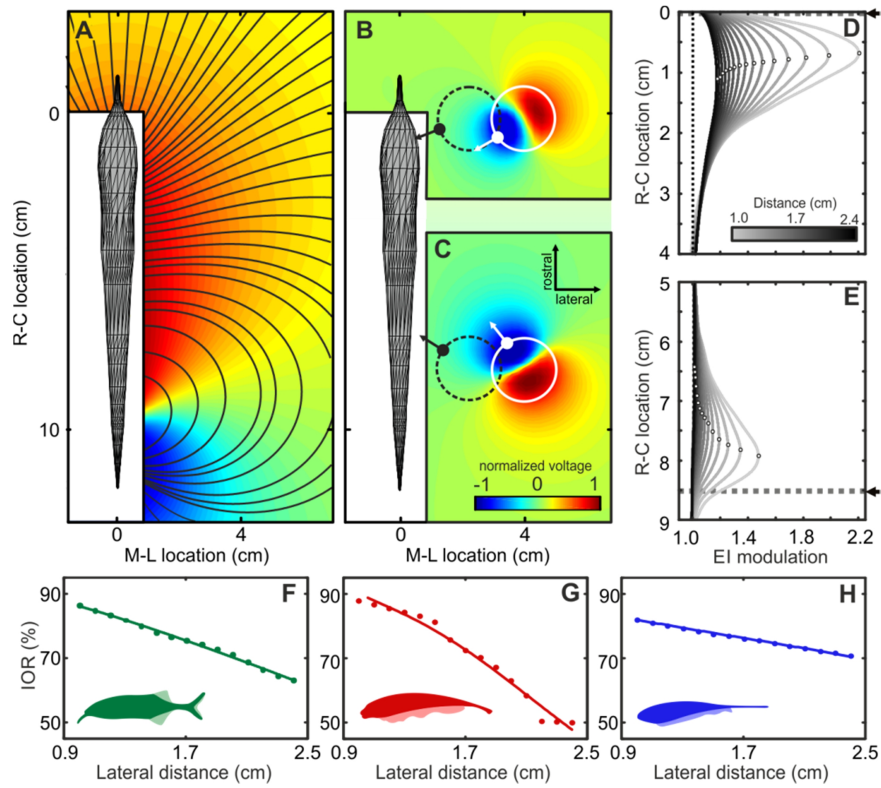
## 4.3 Results

### 4.3.1 Sensory basis of electrosensory motion parallax

To understand the information content of the electric image, we must consider the change in the electric field caused by an object, the *field perturbation* (Figure 4.1B-C)(Caputi and Budelli, 2006; Rasnow, 1996).

The field perturbation shows that the object is polarized, with the gradient of the polarization (Figure 4.1B-C, white arrows) oriented along the electric field lines (black contours, Figure 4.1A). Due to the changing curvature of the field lines, the polarization gradient rotates towards the mid-body as an object moves away from the fish (Figure 4.1B-C, compare black and white arrows; Figure S4.1).

This has marked effects on the electric image (Figure 4.1D-E; Figure S4.2): as the lateral distance of the object increases, the amplitude of the image decreases (compare light to dark curves), while the peak of the image (open circles on each curve) shifts towards the mid-body (caudally in D, rostrally in E), even though the true rostral-caudal location of the object is constant (dashed lines and arrow). Therefore, as a fish swims by an object, the electric image travels a length along the skin ( $\Delta_{\text{image}}$ ) that decreases systematically with increased lateral distance of the object, even when the actual rostral-caudal translation ( $\Delta_{\text{object}}$ ) is constant. We verified this relationship in three species across the lineages of weakly electric fish using the image-object ratio ( $\text{IOR} = \Delta_{\text{image}}/\Delta_{\text{object}}$ ; Figure 4.1F-H; Figure S4.2). From the negative slope of the IOR curves, it follows that the electric image of a nearby object will move faster across the body than the image of a more distant object. Thus, the electric field geometry together with relative motion produces a speed-based cue for distance perception that is similar to motion parallax in vision (Kral, 2003; Ono and Wade, 2005).



**Figure 4.1:** (*Cont. next page*). **Physical basis of electrosensory motion parallax.** **A.** Top view of the basal electric field of *Gnathonemus petersii* computed using a Boundary Element Method (BEM) electric field model (see Methods). Normalized voltage is shown as a color-map (red positive and blue negative); electric field lines are indicated by black contours. The white areas close to the fish comprise points where data could not be obtained in the corresponding physical measurements (see Figure S2). **B-C.** Electric field perturbations due to a metal sphere (1 cm radius) positioned at two different rostral-caudal locations (B: rostral; C: caudal) and a lateral distance of 2.9 cm. The field perturbation (plotted as normalized voltage; see color bar) is defined as the difference between the electric field with and without the object present. The position and size of the sphere is indicated by the white circle. The polarization gradient of the object (white arrows) is roughly aligned with the field lines of the unperturbed field (see black contour lines in A). Accordingly, the gradient differs by almost  $90^\circ$  for the rostral and the caudal object. The dashed black circles represent the spheres at a distance of 1.1 cm from the fish with the corresponding polarization gradient shown by the black arrows. At this closer lateral distance, the angular difference of the polarization gradients is smaller than when the object is further away (white circles, see also Figure S1). **D-E.** Electric images (EI) of the sphere at different lateral distances (1 – 2.4 cm; see greyscale bar) for the same rostral-caudal positions as in B and C, respectively. The location of the object along the rostral-caudal axis is indicated by the dashed lines in both panels (fish mouth at  $x = 0$  cm). Note that the amplitude of the EI decreases with increasing lateral distance, while the EI peak (open circles) shifts towards the mid-body. **F-**

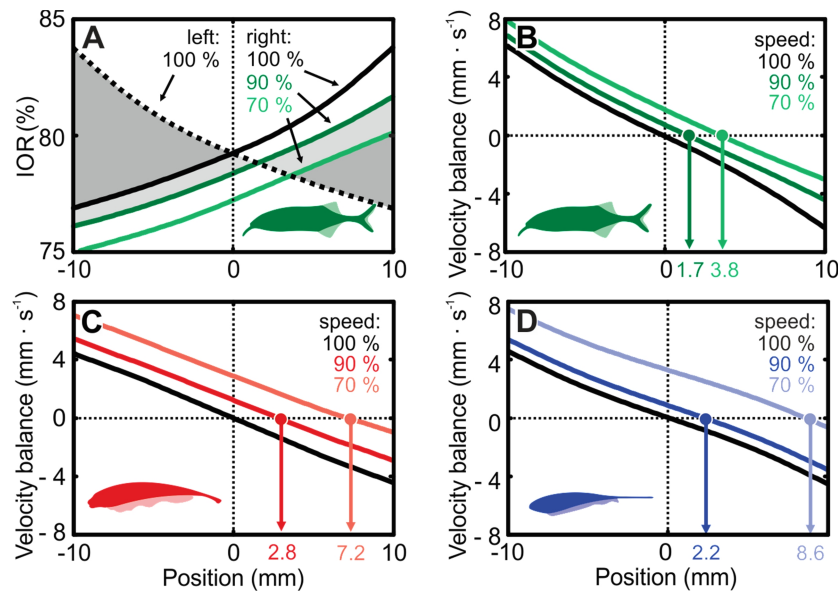
**H.** The image-object ratio (IOR) measured using BEM electric field models for three different species. The IOR is the ratio (in %) of the shift of the EI peak ( $\Delta_{\text{image}}$ ) to the actual physical displacement of the object ( $\Delta_{\text{object}}$ ) for the two rostral-caudal object locations shown in B and C. The IOR decreased with distance in all cases, suggesting that a more distant object would appear to be moving slower during relative motion. Solid lines show power law fits to the measurements: RMSE *Gnathonemus petersii* (green): 0.38 %, *Apteronotus albifrons* (red): 1.82 %, and *Eigenmannia virescens* (blue): 0.14 %.

### 4.3.2 Predicting the magnitude of the parallax-induced shift

We next consider whether weakly electric fish actively exploit this electrosensory-based parallax cue. These fish are well-known to track the sidewalls of a moving shuttle-box while maintaining a centered position (Stamper et al., 2012), reminiscent of natural behaviors such as hovering and active exploration (Heiligenberg, 1973). We hypothesized that electrosensory motion parallax is one of the cues used to perform this behavior. We used the image-object ratio IOR as determined from our BEM simulations (Figure 4.1F - H) to predict how much the fish would shift its position under the different speed conditions (i.e. right shuttle wall moving at 90% and 70% of the left wall speed).

Figure 4.2 shows IOR curves for the right (solid black line) and left (dotted black line) sides of the shuttle in *Gnathonemus*. It is important to note that the IOR will vary quantitatively with the translation range and specific position of an object within the electric field. The IOR curves shown here were calculated using a longitudinal object translation of 8 cm (i.e. the magnitude of the shuttle's movement in the behavioral experiments). For the reduced-speed conditions (70 and 90%), the right side of the shuttle translates across a reduced range of the fish's electric field as compared to the 100% side. Thus, we re-calculated the IOR curves

accordingly (Figure 4.2 dark green: 90% object translation 7.2 cm; light green: 70%, 5.6 cm). Under the assumption that fish use electrosensory parallax, the point where the apparent speeds of left and right sides are the same predicts where the shuttle center position should be perceived.

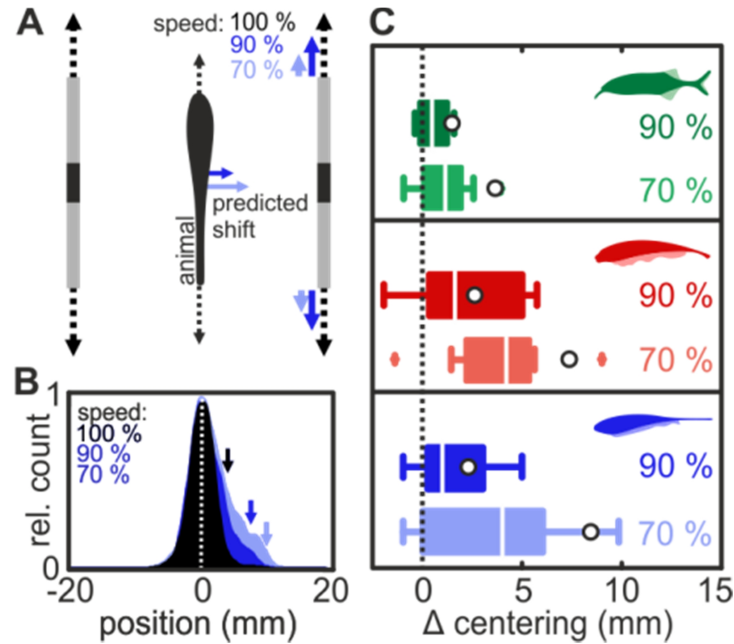


**Figure 4.2: Prediction of the perceptual center of the shuttle under different speed conditions for the different species.** **A.** IOR curves for BEM-data in *Gnathonemus* assuming a rostral-caudal object translation of 8 cm (100% speed condition). Black dotted line shows the IOR for the left side of the shuttle object, and the solid black line shows the data for the right side. For the different speed conditions, the relative translation of the object decreases on one side (dark green: 90% = 7.2 cm; light green 70% = 5.6 cm). As a result, the characteristics of the IOR curves change and the curves are offset along the y-axis. **B.** Velocity balance (difference in left vs. right IOR curves shown in A, and scaled to 2 cm s<sup>-1</sup>) for control (black line) and parallax speed conditions (dark green: 90%; light green: 70%) for *Gnathonemus*. The location at which the velocity balance curve intercepts the abscissa predicts the perceptual center of the shuttle. Based on the IOR data calculated for *Gnathonemus*, this was shifted 1.7 mm (90%) and 3.8 mm (70%) from the actual center towards the slower side of the shuttle. **C-D.** Same as B but for *Apteronotus* (C, predicted perceptual center 90%: 2.8 mm; 70%: 7.2 mm) and *Eigenmannia* (D, 90%: 2.2 mm; 70% 8.6 mm).

We calculated *velocity balance* curves from the left-right IOR differences ( $\text{IOR}_{\text{left}} - \text{IOR}_{\text{right}}$ ) scaled to a reference speed of  $2 \text{ cm} \cdot \text{s}^{-1}$ . Under control conditions (both sides move at 100%), this curve is zero (balanced) at position 0 (Figure 4.2B, solid black line). If the right side moves more slowly, the velocity balance between left and right sides shifts upwards by an amount proportional to the right-left speed difference (Figure 2B, dark green: 90%; light green: 70%). Similarly, we calculated velocity balance curves for *Apteronotus* (Figure 4.2C) and *Eigenmannia* (Figure 4.2D). These curves were used to predict the magnitude of the animals' shift in our behavioral experiments (next section), based on the notion that the centered position is perceived differently in the different speed conditions.

### **4.3.3 Behavioral test of the electrosensory parallax hypothesis**

To elicit centering behavior, we used a shuttle comprising two Perspex sidewalls, each with a narrow vertical slit that produces an object-like electric image (Figure 4.3A; Figure S4.3; see Methods). If our hypothesis is true, moving one sidewall more slowly than the other should cause the fish to perceive the slower side as farther away and then shift its position towards the slower side to maintain the perception of being centered (Figure 4.3A). We estimated the magnitude of this shift using the IOR curves for each species (Figure 4.2) and predicted that the fish should shift its position by an amount that depends on speed condition (slow side moving at 90% and 70% of the reference side; Figure 4.3C open circles).



**Figure 4.3: Behavioral test of the electrosensory parallax hypothesis.** **A.** Schematic drawing of the behavioral setup: Top view of a fish positioned between the moving shuttle walls (grey) with a slit (black) acting as a conductive object. Control condition: both sides move back-and-forth in phase at 2 cm s<sup>-1</sup> (dashed black arrows; Methods). Parallax conditions: one side (left) moving at 2 cm s<sup>-1</sup> and the other (right) moving in phase at 1.8 cm s<sup>-1</sup> (90% speed, blue) or 1.4 cm s<sup>-1</sup> (70% speed, light blue). The colored arrows beside the fish indicate the predicted change in centering for each condition under the assumption that electrosensory parallax is used to estimate lateral distance. **B.** Normalized distributions of fish position during centering behavior in *Eigenmannia*: control condition (N = 21, black), 90% speed (N = 11, dark blue) and 70% speed (N = 10, light blue). Note that for illustrative purposes the position data were adjusted to represent the parallax condition on the right while the experimental conditions were tested on either side at random. With a stronger parallax cue, the skewness of the position distributions increased as quantified by the 90% quantiles (see arrows). **C.** Behavioral change in centering for the three species tested (green: *G. petersii*; red: *A. albifrons*; blue: *E. virescens*). We quantified the behavioral responses as the change in position of the 90% quantile of the position distributions between control and parallax conditions ( $\Delta$  centering); boxplots show shift in position; median, interquartile range (bars), 1.5 times the interquartile range (whiskers) and outliers (+). For each species, we found a significant shift towards the slower side (Wilcoxon-signed-rank test, *G. petersii*: (90%) N = 10, p = 0.04; (70%) N = 9, p = 0.02; *A. albifrons*: (90%) N = 9, p = 0.03; (70%) N = 9, p = 0.01; *E. virescens*: (90%) N = 11 fish, p = 0.02; (70%) N = 10 fish, p = 0.03). Open circles represent the predictions of the perceptual shuttle center during parallax conditions based on our EI simulations for each species (Figure 4.2).

To test our parallax hypothesis, we video-recorded individual fish in the moving shuttle under infrared illumination (Methods). When both sides of the shuttle moved in tandem at the same speed ( $2 \text{ cm} \cdot \text{s}^{-1}$ ), fish remained centered (Figure 4.3B, black). When the speed of one of the sides was decreased while remaining in phase with the opposite side, the fish moved closer to the slower side (Figure 4.3B-C; dark colors:  $1.8 \text{ cm} \cdot \text{s}^{-1}$  or 90% of the reference speed; light colors:  $1.4 \text{ cm} \cdot \text{s}^{-1}$  or 70% speed).

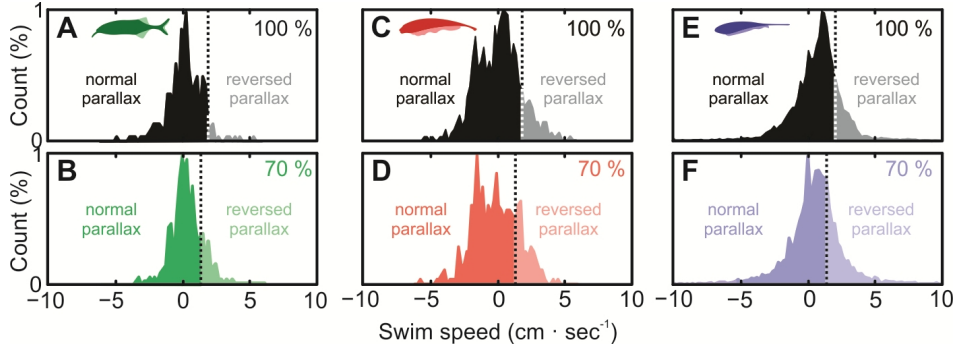
This shift in position was reflected in an increased skewness of the position distributions, so we quantified responses using the change in position of the 90% quantile (Figure 4.3B, see arrows). We found a systematic and significant change in centering in both speed conditions for all species tested (Figure 4.3C;  $F_{3,54} = 3.71$ ,  $p = 0.017$ ). While it is possible that natural centering behavior also involves visual and mechanosensory cues (Nelson et al., 2002; Stamper et al., 2012; Sutton et al., 2016), we were able to rule out these influences in our experiments: first, we performed all experiments in the dark, and thus no visual information was available to the fish (Ciali et al., 1997); second, fish did not shift position when provided with mechanosensory cues alone, i.e. when electrosensory cues were absent (Figure S4.4). In summary, although the lateral position of the shuttle walls was constant, changing their longitudinal speed caused the fish to move towards the slower side. While these shifts are small (1 cm), they are behaviorally relevant, as prey detection and the inspection of larger objects occur on similar spatial scales (Hofmann et al., 2017; Nelson and MacIver, 2006).

As predicted, the shift in position differed in magnitude between speed conditions, but there was also variation across individuals and species



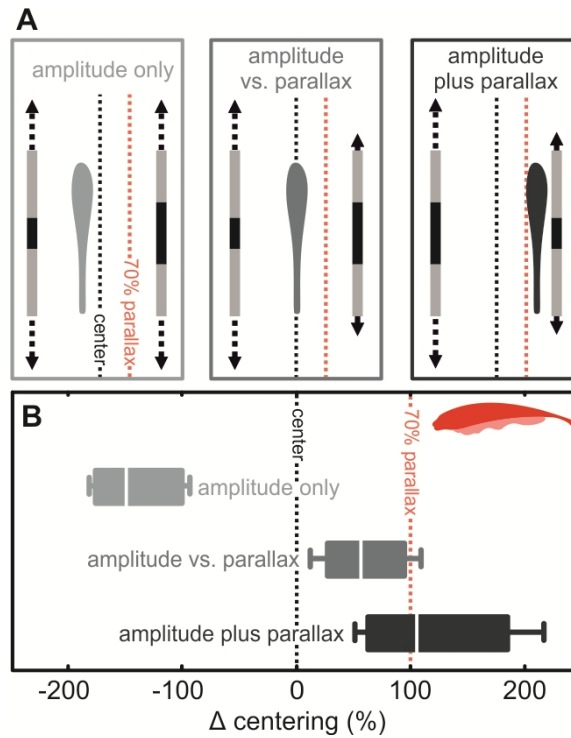
(Figure 4.3C). Some of this variability will be due to differences in fish size and details of the electric field geometry, as well as differences in life history (Moller, 2005), neuronal processing (Bell and Maler, 2005; Caputi et al., 2005), or kinematic abilities (Hofmann et al., 2014; Sutton et al., 2016). As in visual depth perception (Kral, 2003; Ono and Wade, 2005), there are also multiple electrosensory cues that could be used in parallel during this centering task (Lewis and Maler, 2002). Indeed, the skewed distribution of fish positions and smaller-than-predicted shifts suggest that at least one other conflicting cue is involved. One such cue arises from the motion itself. For example, when fish swim faster than the average speed of the two sides of the shuttle, the translation of the electric image (determined by the relative velocity) will in fact be slower on the side of the faster-moving shuttle wall, rather than on that of the slower-moving wall. In this case, the parallax hypothesis predicts a conflicting response: the fish should move towards the faster side of the shuttle (due to its slower relative speed). In general, this occurred only during a fraction of the time (Figure 4.4); nonetheless, such a conflict would lead to a behavioral response that is smaller in magnitude than predicted theoretically.

Another cue fish could use for centering is the electric image amplitude, which is narrower and greater in amplitude when an object is closer (e.g. Figure 4.1D-E; Engelmann et al., 2008; Rasnow, 1996). Thus, an alternative centering strategy could involve comparing the amplitude of the electric image on both sides of the body. If the fish moves towards one side of the shuttle, the image amplitude on that side will increase, so the fish should move in the opposite direction to compensate. Importantly, this strategy is based on a static cue and is independent of the sensory flow (relative motion) required for parallax.



**Figure 4.4: Swimming speed during centering behaviour. Histograms of the swim speed during centering behavior in the three species.** A, C & E. Control data (both shuttle walls moving at the same speed) for each species (green: *G. petersii*; red: *A. albifrons*; blue: *E. virescens*). B, D & F. Data obtained for the 70% parallax condition. In all panels, positive speeds represent the fish moving in-phase with the shuttle walls and negative values out-of-phase. Vertical dotted lines in all graphs depict the critical speed that is the average speed of the two shuttle walls. Swimming at speeds above this critical speed during parallax trials (“reversed parallax”: light shaded regions) potentially leads to contradictory parallax information. For the majority of the data, swim speeds are below this critical value (“normal parallax”: dark solid color).

Therefore, in our centering assay, in which only the speed of the shuttle-wall changes, this *amplitude hypothesis* predicts that fish should remain centered under all speed conditions. To further explore this possibility, we performed a series of experiments during which such amplitude and parallax-based cues were in competition. Indeed, when the amplitude cue alone was presented, fish moved away from the larger amplitude stimulus (Figure 4.5). When both parallax and amplitude cues were presented in conflict (i.e. where amplitude and parallax cues predict shifts in opposite directions), the fish shifted to an intermediate position that was biased towards the slower-moving side predicted by the parallax cue (Figure 4.5). These results confirm that fish use multiple cues during centering behavior, however future work will be required to determine how these sensory cues are integrated.



**Figure 4.5: Static electric image cues contribute to the centering behavior.** **A.** To test the influence of image amplitude comparison between the two shuttle sides, we performed experiments (*Apteronotus*) using various combinations of shuttle motion speeds (slow and fast: 1.4 vs. 2 cm · s<sup>-1</sup>) and cue sizes (small vs. large: 1 vs. 2 cm metal slit). Specifically, we created experimental conditions in which only amplitude information was available (“amplitude only”: light gray & left panel), amplitude and parallax information were contradictory (“amplitude vs. parallax”: intermediate gray & middle panel), and where both cues provided consistent information (“amplitude plus parallax”: dark gray & right panel). The fish schematic depicts the predicted effects on fish centering behavior. **B.** Centering behavior for the three test conditions shown in panel A. The shift in fish position from the center of the shuttle (black dotted line) is shown relative to that observed during 70% parallax condition (red dotted line, see also Figure 2C). The behavioral responses were in line with predictions: (i) when the amplitude cue was presented without parallax information available (light gray), fish moved away from the shuttle center towards the smaller object (Wilcoxon signed rank test, compared to 70% parallax condition indicated by red dotted line; N = 6, p = 0.03); (ii) when parallax and amplitude cues were in conflict (intermediate gray), fish shifted their position towards the slower moving side (parallax) but the magnitude of the shift was reduced (N = 6, p = 0.03); and (iii) when amplitude and parallax cues were consistent (dark gray), the shift magnitude was similar to those observed for the 70% parallax condition (with the distribution skewed to higher values; N = 6, p = 0.56).

That said, a stochastic switch between parallax-based and amplitude-based centering strategies could underlie the skewed position distributions observed experimentally (Figure S4.5). Additional competing or complementary influences may be involved as well. When a fish scans an object, the spatial aspects of the electric image are transformed into a local temporal pattern of input to the skin electroreceptors (the *temporal* electric image). Closer objects, with narrower images, lead to higher rates of change in this temporal input (Hofmann et al., 2017, 2013). Importantly, the temporal electric image and motion parallax cues are inseparable due to their mutual dependence on electric field geometry: motion parallax increases the speed of image translation for closer objects and thus increases the rate of change of the temporal electric image. In conclusion, our behavioral results can be explained by a centering strategy that uses electrosensory parallax and at least one other electrosensory-based cue.

## 4.4 Discussion

The two lineages of weakly electric fish have independently-evolved electrosensory systems, but have similar electric field geometries (Assad et al., 1999; Caputi and Budelli, 2006; Moller, 2005). We describe a novel electrosensory parallax that arises directly from the electric field geometry and provide behavioral evidence that fish use this cue to estimate distance. The fact that independently-evolved species exhibit similar behavioral responses strongly suggests that electrosensory parallax is a robust cue for electric sensing. Both lineages exhibit similar stereotypical swimming movements (e.g. *va-et-vient* scanning) during electrosensory-based behaviors (Hofmann et al., 2014; Lannoo and Lannoo, 1993; Nelson and MacIver, 2006; Stamper et al., 2012; Toerring and Belbenoit, 1979). Such

motion will generate the electrosensory flow that leads to motion parallax (Hofmann et al., 2017, 2013; Stamper et al., 2012), but how the electric fish brain controls the necessary movements remains unknown. The neural coding of image shape and motion is very different between pulse-type Mormyrid (*Gnathonemus*) and wave-type Gymnotiform (*Apteronotus* and *Eigenmannia*) fish; the sensory encoding stage primarily involves a latency code in the former and a rate code in the latter (Sawtell et al., 2005). Recent studies have identified motion sensitive neurons in the midbrain of a Gymnotiform fish (Chacron and Fortune, 2010). The responses of these neurons are likely optimized by specific swimming movements (Hofmann et al., 2013; Stamper et al., 2012; Xiao and Frost, 2013), but how they might be involved in distance perception is not clear. Interestingly, the centering behavior performed by electric fish is similar to that exhibited by flying insects (Srinivasan, 2011) and walking humans (Duchon and Warren, 1994; Koenderink, 1986; Lee, 1980; Serres and Ruffier, 2017), where flow from the right and left visual fields is thought to be actively balanced. Our results suggest that electric fish use a similar strategy during centering behavior; shifting to the slower side effectively increases the speed of electric image translation on that side, therefore balancing the perceived electrosensory flow on both sides of the animal. A better understanding of such strategies, as well as the cues available for electric-field-based sensing, will provide important insight into the worlds of electrosensory animals, and may also lead to better sensing systems for robotics, human-computer interfaces, and medical imaging.

## 4.5 Conclusion

Through specific movements, animals can structure the dynamics of sensory inputs to optimize perception. In vision, side-to-side peering can provide distance information from visual parallax. Weakly electric fish exhibit swimming patterns reminiscent of visual peering, but there is no direct evidence that these fish use motion-related cues for electric sensing. Indeed, how a dynamic environment is perceived through an electrosensory lens remains unclear. By combining computational modeling and a direct behavioral test, we demonstrate that temporal dynamics, along with a dipole electric field geometry, generates a novel parallax-like cue that weakly electric fish from two independent taxa exploit for distance perception. Studying weakly electric fish will lead to a better understanding of active sensing and the fundamental principles of sensory processing.

## 4.6 Bibliography

- Assad C, Rasnow B, Stoddard PK. 1999. Electric organ discharges and electric images during electrolocation. *J Exp Biol* 202:1185-1193.
- Babineau D, Lewis JE, Longtin A. 2007. Spatial acuity and prey detection in weakly electric fish. *PLoS Comput Biol* 3:e38.
- Babineau D, Longtin A, Lewis JE. 2006. Modeling the electric field of weakly electric fish. *J Exp Biol* 209:3636-51.
- Bastian J. 1987. Electrolocation in the presence of jamming signals: behavior. *J Comp Physiol A* 161:811-24.
- Bell C, Maler L. 2005. Central neuroanatomy of electrosensory systems in fish In: Bullock TH, Hopkins CD, Popper AN, Fay RR, editors. *Electroreception*. New York: Springer. pp. 68-111.
- Caputi a. a., Budelli R. 2006. Peripheral electrosensory imaging by weakly electric fish. *J Comp Physiol A Neuroethol Sens Neural Behav Physiol* 192:587-600.
- Caputi AA, Carlson BA, Macadar O. 2005. Electric Organs and Their Control In: Bullock TH, Hopkins CD, Popper AN, Fay RR, editors.

- Electroreception. Springer New York. pp. 410-451.
- Chacron MJ, Fortune ES. 2010. Subthreshold membrane conductances enhance directional selectivity in vertebrate sensory neurons. *J Neurophysiol* 104:449-62.
- Ciali S, Gordon J, Moller P. 1997. Spectral sensitivity of the weakly discharging electric fish *Gnathonemus petersi* using its electric organ discharges as the response measure. *J Fish Biol* 50:1074-1087.
- Clarke S, Naud R, Longtin A, Maler L. 2013. Speed-invariant encoding of looming object distance requires power law spike rate adaptation. *PNAS* 110:13624-13629.
- Clarke SE, Longtin A, Maler L. 2015. The neural dynamics of sensory focus. *Nat Commun* 6:8764.
- Duchon AP, Warren WH. 1994. Robot navigation from a Gibsonian viewpoint. *Proc IEEE Int Conf Syst Man Cybern* 3:2272-2277.
- Engelmann J, Bacelo J, Metzen M, Pusch R, Bouton B, Migliaro A, Caputi A, Budelli R, Grant K, von der Emde G. 2008. Electric imaging through active electrolocation: Implication for the analysis of complex scenes. *Biol Cybern* 98:519-539.
- Engelmann J, Bacelo J, van den Burg E, Grant K. 2006. Sensory and motor effects of etomidate anesthesia. *J Neurophysiol* 95:1231-1243.
- Heiligenberg W. 1973. Electrolocation of objects in the electric fish *Eigenmannia*. *J Comp Physiol* 87:137-164.
- Hofmann V, Geurten BRH, Sanguinetti-Scheck JI, Gómez-Sena L, Engelmann J. 2014. Motor patterns during active electrosensory acquisition. *Front Behav Neurosci* 8.
- Hofmann V, Sanguinetti-Scheck JI, Gómez-Sena L, Engelmann J. 2017. Sensory flow as a basis for a novel distance cue in freely behaving electric fish. *J Neurosci* 37:302-312.
- Hofmann V, Sanguinetti-Scheck JI, Kunzel S, Geurten B, Gómez-Sena L, Engelmann J. 2013. Sensory flow shaped by active sensing: sensorimotor strategies in electric fish. *J Exp Biol* 216:2487-500.
- Koenderink JJ. 1986. Optic flow. *Vis Res* 26:161-179.
- Krahe R, Maler L. 2014. Neural maps in the electrosensory system of weakly electric fish. *Curr Opin Neurobiol* 24:13-21.
- Kral K. 2003. Behavioural analytical studies of the role of head movements in depth perception in insects, birds and mammals. *Behav Process* 64:1-12.
- Lannoo MJ, Lannoo SJ. 1993. Why do electric fishes swim backwards? An hypothesis based on gymnotiform foraging behavior interpreted

- through sensory constraints. *Environ Biol Fishes* 36:157-165.
- Lee DN. 1980. The optic flow field: the foundation of vision. *Phil Trans R Soc Lond B* 290:169-179.
- Lewis JE. 2014. Active electroreception: signals, sensing, and behavior. *The Physiology of Fishes, Fourth Edition*. pp. 375-390.
- Lewis JE, Maler L. 2002. Blurring of the senses: common cues for distance perception in diverse sensory systems. *Neuroscience* 114:19-22.
- Metzen MG, Krahe R, Chacron MJ. 2016. Burst Firing in the Electrosensory System of Gymnotiform Weakly Electric Fish: Mechanisms and Functional Roles. *Front Comput Neurosci* 10:1-17.
- Moller P. 2005. *Electric fishes: history and behavior*. London: Chapman and Hill.
- Nelson ME, MacIver MA. 2006. Sensory acquisition in active sensing systems. *J Comp Physiol A Neuroethol Sens Neural Behav Physiol* 192:573-586.
- Nelson ME, MacIver MA, Coombs S. 2002. Modeling electrosensory and mechanosensory images during the predatory behavior of weakly electric fish. *Brain Behav Evol* 59:199-210.
- Ono H, Wade NJ. 2005. Depth and motion in historical descriptions of motion parallax. *Perception*.
- Pedraja F, Aguilera P, Caputi A a., Budelli R. 2014. Electric Imaging through Evolution, a Modeling Study of Commonalities and Differences. *PLoS Comput Biol* 10.
- Rasnow B. 1996. The effects of simple objects on the electric field of *Apteronotus leptorhynchus*. *J Comp Physiol A* 178:397-411.
- Rother D, Migliaro A, Canetti R, Gómez L, Caputi A, Budelli R. 2003. Electric images of two low resistance objects in weakly electric fish. *Biosystems* 71:169-177.
- Sawtell NB, Williams A, Bell CC. 2005. From sparks to spikes: Information processing in the electrosensory systems of fish. *Curr Op Neurobiol* 15:437-443.
- Serres JR, Ruffier F. 2017. Optic flow-based collision-free strategies: From insects to robots. *Arthropod Struct Dev* 46:703-717.
- Snyder JB, Nelson ME, Burdick JW, Maciver MA. 2007. Omnidirectional sensory and motor volumes in electric fish. *PLoS Biol* 5:e301.
- Srinivasan M V. 2011. Visual control of navigation in insects and its relevance for robotics. *Curr Op Neurobiol* 21:535-43.
- Stamper SA, Fortune ES, Chacron MJ. 2013. Perception and coding of envelopes in weakly electric fishes. *J Exp Biol* 216:2393-2402.



- Stamper SA, Roth E, Cowan NJ, Fortune ES. 2012. Active sensing via movement shapes spatiotemporal patterns of sensory feedback. *J Exp Biol* 215:1567-74.
- Sutton EE, Demir A, Stamper SA, Fortune ES, Cowan NJ. 2016. Dynamic modulation of visual and electrosensory gains for locomotor control. *J R Soc Interface* 13:20160057.
- Toerring MJ, Belbenoit P. 1979. Motor programmes and electroreception in mormyrid fish. *Behav Ecol Sociobiol* 4:369-379.
- von der Emde G, Fetz S. 2007. Distance, shape and more: recognition of object features during active electrolocation in a weakly electric fish. *J Exp Biol* 210:3082-3095.
- von der Emde G, Schwarz S, Gomez L, Budelli R, Grant K. 1998. Electric fish measure distance in the dark. *Nature* 395:890-894.
- Xiao Q, Frost BJ. 2013. Motion parallax processing in pigeon (*Columba livia*) pretectal neurons. *Eur J Neurosci* 37:1103-1111.



Passive and active electroreception during  
agonistic encounters in the weakly electric fish  
*Gymnotus omarorum*

# 5



A version of this chapter has been published:

**Pedraja, F.;** Perrone R.; Silva, A.; Budelli, R.; 2016. *Passive and active electroreception during agonistic encounters in the weakly electric fish Gymnotus omarorum*. Bioinspir. Biomim. 11(6):065002.

*Agonistic behaviour related to territorial defence is likely to be costly in terms of energy loss and risk of injury. The importance of obtaining information of a potential opponent to fight could influence the contest. We here study electric images of the territorial and aggressive weakly electric fish *Gymnotus omarorum* in the context of agonistic behaviour. We show that passive and active electric images may drive the approach towards an opponent. The likelihood of first attacks can be predicted in these fish based on electric image information, suggesting that aggressive interactions may in fact be triggered through the passive electrosensory information.*

## **5.1 Introduction**

Animals fight for limited resources like territory, food and mates (Nelson, 2006). When two fish perceive the presence of a contender, they have to approach each other to evaluate the opponent and eventually initiate or refuse the struggle. Far-range sensory modalities (vision and smell, for example) are particularly important to provide information to approach each other and for pre-contest rival fighting ability (resource holding potential, RHP) assessment. Nocturnal animals or those living in turbid waters, as many electric fish, have developed another sophisticated sense: electroreception (Bullock and Chichibu, 1965; Lissmann, 1958). It has two electrosensory sub-modalities sensitive to transcutaneous electric fields (Lissmann and Machin, 1958). Passive electroreception allows the perception of electric fields produced by external electric sources, e.g. the muscles or electrochemical potentials of prey, predators, as well as the active electric signals of neighboring electric fish. Active electroreception senses and processes environmental perturbations in the electric field

generated by the fish's own electric organ (EO) (Bullock and Chichibu, 1965; Lissmann, 1958; Lissmann and Machin, 1958). These perturbations are induced by objects with impedance different from water (Knudsen, 1975). While ampullary organs detect low frequency environmental electric fields (passive electroreception), tuberous organs of varying morphology measure the high-frequency electric fields of the actively generated EOD (active electrolocation for self-generated EODs and passive electrolocation for EODs from other electric fish) for electroreception and social communication (Baker et al., 2013; Caputi and Budelli, 2006; Feulner et al., 2008; Kawasaki, 2009; von der Emde, 1999, 2006).

Both electroceptive modalities provide a spatially sampled measure of the local field intensity over the skin of the animal. This distribution typically is referred to as the electric image (EI), as defined by Caputi and Budelli (2006). We here distinguish two kinds of images: (1) images produced by the changes in the characteristics of an external electric field, and (2) images generated by distortions of the self-generated electric field. For simplification, we will refer to these as the passive and active EI, respectively.

For the resolution of agonistic encounters, electric fish could remotely assess the RHP of the contender through active or passive properties of the EIs, and thus avoid engaging in aggressive displays to solve the conflict. If these cues initially are insufficient for assessment and fish enter in the aggression phase, they can still use either sub-modality of the EI to localize and then approach their contenders better.

Most research has addressed the potential to obtain information about a conspecific based on passive EIs, since the attenuation of the field produced

by a conspecific is subjected to the spherical dissipation only once. Using playback experiments, in which a conspecific is mimicked through a pair of electrodes that deliver electric pulses, it was shown that fish align their body parallel to the electric field lines as they approach the playback electrodes (Hopkins, 2005). This results in an approach behaviour that is not based on the shortest path towards the EOD's source, but inevitably brings the fish towards the source. A consequence of this approach behaviour is that the passive EI will be located in the foveal region of the head (Hopkins et al., 1997; Westby, 1974).

Active EIs may also serve to localize and/or to assess a contender in agonistic behavioral contexts. In contrast to passive EIs, the animals can be expected to have access to this active EI information only in the near range. Regardless of this obvious disadvantage, active EIs do not depend on the contender emitting its own EOD; hence it may enable assessing quality and position of an electrically silent contender (Batista et al., 2012). For Mormyrid fish, for example, it was shown that they can localize novel objects in their environment based on their active EIs (Hofmann et al., 2013 and 2014). One potential cue that animals might use for this is the spatial pattern of the EI, as this enables the animal to precisely localize an object and to establish how far away the target is (von der Emde et al. 1999). Building on this idea, fish might also use the temporal pattern experienced by a single electroreceptor to extract the same information from a succession of EODs (Hofmann et al., 2012). In fact, recent results suggest that the integration of the own motion should enable fish to dynamically estimate the distance with increased sensitivity (Hofmann and Pedraja, personal communication). Taken together, these evidences suggest that EIs may be crucial in agonistic scenarios.

In this study, we aim to shed light on the role of EIs in the context of agonistic behaviour. For this, we focus on the so-called evaluation phase of the agonistic encounters between two conspecific pulse-like weakly electric fish (*Gymnotus omarorum*) and investigate how active and passive electroreception could aid in the decision of how to approach or retreat from rivals. We show that although size asymmetry between animals is the best proxy of contest outcome, small and large fish have the same chances to produce the first attack (when body sizes differ less than 25 %). Our computer modelling of the electric images shows that: both animals swim in a manner that maintains the maximum of the EIs (active and passive) on the front of their head. Furthermore, passive and active EIs of contenders differ such that passive EIs are most informative when contenders differ in size. This difference predicts the likelihood of first attacks in these fish, suggesting that aggressive interactions may in fact be triggered through the passive electrosensory information. Finally, modelling the fish in parallel and antiparallel disposition shows that theoretically, when the fish are side to side, information about the size of the contender arises. At a first glance, this might indicate that electroreception is important for RHP assessment.

## 5.2 Methods

### 5.2.1 Behavioral Protocol

Behavioural experiments of agonistic contests were conducted in dyads of *G. omarorum* in the non-reproductive period using the gate protocol (Batista et al., 2012; Silva et al., 2007; Silva et al., 2013; Zubizarreta et al., 2012). In this condition, it can be assumed that fish will fight over territory

only. Sixteen adult fish were grouped in dyads in which the weight of the smaller fish was 75% to 95% of the weight of the larger fish.

To characterize the approach trajectories in the evaluation phase of the agonistic contests and evaluate the electrical cues used by the fish, fish were videotaped from below in a glass-tank (110 cm · 80 cm · 25 cm). Three plastic gates initially separated the fish and ensured that animals were electrically isolated prior to the start of the experiment (Figure 5.1A). The isolation was checked by placing a single fish in each compartment and recording its EOD in the other compartments. The partitions separating the fish were opened 10 minutes after lights were turned off and fish were removed from the test arena 10 minutes after resolution of the conflict.

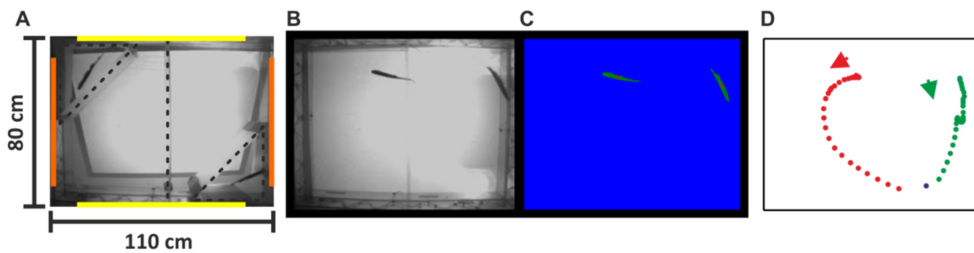
All experimental procedures were approved by the institutional ethical committee (Comisión de etica en el Uso de Animales (CEUA), Instituto de Investigaciones Biologicas Clemente Estable, MEC, 007/02/2010).

### **5.2.2 Behavioural Recording**

Methods of the simultaneous recordings of EOD and behavior have been previously described (Silva et al., 2007). In brief, the tank was fitted with two orthogonal pairs of electrodes; each pair attached to opposites walls (Figure 5.1A, orange and yellow lines). EODs were acquired by the two pairs of electrodes connected to amplifiers with high input-impedance (FLA-01, Cygnus Technologies, Inc.). Fish were held in their separate partitions of the tank for 2 hours before the experiment (water temperature: 20-22° C, conductivity: 100 µS). The experiments were performed in total darkness at night using IR-illumination (L-53F3BT, Fablet and Bertoni Electronics). The tank was filmed at 30 FPS (SONY CCD-Iris) and both



the images and EODs were digitized online (Pinnacle Systems PCTV HD Pro Stick). Using a routine in Matlab the midpoint and head location of each fish was obtained (Figure 5.1B and C). These data served as input to model passive and active EIs prior to the first attack (Figure 5.1D).



**Figure 5.1:** **A.** View of the set up (length 110cm, width 80cm, depth 25cm). The three partitions (dotted lines) are removed just prior to the start of the experiment. Yellow and orange bars represent the position of the electrodes. **B.** Frames from the video after removing the partitions. **C.** Positions (center of mass) of both animals as tracked offline for the frame shown in B. **D.** Sequence of positions of the two fish from the start to the end of an encounter. Here and in the following Figures, the colored arrows indicate the heading direction of both fish at the beginning.

The first attack latency was defined at the time of the first aggressive physical contact (bite or nudge) towards the other fish. Conflict resolution was established as the moment we observed the third consecutive retreat of one fish without attacking back. This criterion unambiguously defined subordination status (dominant and subordinate); fish fulfilling this requirement were never observed to change their status in the following 10 min of interaction (Batista et al., 2012).

### 5.2.3 Modeling the electric organ

To model the electric organ of *G. omarorum*, we used data published by Rodriguez-Cattaneo and colleagues (2013). To set the resistance of the

internal tissues and the skin, we used data from Caputi and colleagues (1995).

The voltage difference between 8 consecutive transverse planes of the fish placed at different sites of the body are mainly produced by the regions of EO encompassed by these planes and, according to Ohm's law, it is equal to the current (I) flowing through the internal tissues between each pair of planes times the resistance (R) of that section of the fish's body (Figure 5.2A). Then, from the resistance of the given section of the fish body (R) and the measured voltage (V) across it, we were able to calculate the current causing the voltage drop:  $I=V/R$ .

This is based on the simplifying assumption that for a small longitudinal region of the EO the electrocyte population is homogeneous and according to the simplest assumption, electrocytes within a short segment of the electric organ are oriented similarly and fire almost synchronously. Thus in the model, the current generated by the series of identical dipoles - mimicking the electrocytes inside a cylindrical body slice - is equivalent to a dipole. This is because the rostral pole of one dipole adds with the caudal pole of the next caudal dipole: consequently, all the intermediate poles are cancelled and the line of dipoles is equivalent to a single dipole with poles situated at the transverse planes limiting that portion of fish.

The longitudinal resistance (R) of a section of fish can be calculated from the geometry and resistivity ( $\rho$ ).

$$R=\dots l/S \quad (1),$$

where  $l$  and  $S$  are respectively the distance between recording electrode planes and the average cross-sectional area of the encompassed body portion.

Hence:

$$I=(V \cdot S) / (\dots \cdot l) \quad (2)$$

The poles lying on the plane separating contiguous longitudinal pieces of the fish can be reduced to one by addition, and the EO can be represented by a set of poles equal in number to the planes limiting the experimentally studied regions of the fish. This method requires to identify whether there are abrupt transitions in the regional EOD waveform and to place gap limiting planes at the transition points (Figure 5.2B). Since the shapes of the fish of a given species, is usually the same (they are homotetic) and the head to tail voltage, outside the water, is almost the same, the parameters of a given fish can be obtained from another fish with different size. The new model can be made from the other by multiplying the parameters from the original with constants of proportionality. Figure 5.2C shows the models of two fish and the resulting head to tail voltages calculated underwater (Pedraja et al., 2014; Sanguinetti-Scheck et al., 2011).

#### **5.2.4 Modeling electric images**

Modeling of EIs was done using software developed by Diego Rother (Rother, 2003). This model has two parts, a geometric reconstruction of the fish's body and a calculation of the transcutaneous field. The model was constructed under the following assumptions:

1) All media are ohmic conductors. This means that the vector representing the current density at the point  $\mathbf{x}$  ( $\mathbf{J}(\mathbf{x})$ ) is proportional to the vector electric field at the same point ( $\mathbf{E}(\mathbf{x})$ ). Then:

$$\mathbf{J}(\mathbf{x}) = \sigma(\mathbf{x}) \cdot \mathbf{E}(\mathbf{x}), \sigma(\mathbf{x}) > 0. \quad (3)$$

The proportionality constant  $\sigma(\mathbf{x})$ , is the volumetric conductivity at the point  $x$ .

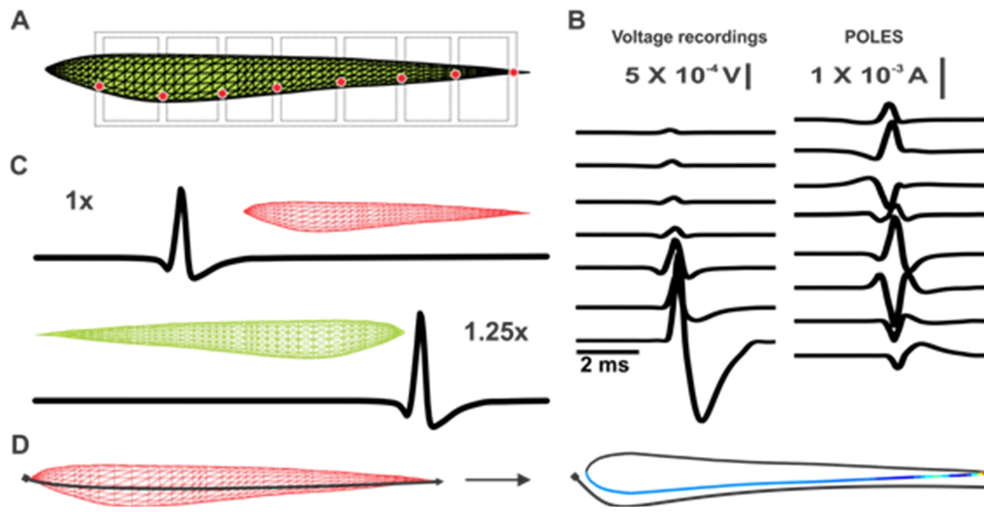
2) Given that the dielectric relaxation of the media is in general shorter than the minimum significant period of the EOD Fourier components, the model is an electrostatic approximation (Bacher, 1983).

3) The fish and other objects are immersed in an infinite water medium. The shapes of the fish body and objects are approximated by an external surface composed by triangles, allowing an approximation of the object shape that is limited only by the computation power available. Every object should be covered by a thin resistive layer (the skin in the case of the fish), which can be homogeneous or heterogeneous in resistance (magnitudes specified as desired).

The model is based directly on the charge density equation which, under our assumptions, implies that the charge generated by the sources ( $f(\mathbf{x})$ ) is equal to the charge diffusion ( $\nabla \cdot \mathbf{J}(\mathbf{x})$ )  $f(\mathbf{x}) = \nabla \cdot \mathbf{J}(\mathbf{x})$ , and therefore  $\sigma \nabla^2 \phi(\mathbf{x}) = \sigma \Delta \phi(\mathbf{x}) = f(\mathbf{x})$ , where  $\phi(\mathbf{x})$  is the local potential at point  $x$ .

This differential equation, the so-called Poisson equation, can be solved for the electric fish boundary using the Boundary Element Method (BEM) as proposed by Assad (Assad, 1997). Briefly, this method determines the boundary electrical distributions solving a linear system of  $S \cdot N$  equations

for  $S$  sources and  $N$  nodes, where the unknown variables are the trans-epithelial current densities and potentials that correspond to each node (for a detailed description of the method see (Hunter and Pullan, 2002)). The known variables were the location of the nodes, the location and magnitude of the poles representing the EO inside the fish, the conductance of the internal tissues, the skin and the water. It is important to note that, differently from Assad's method, a set of important constraints of the model were those posed by the electric organ equivalent sources that we measured experimentally using the air gap method. In the first instance, only trans-epithelial current densities and potentials are calculated at the *skin* nodes and these are then linearly interpolated in the triangles defined by the nodes. This allows the calculation of the potentials in the surrounding space. In this work, after the calculation of the transcutaneous current along the fish skin, a longitudinal section (on a horizontal plane) was taken to represent the EI (Figure 5.2D). Electric images throughout this manuscript are represented by the root mean square (RMS) transcutaneous current on each node. For active EI, we calculated the difference between the EIs in presence of the contender and in its absence. To represent the temporal change of both active and passive EIs we reduced the complexity of the EIs by analysing the along one horizontal line (Figure 5.2D).



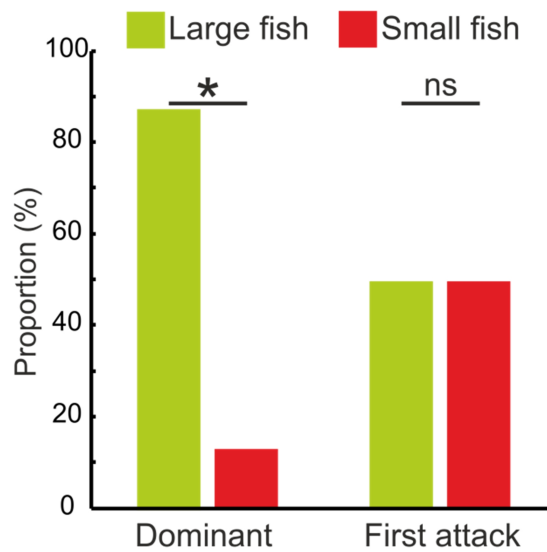
**Figure 5.2:** The model. **A.** The experimental set up for the determination of the EO sources. The fish is placed on a partition with eight electrodes placed at fixed distances (2.5 cm distance between electrodes). Red points show the position of the hypothetical sources (poles) of the EO model. **B.** Left. Voltages measured between neighbouring electrodes. Right. Magnitude of the poles (current sources or poles). **C.** Scheme of the 3D-nodes of a small fish (16 cm, red) and a large fish (20 cm, green) and the modelled head-to-tail EODs. **D.** Scheme showing how simplified 2D electric images were obtained along the horizontal line indicated by the black line on the left. The dorsal view on the fish at the height of this line is shown to the right with the currents density shown in a colour-coded manner. The black line next to the fish shows serves as a reference for the simplified scheme used in the following Figures to show the corresponding points of the skin. The square indicates the extreme frontal region and the arrow, the tip of the tail.

To visualize the spatio-temporal effect of behaviour on the EIs we stacked these simplified EIs for successive EODs to 2D temporal maps that represent the gradual change of the EIs over the body of the animals. Similar maps were created for simplified hypothetical trajectories. In these cases a marker to indicate the position of the maximum in each electrical image was superimposed to the 2D maps (Figure 5.6 and 7 black lines).

## 5.3 Results

### 5.3.1 Experimental analysis of real pre-contest behavior

Videos of both the evaluation phase (prior to first attack) and the contest phase (from first attack to contest resolution) were analyzed. Separating between contenders by size shows that in 7 out of 8 dyads the larger fish won (became dominant; Binomial test,  $p=0.03$ , marked with \* in Figure 5.3).

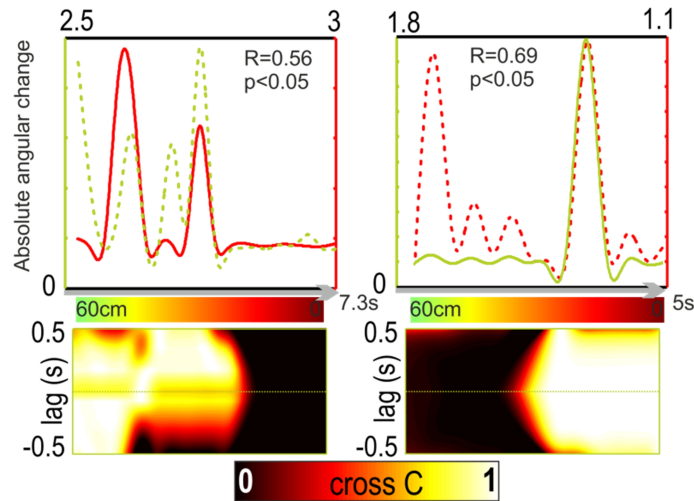


**Figure 5.3:** Proportion of winner (dominant) and first attack in dyadic interactions ( $n=8$ ). In most dyadic interactions, the larger fish won the fight (binomial test, \*  $p=0.03$ ). Instead, the first attack was made by any fish (binomial test, **ns**  $p=0.27$ ). Here and in the following, red indicates smaller and green larger fish.

This clear effect of size indicates that a pre-contest assessment of the size difference could be used by the animals to decide when to attack. If

this were the case we would expect that in the majority of cases the first attack is initiated by the larger fish. Nevertheless, we found no significant differences in the fist-attack rates between small and large fish (binomial test, no significant difference, ns  $p=0.27$ , Figure 5.3).

While these data indicate that contenders either cannot assess or, alternatively, do not use the information on size difference prior to engaging in agonistic behavior, the swimming behavior suggests that the fish used electric information of their contender in general. This is shown in Figure 5.4 where we analyzed the absolute angular body deviation of two exemplary dyads (upper panels) and the time sliding-window cross correlation of these data (bottom panels).



**Figure 5.4:** (*Cont next page*). Upper panels: absolute angular body changes of two dyadic encounters as a function of time. The angular body change was compute between consecutive frames. Throughout the manuscript, green shows data of larger fish and red that corresponding to smaller fish within dyadic pairs. Dotted lines correspond to the fish that made the first attack. R shows the correlation coefficients while p is the p-value computed by transforming the correlation to create a t-statistic having  $n-2$  degrees of freedom. Bottom panels: sliding-1 second's window cross correlation of the angular change showed in the



upper panels. A period of time between angular changes (lag) from the two fish of -0.5 to 0.5 seconds was chosen. Values that tend to 1 (represented with white in the color map) show a strong cross correlation (cross C).

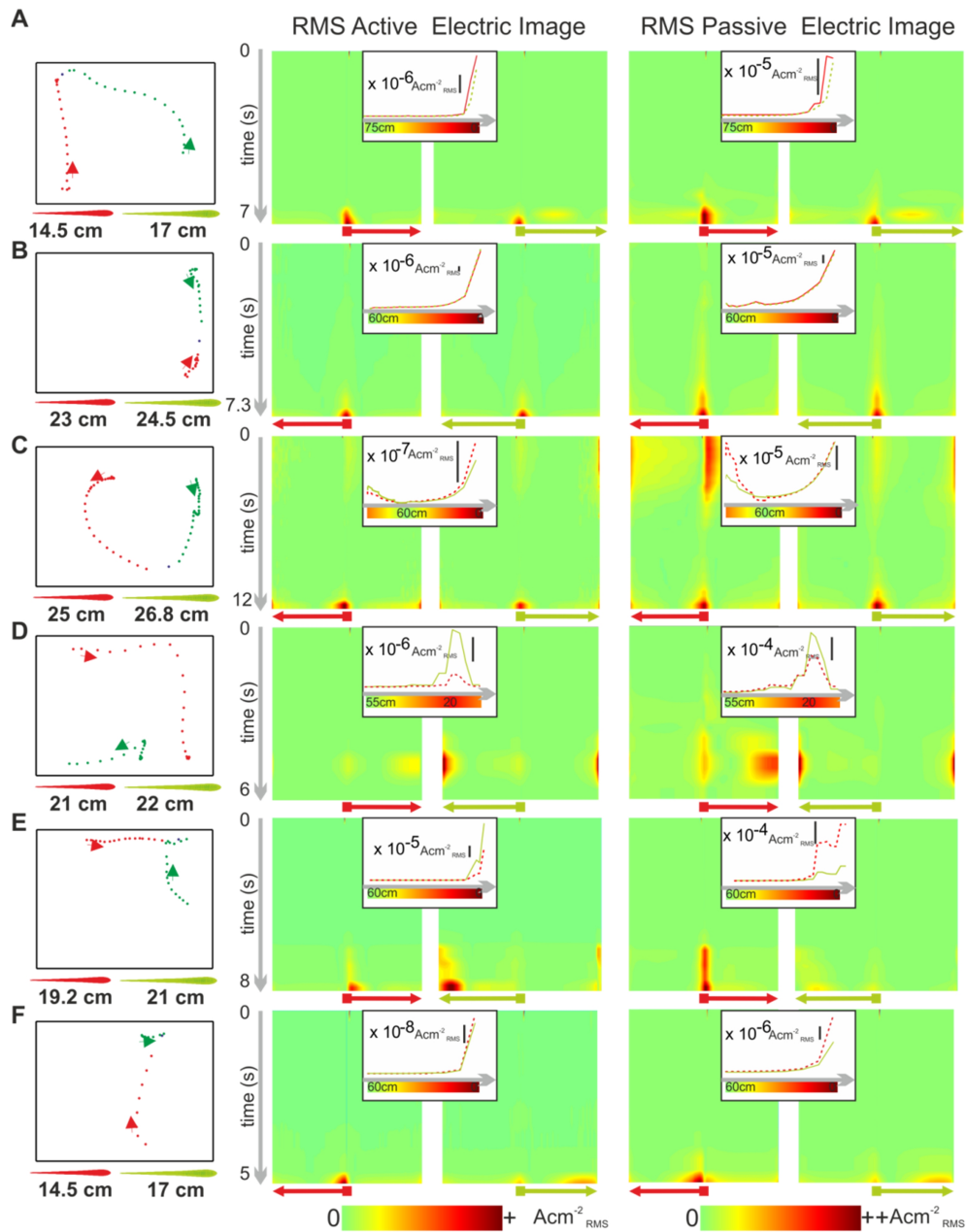
Our results show that the turning behavior was correlated, indicating that the fish have access to information of their rivals behavior and position even without visual input, since these experiments were conducted in darkness using IR-illumination. Similar data were found in five of the six dyads ( $R > 0.5$ , correlation coefficients;  $p < 0.05$ ). This motivated us to analyze the EIs associated with the specific behavior as this arguably is the most likely source of this information given the experimental design.

The above data show that fish use electric information prior to the first attack. Depending on the source of electric information being used, two different approach strategies can be expected: 1) using the passive EI information, following the field lines generated by the contender's EOD, or 2) using the active EI information, following the field lines generated by the perturbation produced by the presence of the contender by its own EOD.

Figure 5.5 shows the pre-contest phase of six dyads. While the left column shows the trajectories of the individuals, images to the right show the temporal series of EIs for these trajectories. EIs were calculated along a horizontal line (as showed in Figure 5.2D), both for the active (middle) and passive (right) EIs. The smaller fish is represented in red and the larger fish in green throughout the Figure. The insets in the middle and right columns show the maximum amplitude of each EI as a function of and proximity between contenders.

The first dyad (Figure 5.5A, left column) shows an indirect approach made by both fish that resulted in the bigger fish making the first attack. When the fish are close, they are placed with the heads almost touching each other and the bodies drawing an angle close to  $100^\circ$ . In this situation the maxima of the active and passive EIs are located at the head of both fish. In the bigger fish a second peak in the passive and active EIs appear on its right trunk. In the smaller fish a second peak appears on the left trunk, the side facing the contender, only for active images. Note that, while the amplitude of the maxima of the EIs is comparable between both fish, it peaks in the small fish for the final frames of the approach sequence (insets). The second dyad (Figure 5.5B) shows a direct frontal approach that resulted in the bigger fish attacking first. Both passive and active EIs are maximal at the rostral regions and the peak values of the sensory images are comparable throughout the approach in both fish (albeit slightly larger in the smaller fish, see insets). In the third dyad (Figure 5.5C) fish approached each other indirectly. Initially they were oriented about perpendicular to each other and the approach ended with fish facing each at an angle close to  $120^\circ$ , at which point the smaller fish attacked. At the beginning of the approach the EIs are located both in the frontal and caudal regions of both fish. As fish increased the distance between each other and turned, the EIs decreased in amplitude but remained maximal at the head until the distance between fish decreased again for the final section of the approach. During this phase the EIs increased, peaking at the rostral region of both fish but with a second maximum at the tail. The active EI maximum is higher in the larger fish at the beginning while it is smaller in this fish for the later phase. The passive EI maxima are higher in the smaller fish throughout the sequence.

The sequence shown in Figure 5.5D is the only initial approach sequence of the dyads where fish initially approach each other, but no physical contact was made and the larger fish retreated after the smaller fish had approached the larger fish in a roughly orthogonal manner. Prior to the larger fish retreating, passive and active EIs are maximal in the caudal regions with a second weaker peak in the frontal region in both fish. The maxima of both EI were larger in the larger fish (inset). However, the magnitude of the second EI-peak at the head region was constantly larger in the smaller fish. In the fifth dyad (Figure 5.5E) fish approach along perpendicular trajectories until the larger fish reaches the collision point, orients towards the approaching opponent which in this case attacked first. During the perpendicular approach the active and passive EI maxima are located in the caudal region in the larger fish while they are found in the frontal region for the smaller fish. While the magnitude of the active EI peak is higher in the bigger fish, it is the opposite for the passive EI. The approach trajectory in the sixth dyad (Figure 5.5F) also was almost perpendicular between the fish and resulted in the smaller fish attacking the larger one from behind. At this point the EIs are maximal in the rostral part of the smaller fish while they are found that the rostral and caudal region at the right side of the larger fish. The magnitude of both active and passive EIs was higher in the smaller fish (inset, note that the difference is higher when comparing EIs in the head region only as opposed to the absolute peaks).



**Figure 5.5:** (*Cont. next page*). Pre-contest phase in the agonistic encounter of *G. omarorum*. **A-F.** Left: approach trajectories. Points represent fish position and arrows indicate the initial heading direction. Green and red symbols represent the large and small fish, respectively; this color-coding applies to the whole Figure. Middle: RMS of active EIs of both fish for the behavior shown in the left. Note that zero in the x-axis represents the rostral part from which the electric image is being analyzed along a horizontal line to the left and right side of the animal (see Figure 5.1D). The zero in the y-axis is the start of the experiment (see grey

arrow) and the display ends at the time of the first attack. Right: RMS of passive EIs of both fish for the behavior shown in the left. The arrows below each panel point towards the side of the fish that is closer to the opponent at the end of the trajectory while the square represents the head region. Inset. Ordinates: maxima of active and passive EI of both fish. Data from the fish that attacked first is shown by the stippled lines. Abscissas: time (grey arrow) and distance between fish (color-coded bar). Note in C the maximum distance occurs in the middle of the time bar since one fish made an approach while the other fish swam away.

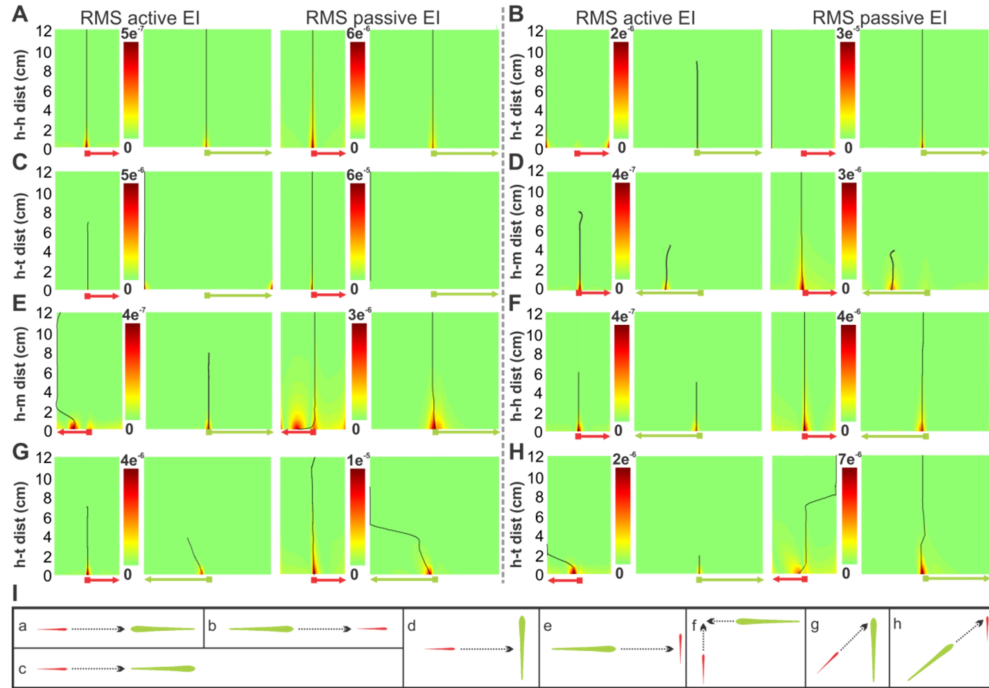
A common finding of the otherwise variable behavior shown in Figure 5.5 is that passive and active EIs are consistently centered on the head and tail regions, almost irrespective of the relative orientation between contenders. This can be explained in part by the elongated body shape tapering off towards the tail. This reduces the cross-sectional area towards the tail, increasing the resistivity and hence funneling electric currents (generated either by the fish itself- or by external sources) towards the head region (the region that also contains the highest density of electroreceptors, (Bacelo et al., 2008; Castello et al., 2000)). As a result the maximal current densities (and transcutaneous voltages) are at the head. A second trend that emerges from this analysis is the finding that the animal that perceives the larger passive EI amplitude is the one more likely to initiate an attack. While this was not significant given the low sample size (binomial test,  $p=0.09$ ,  $n=6$ ), it was found in 5 out of 6 cases. This indicates that information related to the attack is evaluated using passive EIs.

### **5.3.2 Canonical approaches**

To learn how images depend on the size and relative position of the fish, we studied the images produced in simplified collinear, orthogonal and 45° approaches to the head of a stationary fish (fish being 8 and 16cm). The

goal of this analysis is to understand the potential contribution of the two sub-modalities used in electrolocation (active and passive) in agonistic behavior.

When assuming collinear behavior (Figure 5.6A-C) the maxima remain localized at the tail when a fish is being followed, while they are maximal at the head in the follower fish or if animals face each other. Note that the EI-magnitude is almost always bigger in the smaller fish. The exceptions are the cases where the large fish approaches the caudal part of the smaller fish and vice-versa. In the first case the passive EI is larger in the larger fish, whereas in the latter case the active EI is bigger in the large fish (compare Figure 5.6B and C). In Figures 5-6 D and E we model orthogonal approaches. As expected, both active and passive EIs are maximal at the head for the approaching fish. Interestingly, we find that the EIs are bigger in the smaller fish when it is approached by a larger distant fish (Figure 6E). In this case the maxima of the EIs in the smaller fish for active and passive images are found at the tail and head, respectively. As expected, at closer range, both passive and active EIs are located in the middle of the trunk of the stationary fish, irrespective of its size. If both animals move along orthogonal trajectories (Figure 5.6F) the maxima are located at the head region facing towards the contender with the magnitude being bigger in the smaller fish. For an approach at an angle of  $45^\circ$  (Figures 5.6G and H) the maximum is always at the head of the approaching fish while the maxima in the stationary fish transverse from caudal to rostral. Again, EI magnitude is bigger in the smaller fish, except when the larger fish is approaching.



**Figure 5.6:** Electric Images with canonical approaches. **A-C.** Collinear approaches with A showing a frontal approach by a small fish and B an approach of a larger fish towards the rear of a stationary smaller fish. Distance in A is represented as head-to-head distance (h-h dist.) and as the distance from the head of the large fish to the tail of the small fish (h-t dist.) in B. C: same as in B but for the small fish approaching the larger one. **D-F.** Orthogonal approaches with the smaller fish approaching to the centre of a larger fish in D and vice versa in E. The distance is shown as the distance from the head of the approaching fish to the midline of the stationary fish (h-m dist.). F. Both fish approaching orthogonally with the distance being measured from head to head (h-h dist.). **G -H.** Approach at an angle of 45° with the small fish approaching the larger fish's head (G) and vice versa (H) (h-h dist.). The RMS of the current in active and passive EIs is color-coded. RMS values for passive EIs are shown to the left, those for active EIs to the right part, with data for the smaller fish at left. Black lines represent the location of the maximum EI on the body of the fish. Red and green arrow heads and squares represent one of the fish tail extreme and the fish head, respectively. The direction of the arrow shows the skin section closer to the other fish. For symmetric positions of the fish the arrows face to the right. **I.** Schematic representation of the trajectories analysed in A-H.

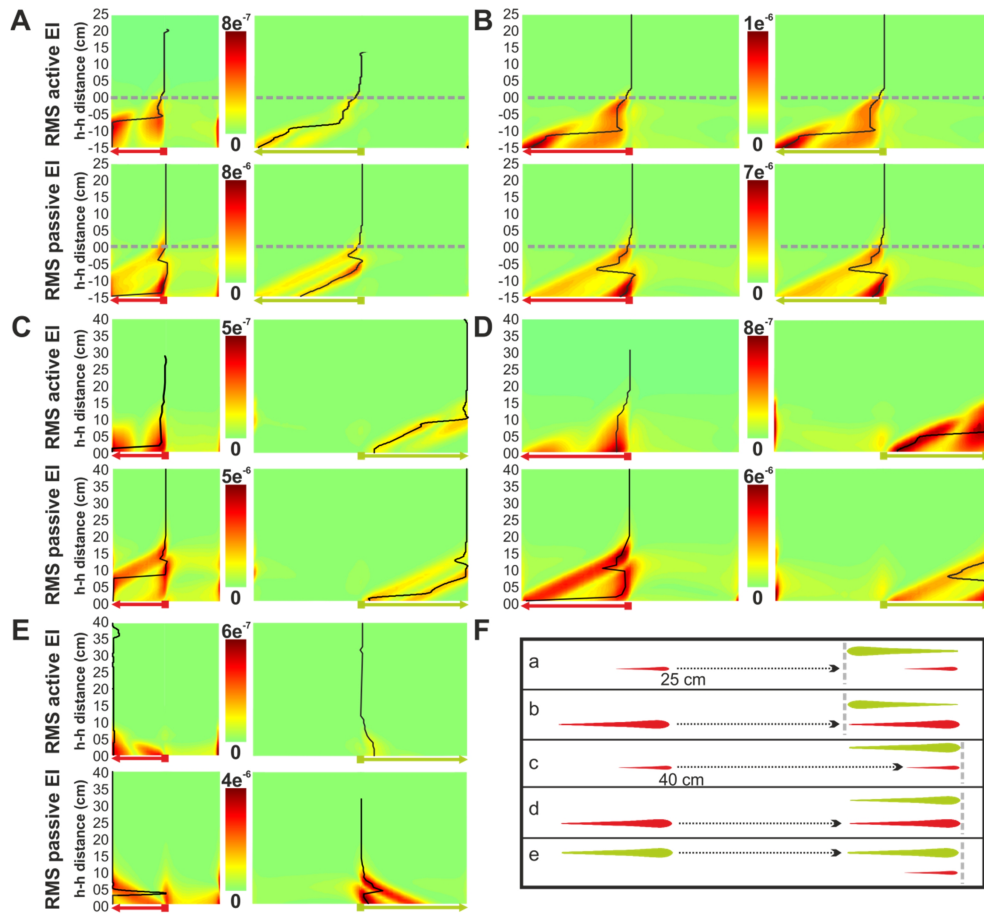
### **5.3.3 Parallel and anti-parallel approaches.**

A frequently observed behavior in electric fish is repetitive back-and-forth swimming along an object, *va-et-vient* (Toerring and Belbenoit, 1979). Such behavior is known to aid in electrolocation (Hofmann et al., 2014), but it also occurs in social interactions. We thus decided to study the impact of this behavior on passive and active EIs, both for parallel and antiparallel orientations, assuming a fixed lateral distance of 2.5 cm between fish. In Figure 5.7 the upper panels show results for active EIs, while lower panels show the corresponding passive EIs. Data in the left column summarizes results for differently sized fish (the smaller being half the size of the other fish), while results on same-sized interactions are shown in the right column. As expected, antiparallel orientation results in maximal EIs close to the tip of the head (Figure 5.7A-B) in both EIs and reach peak amplitude when contenders reach zero head-to-head distance. After this, the maxima move to the side of the trunk that faces the contender. Notably (see below), EIs now become double-peaked and the maxima finally move towards the tail. For same-size interaction (Figure 5.7B), the EIs are similar between contenders, due to the symmetry of the scene. When both fish face in the same direction, the maxima of the EIs are on the head of the approaching and on the tail of the fish being approached (Figures 5.7C-E). When the approaching fish gets closer, EIs maxima move to the tail of the approaching and the head of the approached fish.

Remarkably, there are two inversions of the movement direction of the maximum, which finally are situated at the tail of the moving and the head of the stationary animal. This is particularly evident for the passive EIs. Both for parallel and anti-parallel orientations of the fish, two-peaked EIs



occur. The distance between the peaks changes with difference in sizes between fish, an effect also seen in Figures 5.7A and B. From this, we hypothesized that *G. omarorum* may determine the size of a contender, using the distances between the two maxima during antagonistic displays.



**Figure 5.7:** Passive and active EIs for parallel and antiparallel approaches. **A-B.** Head-to-head approach of a small fish to a large stationary fish (8 and 16cm, A) and of two similarly sized fish (16 and 16 cm, B). Distance is given as head-to-head distance (h-h dist.). **C-E.** Head-to-tail approach of a small fish to the larger fish is shown in C, while D shows the same for two larger fish and E for a large fish approaching a smaller fish. EI amplitude is color-coded as the RMS of the current in each panel with the upper panels showing the active EI and the bottom panels showing the passive EI. Black lines in Figures A-E represent the location of the maximum of the EI on the fish skin. Red and green arrow heads and squares represent tail and head, respectively. The direction of the arrow shows the skin section closer to the other fish. If the position of both fish is symmetrical, the arrows point rightwards. **F.** Scheme of the modeled trajectories.

## 5.4 Discussion

Behavioural decisions are driven both by the expected benefits and the related costs. Agonistic behavior related to territorial defense, as the one studied here, is likely to be costly in terms of energy loss and risk of injury. Hence obtaining information about the opponent should influence aggressive behavior. For our model organism, the weakly electric fish *G. omarorum*, the ability to assess contender's fighting ability should be of particular benefit as it was shown that the difference in body mass is a good proxy for the outcome of agonistic behavior with 80% of fights being won by the heavier fish (Figure 5.3)(Batista et al., 2012). When considering the latency to the first attack in a smaller tank than the one used in our study and with dyad weight differences of either 0 to 5% or 25 to 40% (unpublished data), the first attack time was lower in low weight differences than in large weight differences ( $35.8 \pm 16.58$  s and  $58.4 \pm 17.58$  s respectively). This suggests that weight differences can be assessed by these fish, at least at close distance. If this information could be obtained from longer distances, it is expected that aggression might only occur in interactions of similarly sized fish, while in dyads with high weight asymmetry, smaller fish would give up the resource before engaging in aggressive interactions, or in case of occurring an aggressive encounter, they would never attack first. However, in our dyadic interactions with weight differences between 5% and 25% no correlation between first attack and weight was found (Figure 5.2). These results allow at least two explanations: a) *G. omarorum* do not assess contenders before engaging in physical contact, or b) they assess each other but being in a confined arena makes physical contact inevitable and results in fights.

These uncertainties lead us to the question of the physical information that fish may use for analyzing the RHP in general. At the beginning of an agonistic encounter the distance between the contenders is small enough to assume that the sensory signals used to detect the presence of other fish are: a) the lateral line system (Butler and Maruska, 2015) and/or b) the electrolocation system. While our behavioral data provided no evidence that *G. omarorum* use the electric sense to assess a contender and avoid physical contact, the analysis of the electric images associated with the behavior strongly suggest that EIs carry important information to guide the observed interactions. In 5 out of 6 cases, the fish that attacked first is the one that perceived the higher maximal passive EI amplitude. Most frequently, these passive EIs are larger in the smaller fish (Figure 5.5). Assuming that sensory thresholds are similar, smaller fish are thus more likely to detect a larger fish in most situations (Figures 5-6 and 7). In the case of passive EI, this effect is due to the fact that the EOD of the larger fish is stronger and hence can be sensed from farther away. Similarly, for the active EI, the modulation of the larger fish is stronger. To localize a contender from afar, our data suggest that electric fish should rely on passive information.

One way in which *G. omarorum* could obtain information about the RHP of the contender is making *va-et-vient* movements. Modeling of fish in parallel and antiparallel disposition (Figure 5.7) shows that when fish are side to side, the EIs of a fish on the other fish presents two maxima. The positions of these maxima are near the fish's trunk level. For active electrolocation, this region is especially suited to determine the shape or other properties of large objects (likes a conspecific fish). Probably, it cannot determine qualia of objects as electric-color or texture, but general shape, edges, etc. (Sanguinetti-Scheck et al., 2011). This strategy could be

used by the fish to recognize the contender size. However, we did not find this type of movements in our behavioral experiments.

Our data further show that the fish can use information about the contenders' trajectory to maintain a constant relative angle between the fish's heading directions and its target (Figure 5.4). Playback experiments showed that electric fish approach a static discharging fish (fixed electrodes mimics EODs) by turning their body axis parallel to the local electric field vector (Davis and Hopkins, 1988; Schluger and Hopkins, 1987). Rotation of the electrodes leads to predictable changes in the approaching trajectories (Hopkins et al., 1997). In our work, both fish are in constant movement, which means that the dipole field constantly changes position and orientation. Our analysis shows that these changes elicit a change in the receiving fish's trajectory, probably in order to match the new electric field geometry. As the behavioral analysis revealed that the passive EIs were almost always located at the head, fish simply could follow a strategy to turn toward that side of the body stimulated the strongest (as predicted by Kalmijn, (1988). To answer if this is an optimal chase behavior of constant bearing as known from other animals in prey-capture behaviors (Ghose et al., 2006; Olberg, 2012), further experiments are required. Notably, such a strategy would differ from what was found for prey detection and capture in South American electric fish (MacIver et al., 1999; Nelson and Maciver, 1999) and African mormyrids (von der Emde, 1994; von der Emde and Bleckmann, 1998).

This work can be considered an extension of the passive EI study, product of a conspecific discharge, which used computer models (Gómez-Sena et al., 2014). Trajectories as well as passive and active EIs in dyads of

the species *G. omarorum* were analyzed using the BEM and routines developed in order to assess the information available in the evaluation phase of the agonistic encounter. One limitation of our study is that EIs were modeled as if fish were swimming in a very large medium, not accounting for the actual boundaries of the experimental set up. This was done to keep complexity to a minimum and to reduce the computational load of our calculations, assuming that these limitations are not likely to influence our results on a qualitative level. We also did not account for the curvature of the fish bodies; this is a valid approximation given that in these experiments *G. omarorum* maintain a straight posture most of the time.

Our computational approach might be useful for other applications, for example in robotics. Robots solve different tasks under conditions unfavorable for visual guidance and in conditions where occlusion hinders optical navigation. Objects that generate electric fields could easily be localized; otherwise resistive objects could be detected based on the perturbing field.

## **5.5 Conclusion**

In summary we showed, using a modeling approach, that active and passive EIs provide cues for electric contender evaluation at intermediate distances. However, behavior shows that this important information is not used in RHP assessment. Passive electrosense is not known to be particularly suitable to directly localize distant objects, but was shown to be used in a gradient-balancing way to guide approaches towards sources along their field lines. At very short distances, the active electrolocation

system wins hierarchy producing different active EIs between fish that might be used during the agonistic contest.

## 5.6 Bibliography

- Assad, C., 1997, Electric field maps and boundary element simulations of electrolocation in weakly electric fish: Pasadena, California, California Institute of Technology.
- Bacelo, J., Engelmann, J., Hollmann, M., von der Emde, G., and Grant, K., 2008, Functional foveae in an electrosensory system: *J Comp Neurol*, v. 511, p. 342-59.
- Bacher, M., 1983, A new method for the simulation of electric fields, generated by electric fish, and their distortions by objects: *Biol Cybern*, v. 47, p. 51-8.
- Baker, C.V., Modrell, M.S., and Gillis, J.A., 2013, The evolution and development of vertebrate lateral line electroreceptors: *J Exp Biol*, v. 216, p. 2515-22.
- Batista, G., Zubizarreta, L., Perrone, R., and Silva, A., 2012, Non-sex-biased Dominance in a Sexually Monomorphic Electric Fish: Fight Structure and Submissive Electric Signalling: *Ethology*, v. 118.
- Bullock, T.H., and Chichibu, S., 1965, Further analysis of sensory coding in electroreceptors of electric fish: *Proceedings of the National Academy of Sciences*, v. 54, p. 8.
- Butler, J.M., and Maruska, K.P., 2015, The mechanosensory lateral line is used to assess opponents and mediate aggressive behaviors during territorial interactions in an African cichlid fish: *Journal of Experimental Biology*, v. 218, p. 3284-3294.
- Caputi, A., and Budelli, R., 1995, The electric image in weakly electric fish: I. A data-based model of waveform generation in *Gymnotus carapo*: *J Comput Neurosci*, v. 2, p. 131-47.
- Caputi, A.A., and Budelli, R., 2006, Peripheral electrosensory imaging by weakly electric fish: *J Comp Physiol A Neuroethol Sens Neural Behav Physiol*, v. 192, p. 587-600.
- Castello, M.E., Aguilera, P.A., Trujillo-Cenoz, O., and Caputi, A.A., 2000, Electroreception in *Gymnotus carapo*: pre-receptor processing and the distribution of electroreceptor types: *J Exp Biol*, v. 203 Pt 21, p. 3279-87.
- Davis, E.A., and Hopkins, C.D., 1988, Behavioural analysis of electric signal localization in the electric fish, *Gymnotus carapo* (Gymnotiformes): *Animal behaviour*, v. 36, p. 1658-1671.

- Feulner, P.G., Plath, M., Engelmann, J., Kirschbaum, F., and Tiedemann, R., 2008, Electrifying love: electric fish use species-specific discharge for mate recognition: *Biology letters*, 5(2):225-8.
- Ghose, K., Horiuchi, T.K., Krishnaprasad, P., and Moss, C.F., 2006, Echolocating bats use a nearly time-optimal strategy to intercept prey: *PLoS Biol*, v. 4, p. e108.
- Gómez-Sena, L., Pedraja, F., Sanguinetti-Scheck, J.I., and Budelli, R., 2014, Computational modeling of electric imaging in weakly electric fish: insights for physiology, behavior and evolution: *J Physiol (Paris)*, v. 108, p. 112-28.
- Hofmann, V., Geurten, B.R., Sanguinetti-Scheck, J.I., Gómez-Sena, L., and Engelmann, J., 2014, Motor patterns during active electrosensory acquisition: *Front Behav Neurosci.*, v. 8, p. 186.
- Hopkins, C.D., 2005, Passive electrolocation and the sensory guidance of oriented behavior, *Electroreception*, Springer, p. 264-289.
- Hopkins, C.D., Shieh, K.T., McBride, D.W., Jr., and Winslow, M., 1997, A quantitative analysis of passive electrolocation behavior in electric fish: *Brain Behav Evol*, v. 50 Suppl 1, p. 32-59.
- Hunter, P., and Pullan, A., 2002, FEM/BEM NOTES p [lola.unimo.it/fembemnotes.pdf](http://lola.unimo.it/fembemnotes.pdf).
- Kalmijn, A.J., 1988, Hydrodynamic and acoustic field detection. Sensory biology of aquatic animals, p. 83-130.
- Kawasaki, M., 2009, Evolution of time-coding systems in weakly electric fishes: *Zoological science*, v. 26, p. 587-599.
- Knudsen, E., 1975, Spatial aspects of the electric fields generated by weakly electric fish: *Journal of comparative physiology*, v. 99, p. 103-118.
- Lissmann, H.W., 1958, On the function and evolution of electric organs in fish.: *J. Exp. Biol*, v. 35, p. 156-191.
- Lissmann, H.W., and Machin, K.E., 1958, The mechanisms of object location in *Gymnarchus Niloticus* and similar fish: *J. Exp. Biol*, v. 35, p. 457-486.
- MacIver, M.A., Sharabash, N.M., and Nelson, M.E., 1999, Prey-capture behavior in gymnotid electric fish: motion analysis and effects of water conductivity: *J Exp Biol*, v. 204, p. 543-57.
- Nelson, M.E., and Maciver, M.A., 1999, Prey capture in the weakly electric fish *Apteronotus albifrons*: sensory acquisition strategies and electrosensory consequences: *J Exp Biol*, v. 202, p. 1195-203.
- Nelson, R.J., 2006, *Biology of aggression*, Oxford University Press.

- Olberg, R.M., 2012, Visual control of prey-capture flight in dragonflies: *Curr Opin Neurobiol*, v. 22, p. 267-71.
- Pedraja, F., Aguilera, P., Caputi, A.A., and Budelli, R., 2014, Electric imaging through evolution, a modeling study of commonalities and differences: *PLoS Comput Biol*, v. 10, p. e1003722.
- Rodriguez-Cattaneo, A., Aguilera, P., Cilleruelo, E., Crampton, W.G., and Caputi, A.A., 2013, Electric organ discharge diversity in the genus *Gymnotus*: anatomo-functional groups and electrogenic mechanisms: *J Exp Biol*, v. 216, p. 1501-15.
- Rother, D., 2003, Simulation of the Electric Image in Weakly Electric Fish: Montevideo, Universidad de la Republica
- Sanguinetti-Scheck, J.I., Pedraja, E.F., Cilleruelo, E., Migliaro, A., Aguilera, P., Caputi, A.A., and Budelli, R., 2011, Fish geometry and electric organ discharge determine functional organization of the electrosensory epithelium: *PLoS One*, v. 6, p. e27470.
- Schluger, J.H., and Hopkins, C.D., 1987, Electric fish approach stationary signal sources by following electric current lines: *J Exp Biol*, v. 130, p. 359-67.
- Silva, A., Perrone, R., and Macadar, O., 2007, Environmental, seasonal, and social modulations of basal activity in a weakly electric fish: *Physiol Behav*, v. 90, p. 525-36.
- Silva, A.C., Perrone, R., Zubizarreta, L., Batista, G., and Stoddard, P.K., 2013, Neuromodulation of the agonistic behavior in two species of weakly electric fish that display different types of aggression: *J Exp Biol*, v. 216, p. 2412-20.
- Toerring, M., and Belbenoit, P., 1979, Motor programmes and electroreception in mormyrid fish: *Behav. Ecol. Sociobiol*, v. 4, p. 369-379.
- von der Emde, G., 1994, Active electrolocation helps *Gnathonemus petersii* to find its prey: *Naturwissenschaften*, v. 81, p. 367-369.
- von der Emde, G., 1999, Active electrolocation of objects in weakly electric fish: *J. Exp. Biol.*, v. 202, p. 1205-15.
- von der Emde, G., 2006, Non-visual environmental imaging and object detection through active electrolocation in weakly electric fish: *J Comp Physiol A*, v. 192, p. 601-612.
- von der Emde, G., and Bleckmann, H., 1998, Finding food: senses involved in foraging for insect larvae in the electric fish *Gnathonemus petersii*: *J. Exp. Biol.*, v. 201, p. 969-980.



- Westby, G.M., 1974, Assessment of the signal value of certain discharge patterns in the electric fish, *Gymnotus carapo*, by means of playback: *J. Comp. Physiol.*, v. 92, p. 327-341.
- Zubizarreta, L., Perrone, R., Stoddard, P.K., Costa, G., and Silva, A.C., 2012, Differential serotonergic modulation of two types of aggression in weakly electric fish: *Front Behav Neurosci*, v. 6, p. 77.



Non-breeding territoriality and context-dependent aggression in the weakly electric fish,  
*Gymnotus omarorum*

# 6



A version of this chapter has been published:

Perrone R.; **Pedraja F.**; Valiño G.; Tassino B.; Silva A. 2019. *Non-breeding territoriality and context-dependent aggression in the weakly electric fish, Gymnotus omarorum*. Acta Ethol. 22(2):1-11.

*Agonistic behavior involves all the displays that arise when conspecifics compete for valuable resources. Once the conflict is resolved, dominants obtain priority access to the resource while subordinates lose it. Territoriality is often mediated by agonistic encounters when space is the resource animals compete for, and territory is the area from which subordinates are excluded. We aimed to evaluate how agonistic encounters mediate the acquisition of territories in the weakly electric fish, *Gymnotus omarorum*, which displays a well-documented non-breeding agonistic behavior very unusual among teleosts. When tested in intrasexual and intersexual dyads in small plain arenas, a sex-independent dominant-subordinate status emerges after highly aggressive contests in which subordinates signal submission by retreating and emitting submissive electric signals. We staged dyadic agonistic encounters using a large arena, in which the initial inter-individual distance resembled the one observed in nature. We observed the emergence of a dominant-subordinate status after longer but milder contests with rare electric signaling of submission; the persistence of dominance over time with no outcome reversion; and how dominants exclude subordinates from their conquered resource. Although the territorial behavior of *Gymnotus* has been put forth since pioneer reports, this is the first study to show how agonistic encounters mediate territoriality in this genus. Agonistic encounters of *G. omarorum* in the small arena resemble the characteristics of violent-like behaviors. The ease of shifting from aggression to violence by confinement and the use of electrical signaling of submission make this species superb model to explore new perspectives in territoriality assessment.*

## **6.1 Introduction**

Agonistic behavior, the social behavior related to conflict situations between conspecifics, has shaped sociality across evolution (Lorenz 1963). Conflicts arise because animals compete for different valuable resources

(space, food, mates, shelters, breeding sites, etc.), whose control increases their individual fitness (King 1973; Huntingford and Turner 1987; Briffa and Hardy 2013). In dyadic interactions, conflicts are resolved when one individual obtains priority access to the resource (dominant) while the other contender loses it (subordinate) (Nelson 2006; Briffa and Sneddon 2010). Though the behavioral traits displayed during contests might be extremely diverse across species, agonistic encounters often follow three phases: evaluation (pre-contest), contest, and post-resolution, with overt aggression usually occurring during the contest phase (Summers and Winberg 2006).

When space is the resource animals compete for, territory is the area from which intruders are excluded by some combination of advertisement, threat, and/or attack (Brown 1975). As a form of social dominance, territoriality is often mediated by agonistic encounters between conspecifics (Kaufmann 1983; Wilson 1975). It is well-known in many vertebrates that reproductive males (and also male-female dyads) usually defend territories and prevent the intrusion of competitors during the breeding season (Brown 1964; Clarke 1970; Davies 1976; Armitage 1977; Bakker and Sevenster 1983; Pröhl 2005; Huang et al. 2011). Less frequently, when space itself is the resource animals fight for, territorial defense can also be observed in males and females all year round in several species independently of gonadal hormones (Caldwell et al. 1984; Wingfield and Hahn 1994; Chiver et al. 2014). In these cases, the defense of territories may ensure the access to foraging areas across seasons (Black-Cleworth 1970). In addition, increasing the distance from one's nearest neighbors may give added protection from predators (Kaufmann 1983).

Population density is a well-known factor in determining the strength of intraspecific competition; as density increases (by increasing the number of individuals in a given space, or by space confinement), the rate at which animals interact with competitors obviously increases (King 1973; Kokko and Rankin 2006; Knell 2009). This general rule has been empirically confirmed in a wide variety of animals in which crowding generally increases aggressive behavior (Hazlett 1968; Alexander and Roth 1971; Turner et al. 1999; Buchwalder and Huber-Eicher 2004; Oldfield 2011). In particular, when the size of the territory was experimentally manipulated, an increase in intra-specific aggression was observed both in turkeys (Buchwalder and Huber-Eicher 2004) and Midas cichlids (Oldfield 2011).

South American freshwater weakly electric fish produce an electric organ discharge (EOD) commanded by a very well-known electromotor circuit (Stoddard 2002; Caputi et al. 2005), and shaped by their body into an asymmetric dipole-like electric field (Assad et al. 1999; Caputi and Budelli 2006; Pedraja et al. 2014). By means of this active electrosensory channel, electric fish can locate objects whose electrical properties differ from those of the surrounding water (electrolocation; Lissman 1958), and also communicate with conspecifics (electrocommunication; Hopkins 1972). In particular, fish can obtain important information of both the environment (territory quality) and the fighting ability of their contenders by information encoded in their EODs (Gómez-Sena et al. 2014; Pedraja et al. 2016). In addition, the EOD carries information about an individual's species identity, sex, and physiological state, coded both by the rate and waveform of the EOD (Caputi et al. 2005). Thus, in any given motor behavior, electric fish display not only locomotor traits but also conspicuous

social electric signals. Many studies have reported distinctive agonistic electric displays (either produced by dominants or subordinates) in several species of South American freshwater electric fish (Black-Cleworth 1970; Westby 1975a, b; Hagedorn and Zelick 1989; Hupé and Lewis 2008; Hupé et al. 2008; Triefenbach and Zakon 2008; Perrone et al. 2009; Batista et al. 2012; Perrone and Silva 2016, 2018).

The weakly electric fish, *Gymnotus omarorum*, displays a well-documented non-breeding agonistic behavior very unusual among teleosts (Batista et al. 2012; Silva et al. 2013; Jalabert et al. 2015; Zubizarreta et al. 2015; Quintana et al. 2016). When gonads are regressed, and no reproductive motivation is expected to drive competition, males and females, tested in dyadic encounters in confined arenas, fiercely compete for space in intrasexual and intersexual encounters. Under these experimental conditions, subordinates *G. omarorum* signal submission by both retreating and emitting submissive electric signals. The cessation in the emission of electric signals (offs) has been interpreted as an initial submissive signal; (Hopkins 1974; Westby 1975a; Hagedorn and Carr 1985; Zakon et al. 1991; Triefenbach and Zakon 2008; Fugère et al. 2011), chirps (brief, transient EOD modulations) have been described as late and more unambiguous signals of submission (Batista et al. 2012; Quintana et al. 2016) and an EOD rate rank between dominants and subordinates becomes evident immediately after contest resolution (Silva et al. 2013; Perrone and Silva 2018). The robustness and reliability of the agonistic behavior of *G. omarorum* in these laboratory conditions make this species an advantageous model system to contribute to the understanding of the neuroendocrine control of aggression (Zubizarreta et al. 2012; Silva et al. 2013; Perrone and

Silva 2018). Recent field preliminary observations of *Gymnotus omarorum* spacing in the wild suggest territoriality (L. Zubizarreta, personal communication). In the non-breeding season, adult males and females *G. omarorum* rest more than 1m apart from each other in the natural habitat. Although it is indisputable that in previously reported dyadic contests, individuals of *G. omarorum* compete for space, how agonistic encounters actually mediate territoriality remains unexplored in this species. Territoriality entails, by definition, the persistence of the dominant-subordinate status over time and the demonstration that the dominant proactively excludes the subordinate from the defended territory. Previous studies did not test neither the persistence of the hierarchy nor the exclusion of the subordinate except for a short time (10 min) after resolution. In addition, interindividual distance in the wild is approximately twice larger than the pre-contest interindividual distance of previous reports (L. Zubizarreta, personal communication). Therefore, it also remains unexplored if the size of the space fish compete for influences the characteristics of their agonistic behavior.

In this study, we aimed to demonstrate the territorial behavior of *Gymnotus omarorum* in laboratory settings by evaluating how spatial context impacts on the agonistic behavior of this species. We staged dyadic agonistic encounters using a large arena, in which the initial inter-individual distance resembled the one observed in nature. We were thus able to demonstrate a) the emergence of a clear dominant-subordinate status mediated by longer but milder contests in which electric submission signals are seldom observed; b) the persistence of dominance over time with no outcome reversion; and c) how dominants hold territory after contest resolution and exclude subordinates from their conquered resource.



## 6.2 Methods

### 6.2.1 Animals

We used 42 non-breeding adult *Gymnotus omarorum* (Richer-de-Forges et al. 2009), that ranged from 15 to 27 cm in body length and 9 to 52 g in body weight. Sex in *G. omarorum* is not externally apparent (neither morphologically nor electrophysiologically) and was determined either after the behavioral experiments (experiment 1) or before (experiment 2, in which only males were used) by gonadal inspection (Jalabert et al. 2015).

*Gymnotus omarorum* were collected using a fish detector as described elsewhere (Silva et al. 2003) in Laguna del Sauce (34° 51'S, 55° 07'W, Department of Maldonado, Uruguay), and housed in individual compartments in 500-l outdoor tanks for at least 10 days before the behavioral experiments. All environmental variables were kept within the normal range exhibited in the natural habitat in the non-breeding season. Water temperature ranged from 8 to 21°C, and natural photoperiod ranged from LD10:14 to LD11:13. Water conductivity was adjusted and always maintained below 200  $\mu\text{S} \cdot \text{cm}^{-1}$  by the addition of deionized water. Aquatic plants (*Eichhornia crassipes*, *Pistia stratiotes*, *Salvinia sp.*) covered the surface of the water and provided shelter for the fish. Fish were fed with *Tubifex tubifex* once a week.

Electric fish collection for experimental purposes was authorized by DINARA (National Direction of Aquatic Resources) and MGAP (Ministry of Agriculture and Fisheries), resolution No. 065/2004. All experimental

procedures complied with ASAP/ABS *Guidelines for the Use of Animals in Research* and were approved by our institutional ethical committee (Comisión Bioética, Instituto Clemente Estable, MEC, 007/05/2012).

### **6.2.2 Laboratory Settings**

Fish were placed in an experimental tank that allowed simultaneous video and electric recordings as described elsewhere (Silva et al. 2007). Briefly, the electric signals of freely moving fish were detected by two pairs of orthogonal fixed electrodes attached to each tank wall, connected to two high-input impedance amplifiers (FLA-01, Cygnus Technologies Inc.). We used two types of experimental tanks: a) the small arena, four 30-l glass aquaria (55 · 40 · 25 cm as described in (Batista et al. 2012); and b) the large arena, one 120-l glass aquaria (110 · 80 · 25 cm, as described in (Pedraja et al. 2016). The day–night cycle and the physicochemical parameters (water temperature, conductivity, and pH) of indoor tanks matched those of the outdoor housing tanks. All the experiments were performed in total darkness illuminated by an array of infrared LEDs (L53F3BT, Fablet & Bertoni Electronics) located above the tank. Weakly electric fish are not sensitive to infrared light (Ciali et al. 1997), and IR illumination has become the standard method to eliminate visual influences during behavioral testing (Maciver et al. 2001; Roth et al. 2011; Batista et al. 2012; Zubizarreta et al. 2015; Jun et al. 2016; Pedraja et al. 2018). An infrared-sensitive video camera (SONY CCD-Iris and RoHS CCD Digital Video Camera) was focused on the bottom of the tank. Images and electric signals were captured on a video card (EasyCap) and stored in the computer for analysis. The fish remained in the recording tank at constant

temperature (16–20°C) for 4-5 hours before the experiments.

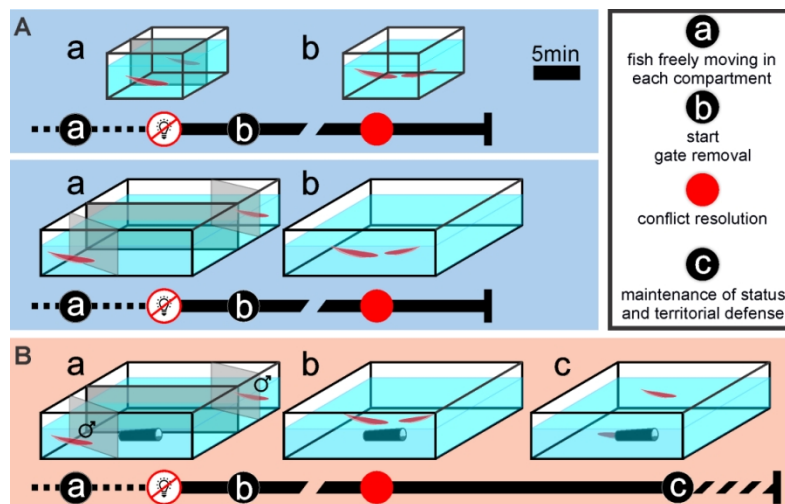
### **6.2.3 Behavioral Experimental Procedures**

All behavioral experiments were performed during the non-breeding season (occurring during the Austral fall-winter time, May-July) of 2016 (Experiment 1) and of 2017 (Experiment 2) to avoid any other type of agonistic interactions related to reproduction. We tested dyadic agonistic interactions of *Gymnotus omarorum* in experimental conditions in which space is the only resource that individuals fight for, providing symmetric resources and resource values for both contestants: equally-sized plain tanks, same residence time, and the same previous experience (Batista et al. 2012). In all cases, animals were kept in their individual housing compartments with no physical contact with conspecifics for at least 15 days before the behavioral experiment. We used dyads whose body weight difference ranged from 7 to 36 % (n = 21), which allowed us to predict the contest outcome (Batista et al. 2012; Pedraja et al. 2016). Contest resolution was established when we observed the third consecutive retreat of one fish without attacking back (Batista et al. 2012; Pedraja et al. 2016).

### **6.2.4 Experiment 1**

To test the effect of territory size on the establishment of the dominant-subordinate status, we recorded the agonistic behavior of *Gymnotus omarorum* in similar conditions in both the small and the large arenas (Figure 6.1A). As originally described in both contexts (Batista et al. 2012; Pedraja et al. 2016), we used indistinctively intrasexual and intersexual adult dyads (small arena: n = 6; large arena: n = 8). In all cases, a removable glass gate was raised 5-10 min after artificial sunset, and

fish were separated 10 min following conflict resolution. While in the small arena fish were freely moving in each compartment prior to the contest, 3 plastic partitions ensured that fish were separated by more than 100 cm in the large arena before the agonistic encounter (Figure 6.1A).



**Figure 6.1:** Experimental design. **A.** Experiment 1. Each fish is placed in one separate compartment (a). In the large arena, 3 plastic partitions are used to separate fish. Five min after the light is turned off, the 23 gate is removed (b) and the agonistic encounter begins. Post-resolution phase starts after conflict resolution (gray circle) and has an arbitrary duration of 10 min. **B.** Experiment 2. (a) and (b) as in A in the large arena. (c) the post-resolution phase is recorded for 36 h after contest resolution. A central shelter was added to enrich territory value.

### 6.2.5 Experiment 2

To test the maintenance of the dominant-subordinate status and dominants' territorial defense over time, we performed a different set of dyadic encounters in the large arena prolonging the recording of the agonistic behavior of *Gymnotus omarorum* up to 36 h after contest resolution, and enriched the resource value of the territory by adding one

shelter in the middle of the arena ( $n = 7$  male-male dyads; Figure 6.1B). In order to identify unambiguously both contenders in the video recordings, potential subordinates were marked with a slight cut in the anal fin, (1-2 mm long, which is harmless for the fish), previous to the agonistic encounter. Similarly, as described above, fish were isolated before the contest in opposite corners of the arena by plastic partitions, which were removed (together with the medial glass gate) 5-10 min after artificial sunset to allow the physical interaction between individuals. The locomotor and electric displays of the agonistic behavior of *G. omarorum* were continuously recorded for 30 min after gate removal, and then recorded in samples of 2 min each 30 min during the following 35 h.

#### **6.2.6 Behavioral data processing**

**Locomotor displays.** In both experiments, we analyzed the locomotor displays of the tested individuals to identify the 3 phases of the agonistic encounter following Batista et al. (2012) a) evaluation phase (pre-contest): from time 0 (gate removal) to the occurrence of the first attack; b) contest phase: from the first attack to conflict resolution (resolution time); and c) post-resolution phase (post-contest), which was recorded for 10 min after conflict resolution in experiment 1, and for 30 min in experiment 2 (early post-resolution, EPR). We measured the following locomotor parameters in all the experiments (experiment 1 in both the small and large arenas, and experiment 2): latency to the first attack, contest duration, contest attack rate (number of attacks/contest duration in seconds) of dominants and subordinates. In experiment 1, we measured post-resolution attack rate of dominants as the number of attacks/600 s, and post-resolution retreat rate of dominants and subordinates as the number of retreats/600 s. In

experiment 2, we measured post-resolution attack rate and retreat rate of dominants and subordinates as the number of attacks or retreats per min performed in the EPR (30 min after resolution). We also measured the number of attacks per min, the number of retreats per min, the position of contenders, and the shelter occupancy of both the dominant and the subordinate in 2-min-samples each 30 min during approximately 35 h (late post-resolution, LPR). We calculated an index of shelter occupancy as the number of samples in which either the dominant or the subordinate were found inside the shelter divided by the total number of samples. We calculated a territory access index using ordinal scores depending on the position of each individual with respect to the shelter in all the samples as follows: score 5 (inside the shelter), score 3 (inside a circle whose diameter was twice the shelter length and was centered in the middle of the shelter), and score 1 (beyond this circle). The maximum score for each 2 min-sample was used as the representative score sample value, and the mean value of all these scores was used as the territory access index for each individual.

**Electric signals.** EOD rate was calculated as the mean instantaneous frequency in 5-10 s samples obtained from the evaluation and post-resolution phases. In all the experiments, the EOD rate change index was calculated as  $((\text{EOD rate in the post-resolution phase}) - (\text{EOD rate in the evaluation phase})) / (\text{EOD rate in the evaluation phase})$  in percentage. Positive values of the index represent an increase in the EOD rate, and negative values of the index a decrease in the EOD rate in the post-resolution phase.

We measured the occurrence and timing of offs (interruptions of EOD emission), and chirps (transient increases in EOD rate with waveform

distortion). We calculated first off and first chirp latency as the time to first off / chirp minus the time of occurrence of the first attack. As EOD cessations are observed in both the contest and post-resolution phase (Batista et al. 2012; Quintana et al. 2016), we calculated off rate as follows: (number of offs during contest + post-resolution phase) divided (contest duration + 600s, the arbitrary recorded duration of the post-resolution phase). As chirps are late submissive electric displays mostly observed after contest resolution (Batista et al. 2012; Quintana et al. 2016), we calculated chirp rate by dividing the number of post-resolution chirps by 600 s. As no submissive electric signals were ever observed after the initial establishment of the dominant-subordinate status, these signals were not evaluated after the first 600s post-resolution in experiment 2.

### **6.2.7 Statistics**

All data were analyzed by non-parametric tests: Mann-Whitney U test (independent variables using sets of data from different fish) for comparing dominants versus subordinates, and small versus large arenas. We used Chi-square tests  $3 \cdot 2$  ( $\chi^2$ ) to test the contest outcome.

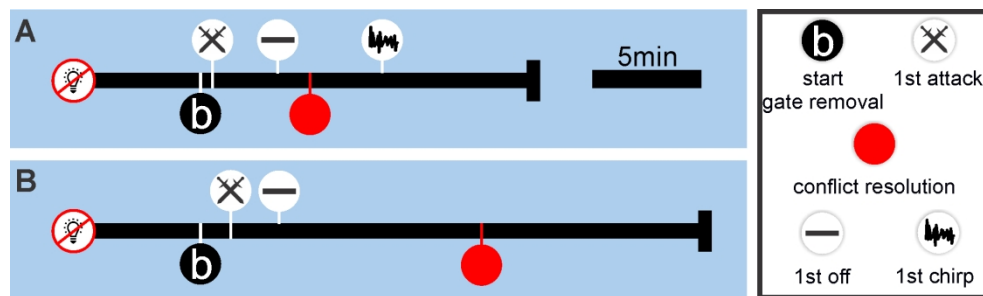
## **6.3 Results**

All dyads of non-breeding *Gymnotus omarorum* tested (small and large arenas) displayed agonistic behavior short after the gate was removed, which ended with the establishment of a clear dominance-subordination status within few minutes in all cases (Figure 6.2; less than 5 min in the small arena,  $n = 6$ ; around 12 min in the large arena,  $n = 15$ ). All the agonistic encounters also followed the typical 3 phases (pre-contest, contest,

post-resolution); and in most cases (6 out of 6 and 13 out of 15 in the small and the large arena, respectively) the larger fish resulted the dominant (Table 6-1).

### 6.3.1 Experiment 1

Although *Gymnotus omarorum* displayed dyadic agonistic interactions that reached to the establishment of the dominance-subordination status in both arenas, we observed important differences between them in the time structure of the agonistic behavior and in its levels of both aggression and subordination (Figure 6.2; Table 6-1).



**Figure 6.2:** Time structure of agonistic encounter in experiment 1. **A.** Small arena. **B.** Large arena. Agonistic behavior has three different stages: evaluation phase, from time 0 (gate removal, b) to the occurrence of the first attack; contest phase from the occurrence of the first attack to conflict resolution; and post-resolution phase. During the contest and post-resolution phase, conspicuous electric signals are observed. The duration of each phase and the latencies of motor and electrical displays are represented by the mean values (small arena: n=6; large arena: n=8).

In line with previous reports (Batista et al. 2012; Quintana et al. 2016; Perrone and Silva 2018), the agonistic behavior of the small arena (Figure 6.2A) was characterized by a) a short pre-contest of around 15 s; b) the contest, with highly aggressive displays by both contenders; and c) the



10 min post-resolution phase, in which dominants persisted in attacking, while subordinates attempted to flee and emitted submissive electric signals. On the other hand, the agonistic behavior of the large arena (Figure 6.2B) was characterized by a) a longer pre-contest of around 1 min; b) a longer contest of more than 10 min, with milder aggressive displays by both contenders; and c) the 10 min post-resolution phase, in which dominants patrolled the conquered territory and excluded subordinates less aggressively inducing subordinates to flee without emitting submissive electric signals.

As shown in Table 6-1, not only the temporal parameters (first attack latency, contest duration) were significantly different between the small and large arenas, but also the intensity of aggression of dominants, subordinates' retreats, and the displays of electric submission. In the small arena, subordinates decreased their EOD rate after contest resolution, and thus showed a negative EOD rate change index  $-7.9 (\pm 1.54)$ ; Table 6-1), while dominants did not change their EOD rate during the contest and showed a nearly null EOD rate change index of  $0.11 (\pm 0.07)$ ; Table 6-1). Interestingly, the EOD rate decrease observed in subordinates after contest resolution in the small arena, was not observed in the large arena, resulting in no significant differences in the EOD rate rank index between dominants and subordinates in the post-resolution phase of the large arena (Table 6-1). In line with this result, chirps were profusely emitted by subordinates in the small arena during the post-resolution phase, but were almost absent in the agonistic encounters held in the large arena (Table 6-1). In contrast, off rate was not significantly different between both arenas (Table 6-1).

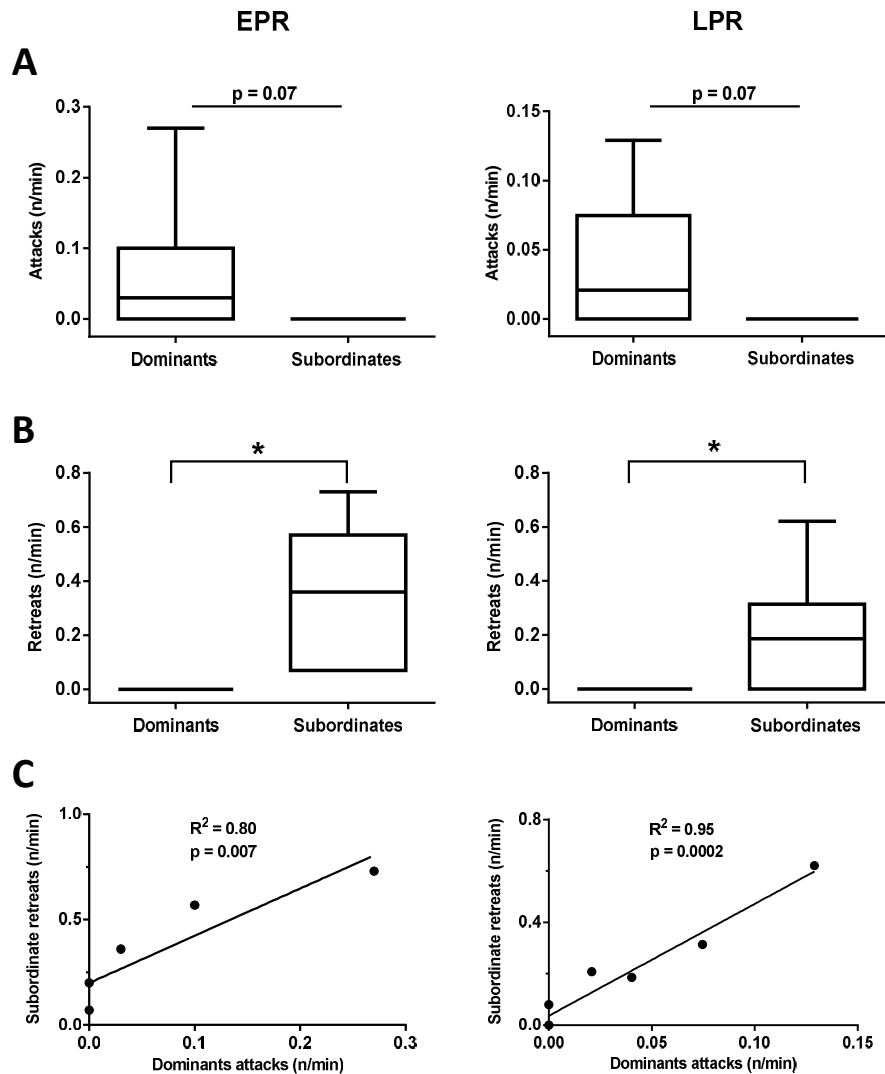
**Table 6-1.** Comparison of the agonistic behavior between the small and the large arenas. Overall comparison (small arena versus large arena) of all parameters (except for contest outcome) was tested by Mann-Whitney U test. Contest outcome was tested by Chi square test (Fisher exact test). Significant p-values are indicated in bold, marginal p-values are indicated in italics. D: dominants. S: subordinates.

		Small arena n=6	Big arena n=8	Overall comparison p-values
<b>Dynamics</b>				
<i>Outcome (% big fish won)</i>		100	87.5	>0.99
<i>contest duration (s)</i>		278.4 (±100.6)	694.25 (±408.15)	<b>0.04</b>
<i>first attack latency (s)</i>		14.25 (±6.25)	62.5 (±39.01)	<b>0.03</b>
<b>Aggression</b>				
<i>Contest attack rate (n/s)</i>	D	0.13 (±0.02)	0,012 (±0.007)	<b>0.001</b>
	S	0.029 (±0.02)	0,008 (±0.008)	0.57
<i>Post resolution attack rate (n/s)</i>	D	0.075 (±0.008)	0.002 (±0.002)	<b>0.001</b>
<i>Post resolution retreats (n/s)</i>	D	0	0	—
	S	0.038 ±(0.012)	0.01 (±0.005)	<b>0.005</b>
<b>Electric submission</b>				
<i>Off rate</i>	S	0.003 (±0.003)	0 (±0)	0.33
<i>Chirp rate</i>	S	0.013 (±0.008)	0 (±0)	<b>0.018</b>
<i>EOD rate change index</i>	S	-7.9 (±1.54)	-4.01 (±3.6)	<b>0.06</b>
	D	0.11 (±0.07)	18.93 (±9.26)	0.14
	D vs S	D: 0.11 (±0.07) S: -7.9 (±1.54)	D: 18.93 (±9.26) S: -4.01 (±3.6)	<b>0.002</b> - 0.16

### **6.3.2 Experiment 2**

Experiment 2 was carried out in the large arena; thus, the timing and general features of the agonistic behavior displayed by the male-male dyads involved in this experiment (n=7) were similar to those observed in the large arena of experiment 1 (Figure 6.2B and Table 6-1). In experiment 2, 6 out of the 7 larger males won the fight; first attack latency was of 65 ( $\pm 49$ ) s; contest lasted 259 ( $\pm 151$ ) s; and contest attack rate of dominants and subordinates was of 0.04 ( $\pm 0.01$ )/s and 0.01 ( $\pm 0.008$ )/s, respectively. None of these characteristics were significantly different from the ones recorded in the large arena of experiment 1 (Mann Whitney U test; large arena experiment 1 versus experiment 2; first attack latency:  $p=0.95$ ; contest duration:  $p=0.18$ ; dominants' contest attack rate:  $p=0.13$ ; subordinates' contest attack rate:  $p=0.23$ ).

During the EPR, 30 min immediately after the dominant-subordinate status was established (Figure 6.3) we observed a clear asymmetry in the locomotor displays of dominants and subordinates. Dominants attacked (0.03( $\pm 0.03$ )) and never retreated (0( $\pm 0$ )) while subordinates retreated (0.36( $\pm 0.21$ )) and never attacked (0( $\pm 0$ )). Further, dominants' attacks and subordinates' retreats were positively correlated (Figure 6.3C,  $r^2=0.80$   $p=0.007$ ). Interestingly, during the LPR (next 35 h of the post-resolution phase), the dominant-subordinate status consolidated with no reversion (Figure 6.3).

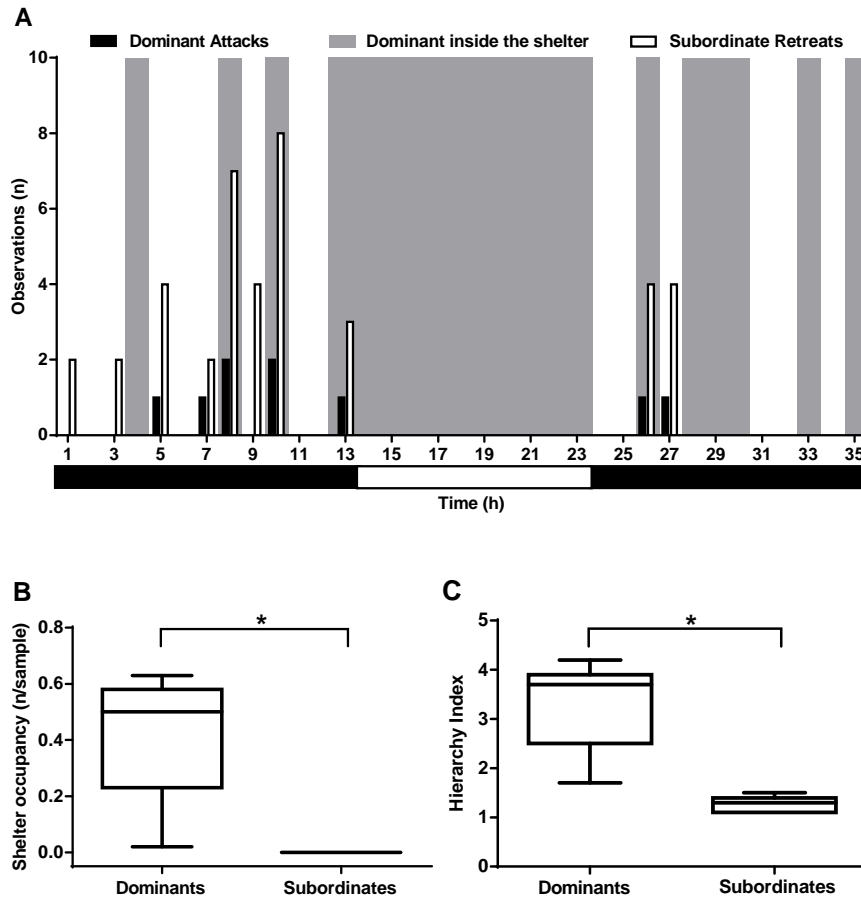


**Figure 6.3:** Locomotor agonistic displays in the post-resolution phase. EPR: early post-resolution, 30 min post-resolution. LPR: late post-resolution, 35 h post-resolution. **A.** Attack rate. EPR: Mann-Whitney U test,  $p = 0.07$ ; LPR: Mann-Whitney U test,  $p = 0.07$ . **B.** Retreats rate. EPR: Mann-Whitney U test,  $p = 0.0006$ ; LPR: Mann-Whitney U test,  $p = 0.02$ . **C.** Correlation between subordinates retreat rate and dominants attack rate. Results in A and B are depicted by boxplots with a dark line representing the median and the whiskers minimum to maximum values.

The same asymmetric behavior between dominants and subordinates was also observed in the LPR. Dominants attacked ( $0.02(\pm 0.02)$ ) and never retreated ( $0(\pm 0)$ ) while subordinates retreated ( $0.19(\pm 0.12)$ ) and never attacked ( $0(\pm 0)$ ). In addition, the correlation between dominants' attacks and subordinates' retreats persisted in long-term recordings (Figure 3C,  $r^2=0.80$ ,  $p=0.007$ ). Furthermore, Figure 6.4A shows the temporal association of dominant attacks usually preceding subordinate retreats.

In experiment 2, the large arena was enriched by the presence of a central shelter, whose occupancy and defense allowed us to make evident both dominant status and territorial behavior. As shown in Figure 6.4A with one representative dyad, only the dominant fish occupied the shelter; it rested inside the shelter during all daytime, and sheltered briefly several times during both active nights. Our video recordings clearly showed how dominants proactively excluded the access of subordinates to the shelter, chasing them when they attempted to approach it. Because of this agonistic interaction, we never found subordinates inside the shelter (Figure 6.4B; Mann-Whitney U test; shelter occupancy dominants versus subordinates;  $p=0.0006$ ).

The overall position of dominants and subordinates with respect to the shelter was evinced by calculating the territory access index. As shown in Figure 6.4C, dominants exhibited a significantly higher territory access index than subordinates, indicating that dominants not only occupied the shelter but also patrolled the surrounding area more than subordinates (Mann-Whitney U test, territory access index dominants versus subordinates;  $p=0,0006$ ).



**Figure 6.4:** Persistence of the dominant-subordinate status and territorial behavior during LPR. **A.** Locomotor agonistic displays recorded in one representative dyad over 35 h. Total time was subdivided in 1 h bins. The white-black bar represents daytime and nighttime, respectively. **B.** Shelter occupancy. Note that subordinates are never found inside the shelter. Mann-Whitney U test,  $p = 0,0006$ ,  $n=7$ . **C.** Territory access index. Note that dominants have priority access to the central part of the arena. Mann-Whitney U test,  $p = 0,0006$ ,  $n=7$ . Results in B and C are depicted by boxplots with a dark line representing the median and the whiskers minimum to maximum values.

## 6.4 Discussion

Territoriality is conceived from both behavioral and ecological perspectives (Maher and Lott 1995). The exclusive use of an area claimed by ecological definitions refers to the allocation of resources among individuals, while the behavioral approach intends to assess how that allocation was produced. This is the first study to show how agonistic encounters mediate territoriality in this genus. In dyadic interactions (experiment 2), males *Gymnotus omarorum* engage in aggressive agonistic encounters, after which a clear dominant-subordinate status emerges with no outcome reversion over time. More importantly, dominants show exclusive access to the most valuable territory (shelter), priority access to its surroundings, and proactively exclude subordinates from this conquered space.

The all-year round territorial behavior of *Gymnotus* has been put forth since pioneer reports (Black-Cleworth 1970). The unusual non-breeding territory defense has been associated with feeding habits in different classes of vertebrates (Crook 1965; Lorenz 1963). Although this assumption needs to be tested in the field, feeding demands is the most likely drive for territorial defense in *Gymnotus omarorum* as the dispersion of conspecifics allows an even exploitation of the habitat. Interestingly, as in other sexually monomorphic species that display territorial defense across seasons, territories are defended equally by both sexes (Randall 1984, Hau et al 2004, Sogge et al 2007).

Territory is defined as a fixed area defended by an animal, from which it excludes rival intruders (Brown 1975). To do so, animals use diverse types of threats as well as actual attacks, usually termed territorial

aggression (Wilson DS1975; Hau et al. 2000). Territory ownership is a major determinant of fitness and the way animals defend territories has important implications for population structure and dynamics (Balthazart et al. 1999; Adams 2001; Morrell and Kokko 2005). There are three criteria for the operational definition of territoriality: 1) defended area, 2) exclusive use, and 3) site-specific dominance (Kaufmann 1983; Maher and Lott 1995). The diagnosis of territoriality for any given species meets at least one of these requirements. For example, the black-capped chickadee (*Parus atricapillus*), was characterized as territorial because they show site-specific dominance, although they do not fulfill the criteria of defended area nor exclusive use (Desrochers and Hannon 1989). As shown in Figure 4, we were able to demonstrate that *G. omarorum* meets all the three criteria of territoriality: 1) dominants defend the central territory and chase subordinates from it, 2) the shelter is exclusively used by dominants that remain inside it during all the diurnal resting phase, and 3) dominants have priority access to a fixed area with no reduction of its boundaries over time. Indirect evidence of the persistence of territory ownership by dominants is also shown in Figure 6.3, in which attacks and retreats are not only asymmetric between dominants and subordinates but also dominant attacks correlate with subordinate retreats in a similar way for 36 h after resolution. As our approach is confined to a restricted area, we are not allowed to conclude that territories will also be fixed in the wild; alternatively, the defended area could change over time and space and constitute mobile or floating territories (Wilson DS 1975; Barrows 2001).

The agonistic behavior allows conspecifics to resolve conflicts aroused by the competition over different resources (Lorenz 1963; King 1973). When space is the resource animals compete for, agonistic encounters mediate the



establishment of territories and thus the space distribution of a given population. As predicted by theory, contest outcome depends on the asymmetries among contenders in their fighting ability (resource holding power) and in how valuable the competing space is for each individual (resource value, (Maynard Smith and Parker 1976; Parker and Rubenstein 1981). Although aggression might be initially necessary to achieve the dominant-subordinate status, once settled, a stable hierarchy suppresses further aggressive contests and unwanted fights among group members and allows the emergence of other types of social interactions (de Boer et al. 2016). The large arena, presented in this study (experiments 1 and 2) and initially reported by (Pedraja et al. 2016), contributes a naturalistic scenario to test the agonistic behavior in *Gymnotus omarorum*. Pre-contest individual distance mimics the one observed in nature (L. Zubizarreta, personal communication). Agonistic contests in the large arena follow the three expected phases (evaluation, contest, and post-resolution), with a stable status establishment in which dominants hold the central territory while subordinates are excluded to the periphery. It is interesting to note that though the volume of water of the large arena is enough to allocate two or more fish, the aggressive contest phase seems unavoidable to solve dyadic agonistic encounters in *G. omarorum*. This is somehow unexpected as individuals of *G. omarorum* can infer the size of their contenders by electric cues at intermediate distances (Pedraja et al. 2016). However, instead of taking advantage of the electric channel of communication to avoid energy demanding and injure costly contests, they disregard this information and always engage in actual fights to settle the use of space.

The time structure, aggression levels, and submissive displays of *G. omarorum* dyadic agonistic encounters show dramatic differences between

the small and the large arenas (Figure 6.2; Table 6-1). Dyads display a more robust and exaggerated agonistic behavior in the small arena (extensively described in previous reports, (Batista et al. 2012; Quintana et al. 2016; Perrone and Silva 2018) than in the large arena. Contest dynamics are extremely short in the small arena, with an evaluation phase of only 15 s and a contest duration of < 3 min. During contest, dominants' aggression levels, but not subordinates', are higher in the small arena with respect to the large one. Even more obvious changes between arenas are observed during the post-resolution phase, which is characterized exclusively in the small arena by the persistence of dominants' aggression and the profuse emission of subordinates' electric signaling of surrender. For example, the status-dependent EOD rate rank attained by the significant decrease in the EOD rate of the defeated fish after contest in the small arena (Perrone and Silva 2018) is not observed in the large arena. In addition, the emission of chirps, the latest signal of submission interpreted as the most explicit and unambiguous one (Batista et al. 2012; Quintana et al. 2016), is only observed in the small arena. This comparative analysis reinforces the idea that the experimental conditions of the large arena resembles the natural agonistic behavior of *G. omarorum* as in these conditions the communication codes exchanged by the contenders during contest lead to a peaceful agreement in how to distribute space. In contrast, when confined in the small arena, a hyper-aggressive agonistic behavior arises. The fact that subordinates cannot flee in the small arena may mislead dominants' interpretation of subordinates' surrender despite subordinates broadcast their defeat by a sequence of progressively unambiguous signals. The comparison of the agonistic behavior of *G.*

*omarorum* between the small and large arenas also contributes a very clear example of how subordinates' signaling is adjusted in response to dominants' behavior. It has already been reported in the small arena that the intensity of aggression is evaluated directly between contenders, and that subordinates assess how hard they are attacked to escalate during contest or to decide when to retreat and to emit submissive electric signals (Zubizarreta et al. 2015; Quintana et al. 2016). In line with these results, we observed in this study that the milder contests of the large arena did not force subordinates to increase their signaling of submission.

Contest outcome in *G. omarorum* depends on body size asymmetry regardless the size of the arena in which the agonistic behavior has been tested (Table 6-1). Body size is the most common predictor of fighting ability and thus of contest outcome across taxa (Jennions and Backwell 1996; Umbers et al. 2012). In theory, if resource value is symmetric among contestants, contest outcome is expected to depend only on fighting ability asymmetries (Maynard Smith and Parker 1976; Parker and Rubenstein 1981). This is indeed the case of the non-breeding agonistic behavior of *G. omarorum*, in which no resource value asymmetry is observed between contenders, and hence, their body mass difference is the only predictor of contest outcome (Batista et al. 2012). Assuming that *G. omarorum* natural territorial behavior is also mediated by agonistic encounters, two predictions arise from this study to be tested in the wild during the non-breeding season: 1) we expect body size to be the only proxy of territory size; and 2) we expect no sex differences in territory size.

In addition to the evidence that confinement intensifies competition and therefore aggressive interactions (Hazlett 1968; Alexander and Roth

1971; Turner et al. 1999; Buchwalder and Huber-Eicher 2004; Oldfield 2011), when the population density increases, many species adjust their territorial behavior by decreasing the territory size they defend (Brown 1964; Adams 2001). A previous report showed that increasing population density in *Gymnotus*, by increasing the number of conspecifics in the same tank, promotes the emergence of a more obvious territoriality (Black-Cleworth 1970). In this study, the increase in population density obtained by reducing the size of the tank did not induce neither a decrease in the territory size to adjust to confinement nor the establishment of more precise territory boundaries. Rather, confinement in the small arena promoted an increase in the fierceness of the agonistic encounter in which dominants kept attacking and chasing subordinates in an attempt of excluding them from a territory whose size is obviously not enough for both. Thus, our observations indicate that the territory size *G. omarorum* defend is not that flexible, and that its minimum size is larger than the size of the small arena.

The features displayed in the agonistic behavior of *G. omarorum* in the small arena resemble the characteristics of violent-like behaviors (de Boer et al. 2009, 2016). From this perspective, violence is defined as an exaggerated form of escalated aggressive behavior that has lost its adaptive function in social communication. Violence is expressed out of context, out of inhibitory control; and it is thus characterized by highly aggressive short-latency agonistic encounters in which dominants persist attacking even after subordinates' surrender (de Boer et al. 2009). Accordingly, the agonistic encounter of *G. omarorum* in the small arena shows an extremely short latency (around 15 s), after which dominants display an escalated and persistent aggression regardless subordinates' defeat and their profuse

electric signaling of submission. Traditional models for the study of violence have been developed in laboratory-bred feral rats and mice (Miczek et al. 2007). These studies claim for novel models to test predictions of probably conserved mechanisms governing exaggerated aggression across evolution. The inclusion of *G. omarorum* as a novel model of violent-like behavior is thus timely and promising as it contributes a teleost model whose territorial behavior is crucial for population structure in nature, can be mimicked in laboratory settings, it only requires confinement to shift from normal adaptive aggression into violent behavior, and it offers an interesting additional dimension to the assessment of territoriality by means of its electric signaling.

## 6.5 Bibliography

- Adams ES. 2001. Approaches to the study of territory size and shape. *Annu Rev Ecol Syst* 32:277–303.
- Armitage KB. 1977. Social variety in the yellow-bellied marmot: a population-behavioural system. *Anim Behav* 25:585–593.
- Assad C, Rasnow B, Stoddard PK. 1999 Electric organ discharges and electric images during electrolocation. *J Exp Biol* 202:1185–1193.
- Bakker TCM, Sevenster P. 1983. Determinants of dominance in male sticklebacks (*Gasterosteus aculeatus L.*). *Behaviour* 86:55–71.
- Balthazart J, Foidart A, Baillien M, Silverin B. 1999. Brain aromatase in laboratory and free-living songbirds. Relationships with reproductive behaviour. 1257–1289.
- Batista G, Zubizarreta L, Perrone R, Silva A. 2012. Non-sex-biased dominance in a sexually monomorphic electric fish: fight structure and submissive electric signalling. *Ethology* 118:398–410.
- Black-Cleworth P. 1970. The role of electrical discharges in the non-reproductive social behaviour of *Gymnotus carapo*. *Anim Behav Monogr* 3:1–77.
- Brown JL. 1975. The evolution of behavior. W. W. Norton, New York

- Brown JL. 1964. The evolution of diversity in avian territorial systems. *Wilson Bull* 160–169.
- Caldwell GS, Glickman SE, Smith ER. 1984. Seasonal aggression independent of seasonal testosterone in wood rats. *Proc Natl Acad Sci* 81:5255–5257.
- Caputi AA, Budelli R. 2006. Peripheral electrosensory imaging by weakly electric fish. *J Comp Physiol A Neuroethol Sens Neural Behav Physiol* 192:587–600.
- Caputi A, Carlson B, Macadar O. 2005. Electric organs and their control. In: Bullock TH, Hopkins CD, Popper AN, Fay RR (eds) *Electroreception*. Springer, New York, pp 410–451
- Chiver I, Stutchbury BJM, Morton ES. 2014. Seasonal variation in male testosterone levels in a tropical bird with year-round territoriality. *J F Ornithol* 85:1–9.
- Ciali S, Gordon J, Moller P. 1997. Spectral sensitivity of the weakly discharging electric fish *Gnathonemus petersi* using its electric organ discharges as the response measure. *J Fish Biol* 50:1074–1087.
- Clarke TA. 1970. Territorial behavior and population dynamics of a pomacentrid fish, the garibaldi, *Hypsypops rubicunda*. *Ecol Monogr* 40:189–212.
- Davies NB. 1976. Food, flocking and territorial behaviour of the pied wagtail (*Motacilla alba yarrellii* Gould) in winter. *J Anim Ecol* 235–253.
- de Boer SF, Buwalda B, Koolhaas JM. 2016. Aggressive Behavior and Social Stress. In: *Stress: Concepts, Cognition, Emotion, and Behavior*. Elsevier, pp 293–303
- de Boer SF, Caramaschi D, Natarajan D, Koolhaas JM. 2009. The vicious cycle towards violence: focus on the negative feedback mechanisms of brain serotonin neurotransmission. *Front Behav Neurosci* 3:52.
- Desrochers A, Hannon SJ. 1989. Site-related dominance and spacing among winter flocks of Black-capped Chickadees. *Condor* 317–323.
- Fugère V, Ortega H, Krahe R. 2011. Electrical signalling of dominance in a wild population of electric fish. *Biol Lett* 7:197–200.
- Gómez-Sena L, Pedraja F, Sanguinetti-Scheck JI, Budelli R. 2014. Review Paper: Computational modeling of electric imaging in weakly electric fish: Insights for physiology, behavior and evolution. *J Physiol –(Paris)* 108:112–128.

- Hagedorn M, Carr C. 1985. Single electrocytes produce a sexually dimorphic signal in South American electric fish, *Hypopomus occidentalis* (Gymnotiformes, Hypopomidae). *J Comp Physiol A* 156:511–523.
- Hagedorn M, Zelick R. 1989. Relative dominance among males is expressed in the electric organ discharge characteristics of a weakly electric fish. *Anim Behav* 38:520–525.
- Hau M, Wikelski M, Soma KK, Wingfield JC. 2000. Testosterone and year-round territorial aggression in a tropical bird. *Gen Comp Endocrinol* 117:20–33.
- Hopkins CD. 1972. Sex differences in electric signaling in an electric fish. *Science* 176:1035–1037.
- Hopkins CD. 1974. Electric communication: functions in the social behavior of *Eigenmannia virescens*. *Behaviour* 50:270–304.
- Huang W-S, Greene HW, Chang T-J, Shine R. 2011. Territorial behavior in Taiwanese kukrisnakes (*Oligodon formosanus*). *Proc Natl Acad Sci* 108:7455–7459.
- Hupé GJ, Lewis JE. 2008. Electrocommunication signals in free swimming brown ghost knifefish, *Apteronotus leptorhynchus*. *J Exp Biol* 211:1657–1667.
- Hupé GJ, Lewis JE, Benda J. 2008. The effect of difference frequency on electrocommunication: chirp production and encoding in a species of weakly electric fish, *Apteronotus leptorhynchus*. *J Physiol-(Paris)* 102:164–172.
- Jalabert C, Quintana L, Pessina P, Silva A. 2015. Extra-gonadal steroids modulate non-breeding territorial aggression in weakly electric fish. *Horm Behav* 72:60–67.
- Jennions MD, Backwell PRY. 1996. Residency and size affect fight duration and outcome in the fiddler crab *Uca annulipes*. *Biol J Linn Soc* 57:293–306.
- Jun JJ, Longtin A, Maler L. 2016. Active sensing associated with spatial learning reveals memory-based attention in an electric fish. *J Neurophysiol* 115:2577–2592.
- Kaufmann JH. 1983. On the definitions and functions of dominance and territoriality. *Biol Rev* 58:1–20.
- King JA. 1973. The ecology of aggressive behavior. *Annu Rev Ecol Syst* 4:117–138.

- Lissman H. 1958. On the function and evolution of electric organs in fish. *J Exp Biol* 35:156-191.
- Lorenz K. 1963. On aggression. Harcourt, Brace and World, New York
- Maciver MA, Sharabash NM, Nelson ME. 2001. Prey-capture behavior in gymnotid electric fish: motion analysis and effects of water conductivity. *J Exp Biol* 204:543–557.
- Maher CR, Lott DF. 1995. Definitions of territoriality used in the study of variation in vertebrate spacing systems. *Anim Behav* 49:1581–1597.
- Maynard Smith J, Parker GA. 1976. The logic of asymmetric contests. *Anim Behav* 24:159–175.
- Miczek KA, de Almeida RMM, Kravitz EA, et al. 2007. Neurobiology of escalated aggression and violence. *J Neurosci* 27:11803–11806.
- Morrell LJ, Kokko H. 2005. Bridging the gap between mechanistic and adaptive explanations of territory formation. *Behav Ecol Sociobiol* 57:381–390.
- Nelson RJ. 2006. Biology of aggression. Oxford University Press
- Parker GA, Rubenstein DI. 1981. Role assessment, reserve strategy, and acquisition of information in asymmetric animal conflicts. *Anim Behav* 29:221–240.
- Pedraja F, Aguilera P, Caputi AA, Budelli R. 2014. Electric imaging through evolution, a modeling study of commonalities and differences. *Plos Comput Biol* 10:e1003722–e1003722.
- Pedraja F, Hofmann V, Lucas KM, et al 2018. Motion parallax in electric sensing. *Proc Natl Acad Sci* 115:573–577.
- Pedraja F, Perrone R, Silva A, Budelli R. 2016. Passive and active electroreception during agonistic encounters in the weakly electric fish *Gymnotus omarorum*. *Bioinspir Biomim*. 21;11(6):065002
- Perrone R, Macadar O, Silva A. 2009. Social electric signals in freely moving dyads of *Brachyhypopomus pinnicaudatus*. *J Comp Physiol A* 195:501–514.
- Perrone R, Silva A. 2016. Vasotocin increases dominance in the weakly electric fish *Brachyhypopomus gauderio*.
- Perrone R, Silva AC. 2018. Status-dependent vasotocin modulation of dominance and subordination in the weakly electric fish *Gymnotus omarorum*. *Front Behav Neurosci* 12:1.



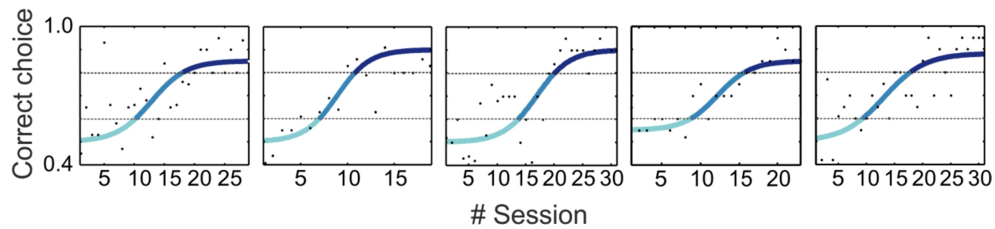
- Pröhl H. 2005. Territorial behavior in dendrobatid frogs. *J Herpetol* 39:354–365.
- Quintana L, Zubizarreta L, Jalabert C, et al. 2016. Building the case for a novel teleost model of non-breeding aggression and its neuroendocrine control. *Journal of Physiology-(Paris)* 110(3):224–232
- Richer-de-Forges MM, Crampton WGR, Albert JS. 2009. A new species of *Gymnotus* (Gymnotiformes, Gymnotidae) from Uruguay: description of a model species in neurophysiological research. *Copeia* 2009:538–544.
- Roth E, Zhuang K, Stamper SA, et al. 2011. Stimulus predictability mediates a switch in locomotor smooth pursuit performance for *Eigenmannia virescens*. *J Exp Biol* 214:1170–1180.
- Silva A, Perrone R, Macadar O. 2007. Environmental, seasonal, and social modulations of basal activity in a weakly electric fish. *Physiol Behav* 90:525–536.
- Silva A, Quintana L, Galeano M, Errandonea P. 2003. Biogeography and breeding in Gymnotiformes from Uruguay. *Environ Biol Fishes* 66:329–338.
- Silva AC, Perrone R, Zubizarreta L, et al. 2013. Neuromodulation of the agonistic behavior in two species of weakly electric fish that display different types of aggression. *J Exp Biol* 216:2412–2420.
- Stoddard P. 2002. The evolutionary origins of electric signal complexity. *J Physiol* 96:485–491.
- Summers CH, Winberg S. 2006. Interactions between the neural regulation of stress and aggression. *J Exp Biol* 209:4581–4589.
- Triefenbach F, Zakon H. 2008. Changes in signalling during agonistic interactions between male weakly electric knifefish, *Apteronotus leptorhynchus*. *Anim Behav* 75:1263–1272.
- Umbers KD, Osborne L, Keogh JS. 2012. The effects of residency and body size on contest initiation and outcome in the territorial dragon, *Ctenophorus decresii*. *PLoS One* 7:e47143.
- Westby G. 1975a. Further analysis of the individual discharge characteristics predicting social dominance in the electric fish. *Anim Behav* 23:249–260.
- Westby G. 1975b. Comparative studies of the aggressive behaviour of two gymnotid electric fish (*Gymnotus carapo* and *Hypopomus artedi*). *Anim Behav* 23:192–213.

- Wilson DS. 1975. The adequacy of body size as a niche difference. *Am Nat* 109:769–784.
- Wilson EO. 1983. Sociobiology: The New Synthesis. *Pap Rev Sociol* 149–154.
- Wingfield JC, Hahn TP. 1994. Testosterone and territorial behaviour in sedentary and migratory sparrows. *Anim Behav* 47:77–89.
- Zakon HH, Thomas P, Yan H-Y. 1991. Electric organ discharge frequency and plasma sex steroid levels during gonadal recrudescence in a natural population of the weakly electric fish *Sternopygus macrurus*. *J Comp Physiol A Neuroethol Sensory, Neural, Behav Physiol* 169:493–499.
- Zubizarreta L, Perrone R, Stoddard PK, et al. 2012. Differential serotonergic modulation of two types of aggression in weakly electric fish. *Front Behav Neurosci*. 6: 77.
- Zubizarreta L, Stoddard PK, Silva Barbato AC. 2015. Aggression levels affect social interaction in the non-breeding territorial aggression of the weakly electric fish, *Gymnotus omarorum*. *Ethology* 121:8–16.

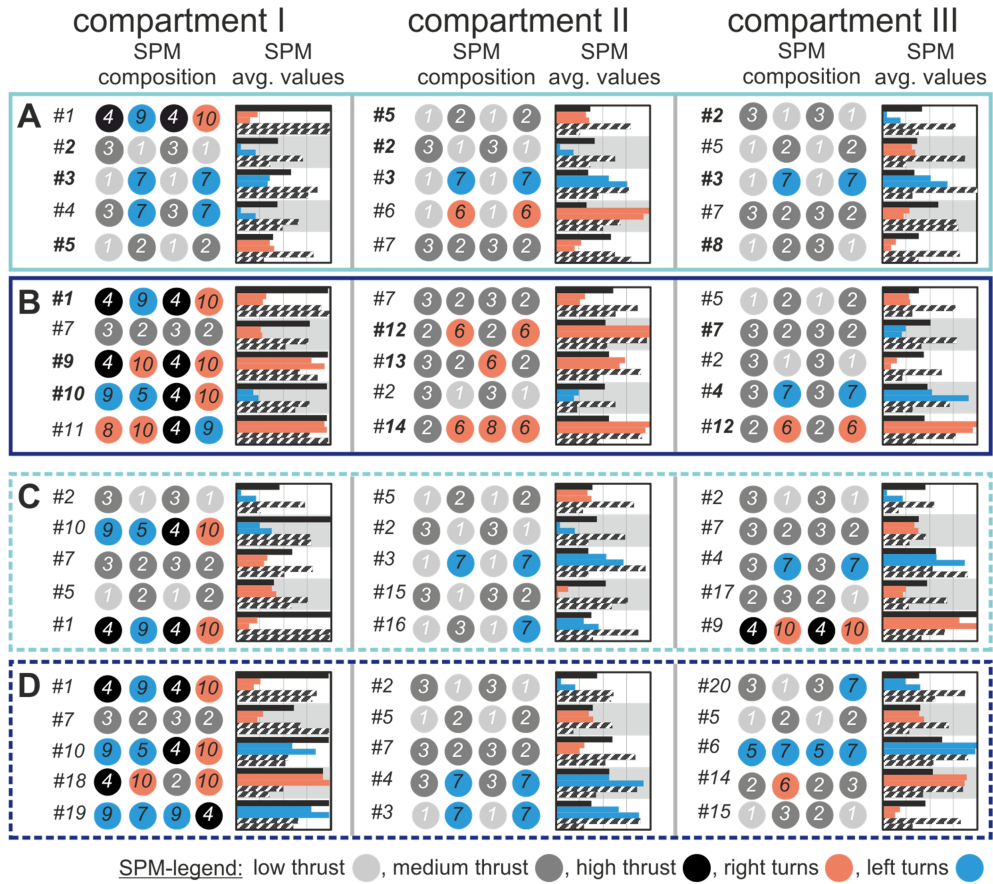
## Supplementary Material

7

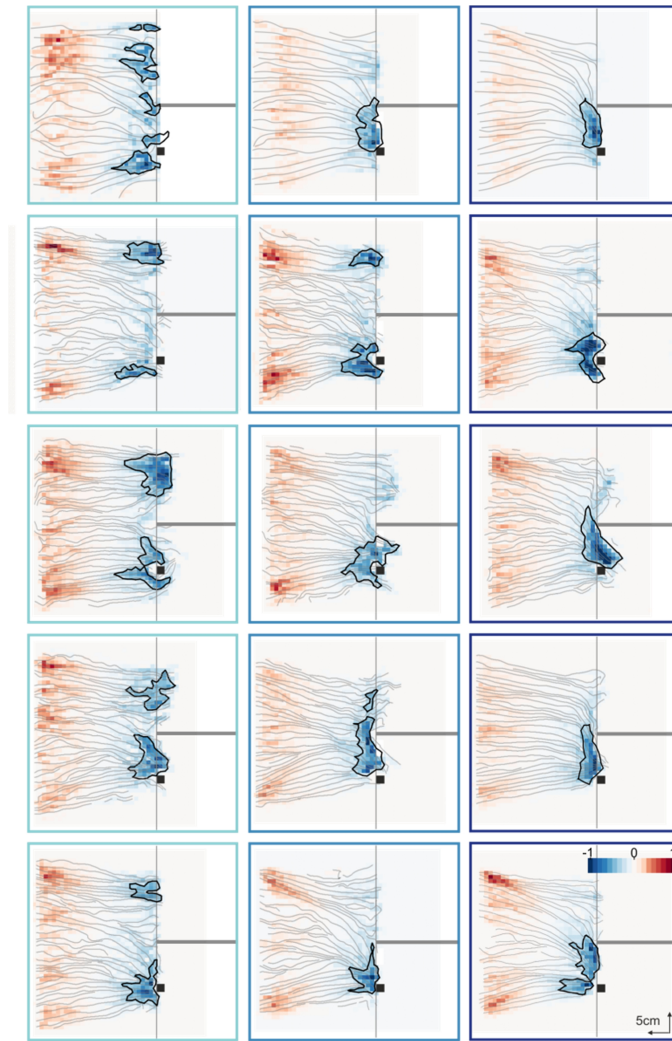
## 7.1 Supplementary figures



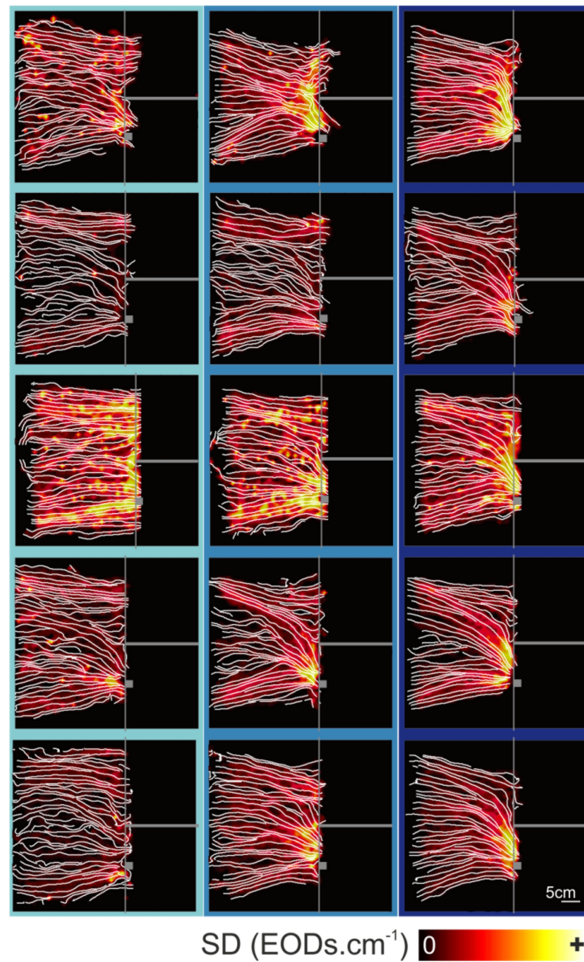
**Figure S2.1: Psychometric function following learning for all five fish.** The learning process was divided in stage I-III (< 60% of correct decision, light green; > 60 to 80%, green; > 80%, dark green).



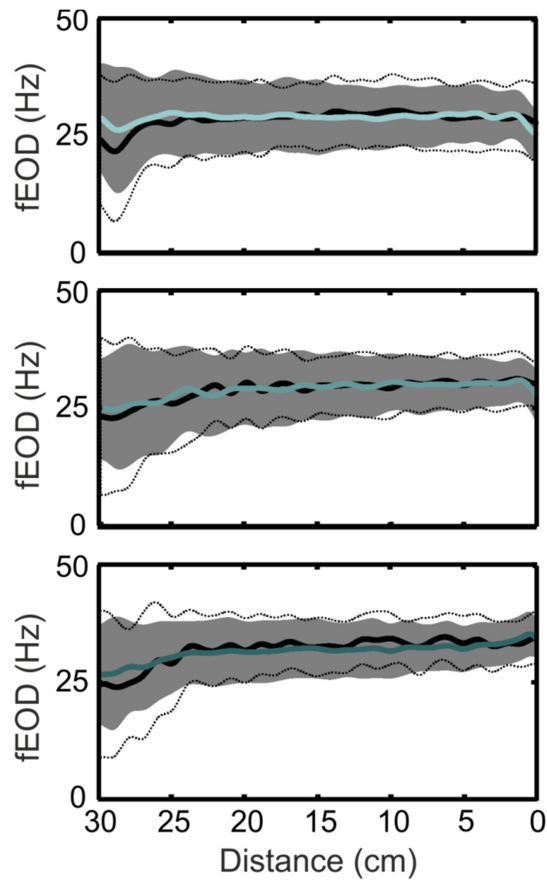
**Figure S2.2: Most frequent superprototypes (SPMs).** Composition and average values of the five most frequent SPMs for correct choices during stage I (A) and III (B) and for the wrong choices in stage I (C) and stage III (D). Columns from left to right show the data for compartments I to III, respectively. The PM-transitions characterizing the SPMs are shown by the series of colored circles. The number in each circle represents the PM being shown (see legend on the bottom for details regarding coloration). SPM average values are shown as bars and corresponds to thrust (black), slip and yaw (red and blue), duration and distance (black and white pattern). SPMs were classified with respect to average values. < 25%, between 25% and 75% and > 75% average thrust speed correspond to low, intermediate and high thrust SPM. > 75% slip or yaw speeds correspond to right or left turn. SPMs that changed the most between learning stages are shown in bold font.



**Figure S2.3: Attractor systems maps.** Attractor landscape diagrams for individual fish for the three learning stages from left to right. Red color represents hills (unstable states) while blue color represents valleys (stable states) in a dynamic system with attractors. As in previous figures, the decision line is marked with a thin vertical grey line. Data was flipped in order of keep the object in the bottom part (black square). The plastic wall dividing the two compartments is shown as a horizontal grey line.

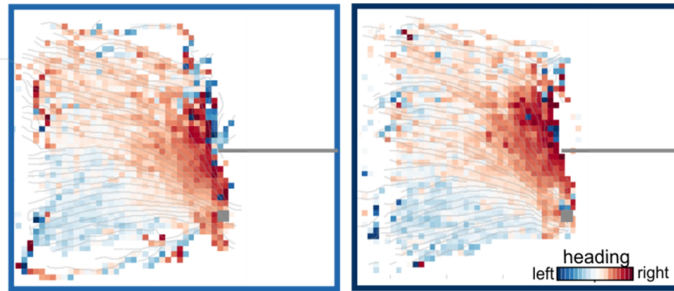


**Figure S2.4: Spatial maps of the sampling density (color-code) and mean trajectories (white lines).** Each row represents the data of a single fish with learning stage I on the left, II in the middle and III on the right. The decision line is marked with a thin vertical grey line. Data was flipped in order of keep the object in the bottom part (grey square). Plastic wall dividing the two compartments is shown as a horizontal grey line.

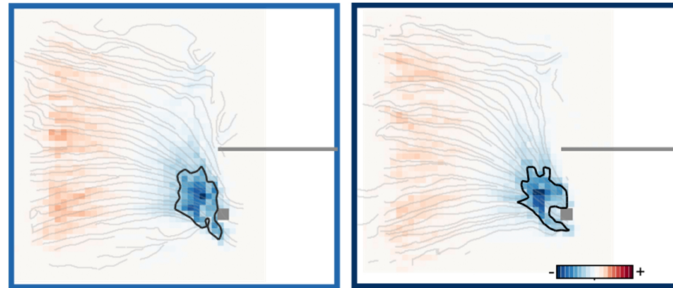


**Figure S2.5: EOD frequency.** Median and median absolute deviation of the EOD frequency with respect to the Euclidian distance from the object. Data was separated in correct trials (blue, N=5, 1119 trials) and incorrect trials (black, N=5, 514 trials). In the latter case, distance is calculated to the virtual position of the object in the compartment that the fish swam to, i.e., we treated the data as if an object had been present. Data for learning stages I-III is shown from top to bottom, respectively.

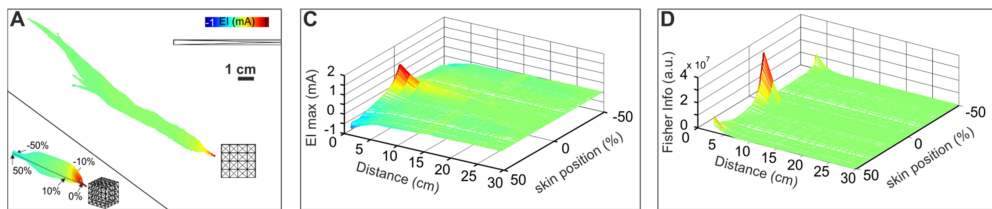




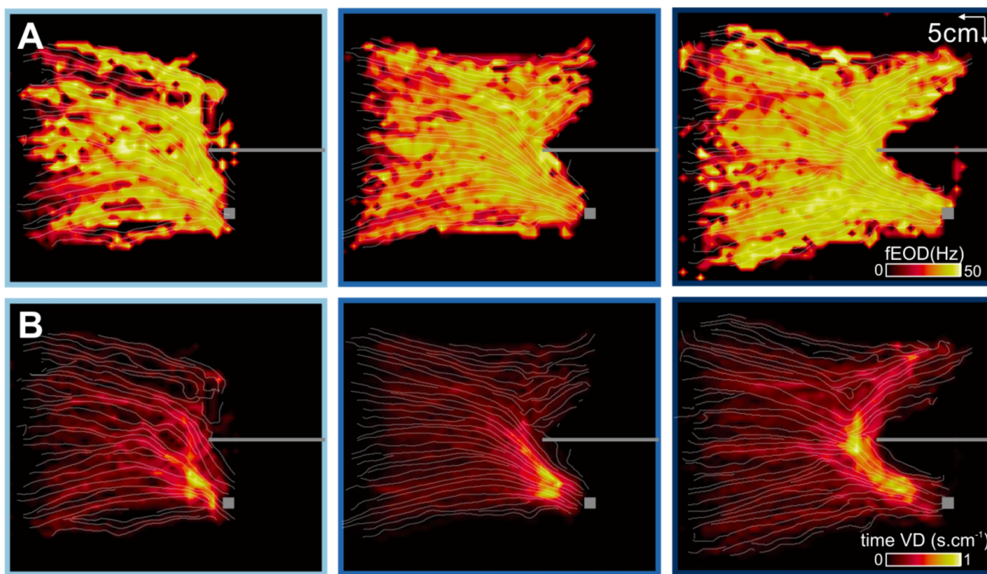
**Figure S3.1:** Top view of parts of the experimental arena showing the averaged trajectories (grey lines) of the fish performed for levels II-III control trials. The superimposed color code shows heading direction. The partition and object are shown by the grey horizontal bar and the grey cube, respectively.



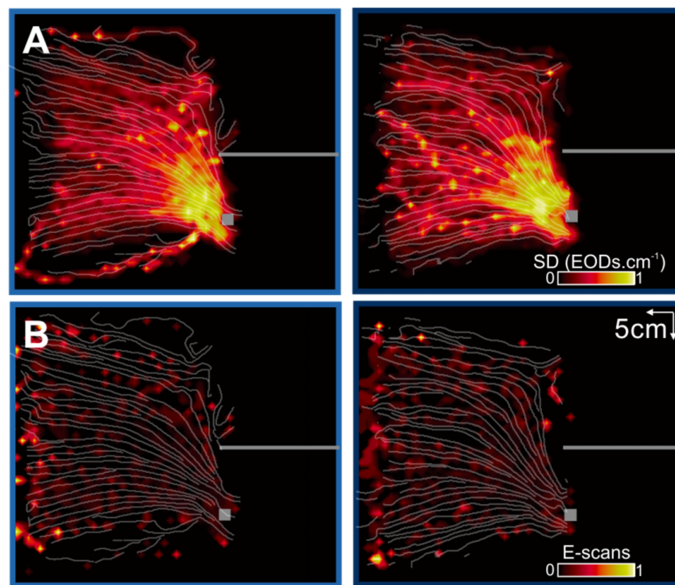
**Figure S3.2:** Top view of parts of the experimental arena showing the averaged trajectories (grey lines) of the fish for levels II-III control trials. The superimposed color code shows the attractor formation. The partition and object are shown by the grey horizontal bar and the grey cube, respectively.



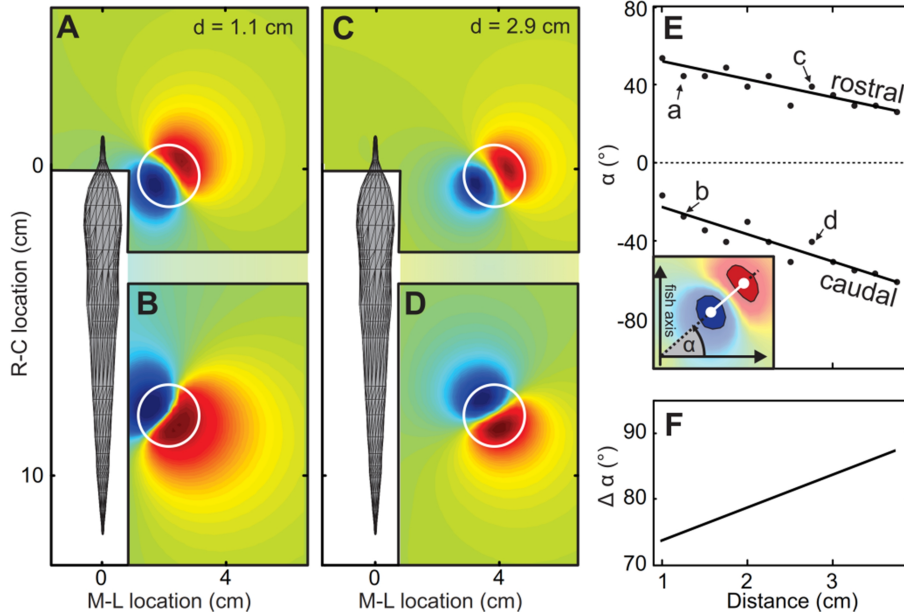
**Figure S3.3: Electric image modelling.** **A.** Example of the electric image calculated with the BEM for a typical approach of a fish to the metal cube, shown for consecutive EODs. The inset shows the cut used for the EI and Fisher information analysis. **B.** Electric image calculated along the fish's midline for the approach sequence shown in A. **C.** As in B but for the Fisher information.



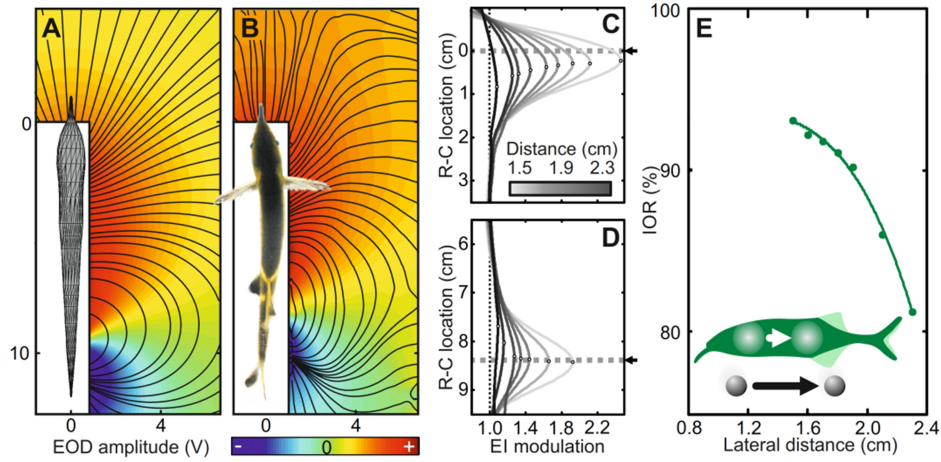
**Figure S3.4:** Top view of parts of the experimental arena showing the averaged trajectories (white lines) of the fish performed for the three levels. The superimposed color code represents the EOD frequency (**A**) and the binned normalized time for visit density (**B**). The partition and object are shown by the grey horizontal bar and the grey cube, respectively.



**Figure S3.5:** Top view of parts of the experimental arena showing the averaged trajectories (white lines) of the fish performed for levels II-III control trials. The superimposed color code represents the sampling density (**A**) and the normalized E-scan occurrence (**B**). The partition and object are shown by the grey horizontal bar and the grey cube, respectively.



**Figure S4.1: The electric field geometry provides a basis for the electrosensory parallax cue.** **A–D.** Electric field perturbations due to a metal sphere (1-cm radius) positioned at different rostral–caudal locations and lateral distances (A and B,  $d = 1.1$  cm; C and D,  $d = 2.9$  cm). **E.** The object polarization direction for rostral (Upper curve) and caudal (Lower curve) object positions at varying distances relative to the fish’s rostral caudal axis. The letters in the plot refer to points corresponding to the data shown in A–D. (Inset) Angle  $\alpha$  was defined by the direction of the polarization gradient (white line) and the fish axis. Both for the rostral as well as for the caudal object location, the orientation angle ( $\alpha$ ) of this polarization systematically changes with increasing lateral distance. Linear fits to the model data are shown by the black lines. **F.** The difference in the polarization direction between rostral and caudal positions (angle difference  $\Delta \alpha$ ) as a function of lateral distance. The angle difference increases linearly with increasing lateral distance and reflects the dependency of the EI translation (image) on lateral distance. As such, the electric field geometry and the resultant direction of object polarization are the physical bases of the electrosensory parallax cue.

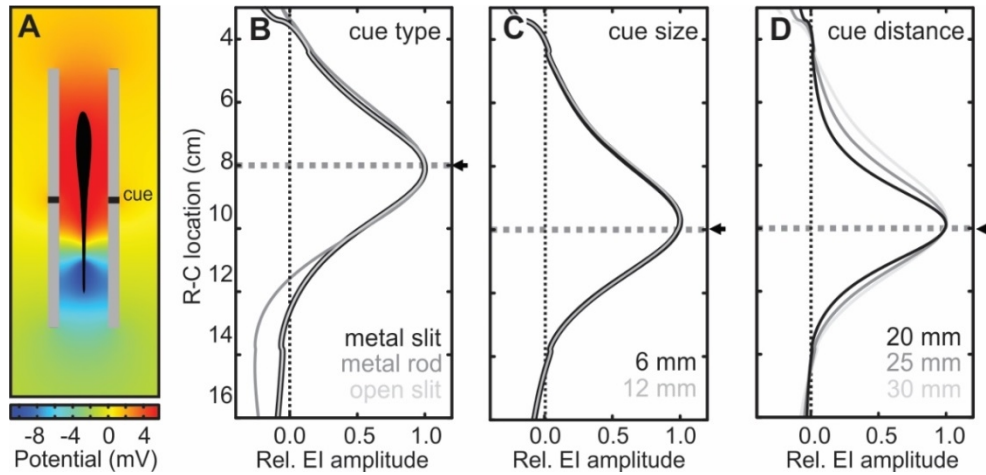


**Figure S4.2: Experimental validation of the model in *Gnathonemus petersii***

**A&B.** Top view of the BEM-modeled (see also Figure 4.1A) and experimentally-measured basal electric fields of *G. petersii*. Voltage is shown as a color-map (red positive and blue negative), black contour lines show the current flow (i.e. electric field). The white areas close to the fish comprise points where experimental measurements were not carried out.

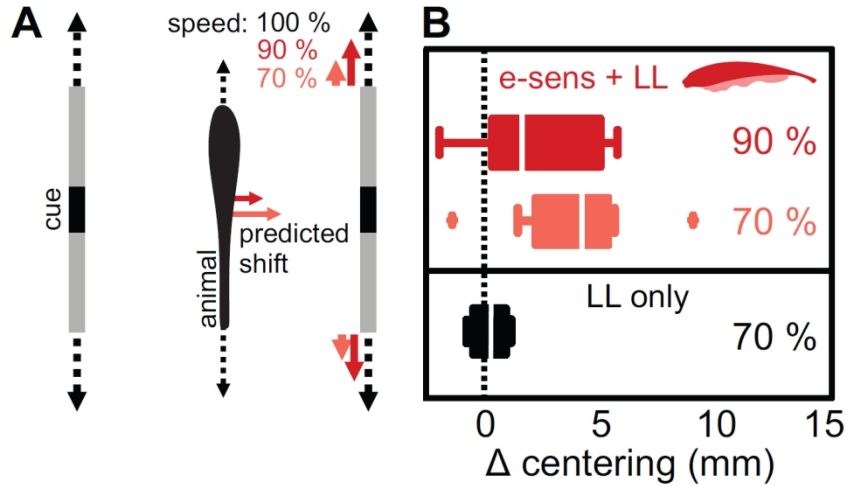
**C& D.** Experimentally-measured electric images of a metal sphere (2 cm diameter) located at rostral (C) or caudal (D) locations along the body but at different lateral distances (1.5 – 2.3 cm; see gradient). The location of the object along the rostral-caudal axis of the animal is indicated by the gray dotted lines (C: 0 cm; D: 8.2 cm; location of the fish mouth was at 0 cm). Note that the amplitude of the EI decreases with increasing lateral distance, while the EI peak (open circles) shifts towards the mid-body.

**E.** The image-to-object ratio, IOR (see main text) for the two rostral-caudal object locations shown in C and D. The ratio decreases with increasing lateral distance indicating that a more distant object would appear to be moving slower during relative motion. Solid line shows a power-law fit to the data; RMSE: 0.23 %. Inset: sketch of fish illustrating the IOR, which is the ratio of the length of the white and the black arrows.

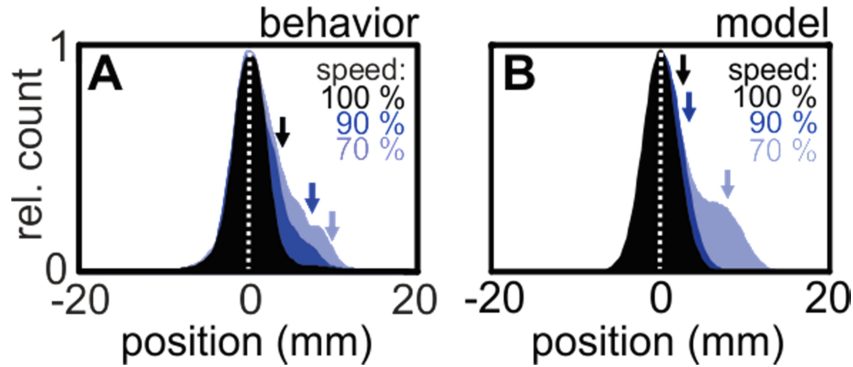


**Figure S4.3: FEM model of the electric field perturbed by the behavioral shuttle setup.** **A.** Voltage map for the fish in a shuttle with a 6 mm open slit. These results are based on the finite-element model and were used to compare electric images of the Perspex shuttle and a metal rod; see Supplementary Information for more details. **B.** Normalized (by peak value) electric images produced for different cue types (black: metal rod with radius = 2.5 cm and metal conductivity  $3.8 \cdot 10^{11} \mu\text{S} \cdot \text{cm}^{-1}$ ; dark gray: shuttle with metal-filled slit, width = 6 mm; light gray: shuttle with open slit, width = 6 mm). Position of the electrosensory cue was 8 cm (gray dotted line, fish mouth was at 0 cm) and at 3 cm lateral distance. **C.** Normalized electric images produced by different cue sizes (slit width). Cue was an open slit in the shuttle wall (black: 6 mm width; gray: 12 mm width) located at 10 cm (gray dotted line) and 3 cm lateral distance. **D.** Normalized electric images produced by the cue at different distances. Cue was an open slit in the shuttle wall with a width of 6 mm located at 10 cm (gray dotted line) at varying distance (black: 20 mm; dark gray: 25 mm; light gray: 30 mm). Similar to the EI parameters known for a sphere, the shuttle slit produced an EI that increased in relative slope with proximity (i.e. image width decreased and slope increased). Note that the 30 mm condition represents the EI a fish would experience when being centered in our behavioral apparatus.





**Figure S4.4: Hydrodynamic cues do not contribute to distance estimation in our setup.** **A.** Top view of the fish between the shuttle walls. The motion of the shuttle walls, and specifically the edges of the shuttle and the slit will produce water motions which fish can detect and analyze using the mechanosensory lateral line system. To determine if the shuttle walls themselves produce mechanosensory cues, we performed an additional set of experiments using a shuttle without slits, and with and without electrosensory cues. Fish (*Apteronotus*) were tested in the 70% parallax condition (motion of shuttle wall  $1.4 \text{ cm} \cdot \text{s}^{-1}$  vs  $2 \text{ cm} \cdot \text{s}^{-1}$ ) with either a metal-filled slit in the shuttle wall or a solid shuttle wall in addition to the usual control condition. **B.** The fish consistently shifted their position towards the slower moving side of the shuttle when both mechanosensory lateral line (LL) and electrosensory (metal-filled slit) cues were available (“e-sens + LL”: dark and light red; Wilcoxon-signed-rank test: 70%,  $N = 9$ ,  $p = 0.01$ , data is the same as in Figure 4.3C). However, with only mechanosensory cues present, the position did not change significantly (“LL only”: black; Wilcoxon-signed-rank test: 70%,  $N = 4$ ,  $p = 0.62$ ). This indicates that the mechanosensory cues are not sufficient to mediate the observed behavior.



**Figure S4.5: A stochastic switch between competing sensory cues can explain the shape of the position distributions obtained during behavioral experiments.** **A.** Position distributions obtained during behavioral experiments for *Eigenmannia* (black: control; dark blue: 90% speed; light blue: 70%, data is the same as in Figure 4.3B). **B.** Position distributions obtained from a stochastic behavioral model ( $\xi = 0.3$ ,  $\tau = 1$ ,  $\sigma = 0.25$ , and  $p = 0.8$ ). Two competing cues were used as sensory inputs to obtain each position distribution. While one cue was independent of the speed conditions (i.e. amplitude balance cue) the other was dependent on speed conditions (i.e. parallax cue). While the independent cue predicted the shuttle center to be at position 0 in all cases, the prediction of the dependent cue was varied based on the predictions presented in Figure 4.2D (black: control = 0 mm; dark blue: 90% = 2.2 mm; light blue: 70% = 8.6 mm). Similar to the experimental data, the position distribution obtained from our model increased gradually in skewness.

## **7.2 List of Acronyms**

<b>AUC</b>	area under the ROC-curve
<b>BEM</b>	boundary element method
<b>CD</b>	corollary discharge
<b>EI</b>	electric image
<b>tEI</b>	temporal electric image
<b>ELL</b>	electrosensory lateral line
<b>EMNs</b>	electromotorneurons
<b>EO</b>	electric organ
<b>EOD</b>	electric organ discharge
<b>EPR</b>	early post-resolution
<b>ESCAN</b>	transient increase in EOD rate
<b>fEOD</b>	electric organ discharge frequency
<b>FEM</b>	finite element method
<b>FI</b>	Fisher information
<b>IOR</b>	image-object ratio
<b>LGN</b>	lateral geniculate nucleus
<b>LPR</b>	late post-resolution
<b>MAD</b>	median absolute deviation
<b>PM</b>	prototypical movement
<b>PMA</b>	probing motor acts
<b>PP</b>	peak-to-peak
<b>RMS</b>	root-mean-square
<b>SD</b>	sampling density
<b>SPM</b>	super-prototypical movement
<b>STD</b>	standard deviation



Documentation

8

### **Author contributions**

Due to the cumulative layout of this thesis some chapters have been published in scientific journals while others are in preparation to being published in the near future. In this summary I want to provide an overview and detail author's contributions to the work.

#### **Chapter 1: Introduction**

Federico Pedraja conceptualized and wrote this chapter.

#### **Chapter 2: Task related sensorimotor adjustments increase the sensory range in electrolocation**

Jacob Engelmann, Federico Pedraja and Volker Hofmann designed the study. Federico Pedraja and Volker Hofmann conducted the experiments. Federico Pedraja, Julie Goulet and Volker Hofmann analyzed the data. Jacob Engelmann and Federico Pedraja drafted the manuscript with intellectual contributions of Volker Hofmann and Julie Goulet.

#### **Chapter 3: Shaping sensorimotor behavior in response to changes of cue saliency in active electrolocation**

Jacob Engelmann and Federico Pedraja designed the study. Federico Pedraja conducted the experiments and analyzed the data. Jacob Engelmann and Federico Pedraja drafted the manuscript.

**Chapter 4: Motion parallax in electric sensing**

John Lewis conceptualized the study. John Lewis, Jacob Engelmann, Volker Hofmann and Federico Pedraja designed the study. Federico Pedraja, Volker Hofmann, Kathleen M Lucas and Colleen Young conducted the experiments. John Lewis, Jacob Engelmann, Volker Hofmann and Federico Pedraja analyzed the data. John Lewis, Jacob Engelmann, Volker Hofmann and Federico Pedraja drafted the manuscript.

**Chapter 5: Passive and active electroreception during agonistic encounters in the weakly electric fish *Gymnotus omarorum***

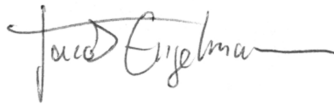
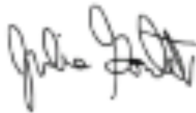



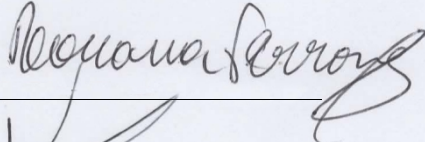
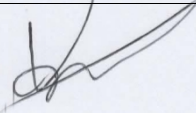
Federico Pedraja, Ana Silva and Ruben Budelli designed the study. Federico Pedraja and Rossana Perrone conducted the experiments. Federico Pedraja analyzed the data. Federico Pedraja, Rossana Perrone, Ana Silva and Ruben Budelli drafted the manuscript.

**Chapter 6: Non-breeding territoriality and context-dependent aggression in the weakly electric fish, *Gymnotus omarorum***

Ana Silva, Bettina Tassino, Rossana Perrone, Guillermo Valiño and Federico Pedraja designed the study. Federico Pedraja, Rossana Perrone and Guillermo Valiño conducted the experiments. Federico Pedraja, Rossana Perrone and Guillermo Valiño analyzed the data. Ana Silva drafted the manuscript with intellectual contributions from Bettina Tassino, Federico Pedraja, Rossana Perrone and Guillermo Valiño.

**Co-authors Affirmation**

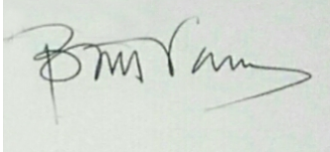
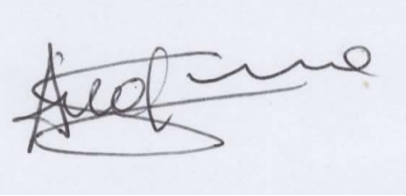
Hereby I affirm the correctness of the above detailed author contributions. I neither did submit, nor intend to use the data reported in this thesis as part of a dissertation, habilitation or other form of graduation.

<b>Prof. Dr. Jacob Engelmann</b> Active Sensing; Faculty of Biology/CITEC Universität Bielefeld; Bielefeld; Germany.	
<b>Dr. Julie Goulet</b> Active Sensing; Faculty of Biology/CITEC Universität Bielefeld; Bielefeld; Germany.	
<b>Dr. Volker Hofmann</b> Department of Physiology McGill University; Montreal; QC; Canada	
<b>Dr. Kathleen M. Lucas</b> Department of Biology University of Ottawa; Ottawa; Canada	 for KM Lucas
<b>MSc. Colleen Young</b> Department of Biology University of Ottawa; Ottawa; Canada	 for C Young
<b>Prof. Dr. John E. Lewis</b> Brain and Mind Research Institute/Department of Biology University of Ottawa; Ottawa; Canada	
<b>Dr. Rossana Perrone</b> UBNC, Instituto de Investigaciones Biológicas Clemente Estable; Montevideo; Uruguay	
<b>Guillermo Valiño</b> UBNC, Instituto de Investigaciones Biológicas Clemente Estable; Montevideo; Uruguay	



*Documentation*

---

<p><b>Prof. Dr. Bettina Tassino</b> Sección Etología; Facultad de Ciencias, Universidad de la República; Montevideo; Uruguay</p>	
<p><b>Prof. Dr. Ana Silva</b> UBNC, Instituto de Investigaciones Biológicas Clemente Estable; Montevideo; Uruguay Laboratorio de Neurociencias; Facultad de Ciencias; Universidad de la República; Montevideo; Uruguay</p>	

## **Acknowledgements**

I have much to thank and the space is limited to do it properly. I hope you could understand.

To Jacob, because he let me be part of an incredible human group and gave me the opportunity to work on what I really like. Thank you for allowing me to do my PhD here, thanks for the advice, teaching and friendship and for sharing with us all the nice moments.

To all the co-authors for the hard work and nice discussion which lead to the publication of our work.

Volker, Julie, John, Rossana, Ana, Bettina, Wally, Kathleen, Colleen.

Everyday life is much easier when you can share it with wonderful people, and those small moments of joy are the ones that I will always remember.

Thanks to the active sensing group, to all old and current members.

Volker, Vanessa, Silke, Damaris, Valerie, Johanna, Rahul, Keshav, Nicola & Lemon, Dennis, Maria Paula, Anika, Tim, Simon, Martin.

Thanks for sharing your time and experiences with me, specially the cooking party times.

To Valerie, Keshav and Maria Paula for the great time at the office. Also thanks Valerie for all your help in these years and for the revision of this thesis.

To all my colleagues from the 4th floor of faculty of Science and the UBNC in the Clemente Estable. I specially thank Ruben, I will never forget you.

To the people from TENS, we have a great time in Transylvania.

I would like to thank all my friends from Uruguay, the ones that are far and the ones that are close. Independent of the distance you all stay always in my mind.

To Vale, we hope to meet you soon.

Gracias a mis padres por todo el esfuerzo, las ganas y amor que dedicaron en criarme y darme todo lo que necesite, quisiera devolverles todo lo que me han dado, pero no me alcanzaría la vida.

Gracias a mis abuelos, tíos, y primos por compartir grandes momentos conmigo, entre ellos recuerdo gratamente las reuniones de fin de año con toda la familia reunida alrededor de una mesa.

Gracias Lu por todos estos años, por compartir este camino, por disfrutar, reír, llorar, soñar, empujar, resistir, y volar juntos.

Gracias a la familia extendida, Sylvia, Mario, Santiago, Flor, Inés y al nuevo integrante Teo, esperamos conocerte pronto.

## Curriculum Vitae

### Personal Data

#### Eduardo Federico Pedraja Muñoz

Name in bibliography citations: PEDRAJA, F - PEDRAJA, EF

Born: 15.07.1987, Montevideo, Uruguay

Address: Große Kurfürstenstraße 32, 33615, Bielefeld, Germany

federico.pedraja@uni-bielefeld.de

<http://web.biologie.unibielefeld.de/activesensing/index.php/en/mitarbeiterinnen/fede>

Institutional address: University of Bielefeld, Faculty of Biology,  
Universitätsstraße 25, 33615, Bielefeld, Germany

Phone: (+49) 521 106 00

### Academic degrees

2014–Present: PhD Student in Biology. Faculty of Biology, Bielefeld University, Germany. Supervisor: Prof. Dr. Jacob Engelmann

2012–2014: Masters Degree in Biological Sciences (option Neurosciences). PEDECIBA, University of the Republic, Uruguay. Title: *Electrorepción en Gymnotus omarorum: desde la interacción con objetos simples a comportamientos sociales complejos*. Supervisor: Prof. Dr. Ruben Budelli. Scholarship from Agencia Nacional de Investigación e Innovación (ANII), Uruguay

2006 – 2012: Bachelors Degree in Biological Sciences (option Biomathematics). Faculty of Science, University of the Republic, Uruguay. Title: *Modelo computacional de Gymnotus omarorum: Un pez eléctrico de pulso con órgano distribuido*. Supervisor: Prof. Dr. Ruben Budelli

## Bibliography

### Publications

**PEDRAJA, F;** ENGELMANN, J. *Shaping sensorimotor behaviour as response of decrease in object's saliency*. In preparation

**PEDRAJA, F;** HOFMANN, V; GOULET, J; ENGELMANN, J. *Task related sensorimotor adjustments increase the sensory range in electrolocation*. Under review in J. Neuroscience

PERRONE, R; **PEDRAJA, F;** VALIÑO, G; TASSINO, B; SILVA, A. *Non-breeding territoriality and context-dependent aggression in the weakly electric fish, *Gymnotus omarorum**. Acta ethologica, 2019

**PEDRAJA, F\*;** HOFMANN, V\*; LUCAS, KM; YOUNG, C; ENGELMANN, J; LEWIS, JE. *Motion parallax in electric sensing*. Proceedings of the National Academy of Sciences, 2018

**PEDRAJA, F;** PERRONE, R; SILVA, A; BUDELLI, R. *Passive and active electroreception during agonistic encounters in the weakly electric fish *Gymnotus omarorum**. Bioinspiration & Biomimetics, 2016

GÓMEZ-SENA L; **PEDRAJA, F;** SANGUINETTI-SCHECK, JI; BUDELLI, R. *Computational modeling of electric imaging in weakly electric fish: insights for physiology, behavior and evolution*. Journal of Physiology (Paris), 2014

**PEDRAJA, F;** AGUILERA, P; CAPUTI, AA; BUDELLI, R. *Electric Imaging through Evolution, a Modeling Study of Commonalities and Differences*. PLoS Computational Biology, 2014

SANGUINETTI-SCHECK, JI; **PEDRAJA, EF;** CILLERUELO, E; MIGLIARO, A; AGUILERA, P; CAPUTI, A; BUDELLI, R. *Fish geometry and electric organ discharge determine functional organization of the electrosensory epithelium*. PLoS ONE, 2011

## Conference Proceedings

### Talks

**PEDRAJA, F.** *Learning to behave: shaping sensory flow to enable and enhance active electrolocation.* 109th Annual Meeting of the DZG, Bielefeld, Germany, 2017

ENGELMANN, J; HOFMANN, V; **PEDRAJA, F;** *Electrosensory parallax: electric field geometry gives rise to a dynamic cue of relative depth.* Electric Fish: Electrosensory and Electromotor Systems Satellite Meeting to the International Congress of Neuroethology, Montevideo, Uruguay, 2016

**PEDRAJA, F.** *Motion parallax cues as a determinant of relative depth in the electrosensory system.* German electric fish' workshop, Bonn, Germany, 2015

**PEDRAJA, F.** *Advances in electrolocation models: G. omarorum: a fish with a distributed electric organ.* ANGELS' workshop, Montevideo, Uruguay, 2011

### Posters

**PEDRAJA, F;** HOFMANN, V; KLOCKE, D; ENGELMANN, J; *Object detection in electrosensory learning: the action-perception loop in Gnathonemus petersii.* XII International Congress of Neuroethology, Montevideo, Uruguay, 2016

**PEDRAJA, F;** HOFMANN, V; ENGELMANN, J; *Action for perception: electric flow during parallax motion as a source of object distance information.* 108th Annual Meeting of the DZG, Graz, Austria, 2015

**PEDRAJA, F;** PERRONE, SILVA, A; R; BUDELLI, R. *Electroreception in agonist contests of weakly electric fish.* 9th World Congress International Brain Research Organization, Rio de Janeiro, Brazil, 2015

HOFMANN, V; **PEDRAJA, F;** ENGELMANN, J; *Estimation of object distance based on electrosensory input dynamics.* 107th Annual Meeting of the DZG, Goettingen, Germany, 2014

**PEDRAJA, F;** PERRONE, R; BUDELLI, R. *Electric fights: electroreception during agonistic encounters in Gymnotus omarorum.* XXVIII congreso anual de la sociedad argentina de investigación en neurociencias & Reunión satélite sobre Neurobiología del Comportamiento: "Neuroetología y Neurobiología de la Memoria en el cono sur" Un homenaje a Héctor Maldonado, Córdoba, Argentina, 2013

MIGLIARO, A; **PEDRAJA, F;** SILVA, A. *Daily changes in electric behavior in two species of south american weakly electric fish.* XII latin american symposium on chronobiology, Mendoza, Argentina, 2013

**PEDRAJA, F;** CAPUTI, A; BUDELLI, R. *Commonalities and differences in active electro-reception by electric fish.* Neuroscience 2013, San Diego, USA, 2013

**PEDRAJA, F;** CAPUTI, A; BUDELLI, R. Estudio comparativo de la electrolocalización en peces eléctricos de pulso y de onda con órgano extendido. XIV Jornadas de la Sociedad Uruguaya de Biociencias , Piriapolis, Uruguay, 2012

**PEDRAJA, F;** CAPUTI, A; BUDELLI, R. *A comparative study of electrolocation in wave and pulse-like electric fish with extended organ.* I Congreso FALAN, Cancún, Mexico, 2012

**PEDRAJA, F;** QUINTANA, L; MACADAR, O; VALLE-LISBOA, JC. *Two models for the reproduction of the basic electrophysiological properties of the Pacemaker Nucleus of Brachyopomus gauderio.* I Congreso FALAN, Cancún, Mexico, 2012

**PEDRAJA, F;** SANGUINETTI-SCHECK, JI; BUDELLI, R. *Passive and active electroreception images in the interaction of two weakly electric fish.* I Congreso FALAN, Cancún, Mexico, 2012

SANGUINETTI-SCHECK, JI; **PEDRAJA, F;** CILLERUELO, E; MIGLIARO, A; AGUILERA, P; CAPUTI, A; BUDELLI, R. *Fish geometry and electric organ discharge determine differential functions of the electrosensory epithelium.* Neuroscience 2011, Washington DC, USA, 2011

**PEDRAJA, F** SANGUINETTI-SCHECK, JI; MIGLIARO, A; GÓMEZ-SENA L; CILLERUELO, E; AGUILERA, P; CAPUTI, A; BUDELLI, R; *Modelo computacional de Gymnotus omarorum: Un pez eléctrico de pulso con órgano distribuido.* XIII Jornadas de la Sociedad Uruguaya de Biociencias , Piriapolis, Uruguay, 2010

BUDELLI, R; **PEDRAJA, F;** SANGUINETTI-SCHECK, JI; MIGLIARO, A; GÓMEZ-SENA L; CILLERUELO, E; AGUILERA, P; CAPUTI, A. *A Electric images of a fish with a distributed electric organ.* IX international neural coding workshop (NC2010) Limassol, Chipre , 2010

### **Academic contents and Positions**

2014-Present: PhD student/TV L-13, (40hs week), Faculty of Biology, University of Bielefeld, Germany

2013-2014: Assistant Grade 1 (10hs week), Institute for biological investigation Clemente Estable, Ministry of education and culture, Uruguay

2011-2013: Assistant Grade 2, (20hs week), Faculty of Science, University of the Republic, Uruguay.

2009-2012: Assistant Grade 1, (20-40hs week), Faculty of Science, University of the Republic, Uruguay.

### **Research projects**

2014 - Present: Quantification and analysis of dynamic sensory information: from behavior to processing of sensory flow in the electrosensory system. Responsible: Jacob Engelmann. DFG.

2013 - 2014: Hormonal bases of the non-reproductive territorial aggression. Responsible: Ana Silva & Laura Quintana. ANII

2011 - 2013: Neural bases of social behavior: A multidisciplinary approach. Responsible: Ana Silva & Milka Radmilovich. CSIC (Comisión Sectorial de Investigación Científica)

2009 - 2013: Strategies for identification and characterization of objects by electrolocation. Responsible: Ruben Budelli & Rafael Canetti. CSIC & 7th Frame Program of the European Union/ANGELS

### **Teaching in practical courses**

#### Master

2014-Present: Module A "Probing Behaviour"- Data Acquisition, Analysis and Presentation. Behaviour: From Neural Mechanisms to Evolution, MSc. Faculty of Biology, Bielefeld University, Germany. Role: Assistant

2016: Electrosensory system, development and evolution & Reproduction of tropical freshwater fishes with special focus on gymnotiforms and mormyrids. Institute for biological investigation Clemente Estable, Ministry of education and culture, Uruguay. Role: Assistant

2012: Mathematics for Cognitive Sciences. Interdisciplinary Nucleus of Cognitive Sciences, Interdisciplinary Center, University of the Republic, Uruguay. Role: Assistant

#### Bachelor

2010: Neuroscience 1. Faculty of Science, University of the Republic, Uruguay. Role: Assistant

### **Awards and Memberships**

2013-2014: Scholarship from ANII, to finish the master degree.

2013-2014: Scholarship from CAP (Comisión Académica de Posgrado) to finish the master degree.

2012: Scholarship from CSIC to participate in the "I Congreso Falan 2012, Cancún, México".

2012: International Scholarship por IBRO (International Brain Research Organization) to participate in the "Latin American Summer School in Computational Neuroscience 2012. Instituto de sistemas complejos, Valparaiso, Chile"

### **Academic Extension Activities**

2011-2014: Brain awareness week, Montevideo, Uruguay. Scientific society: Sociedad de Neurociencias del Uruguay. Role: Assistant

2013: Primary school visits. Institute for biological investigation Clemente Estable, Ministry of education and culture, Uruguay. Role: Assistant

### **Complementary formation**

2018: Transylvanian Experimental Neuroscience Summer School. The Pike lake, Transylvania, Romania

2012: Latin American Summer School in Computational Neuroscience  
Instituto de sistemas complejos, Valparaiso, Chile.



## **Affirmation**

### **Affirmation in lieu of an oath**

This thesis “Dynamics of sensorimotor behavior in electrolocation and electrocommunication” is a presentation of my own original research. All external resources and intellectual contributions of others have been indicated. Citations have been provided in all cases where the published work of others was consulted.

I have neither acquired nor tried to acquire a PhD or an equal degree at the Faculty of Biology, University of Bielefeld, or anywhere else before.

This thesis was written under the advice of Professor Dr. Jacob Engelmann, at the Active Sensing-Lab, Faculty of Biology, Bielefeld University.

Bielefeld, 20.05.2019 Federico Pedraja